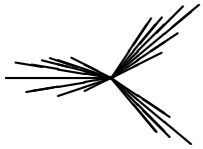

IFT

Instituto de Física Teórica
Universidade Estadual Paulista

MASTER DISSERTATION IFT–D.003/2014

Bright solitons in a quasi-one-dimensional dipolar Bose-Einstein condensate

Emerson Evaristo Chiquillo Márquez

Advisor

PhD. Sadhan Kumar Adhikari

February 2014

Agradecimientos

En primer lugar quiero dar gracias a Dios por estar siempre conmigo en las buenas y en las malas. De igual forma agradezco a mis padres y a mi hermana por su paciencia y apoyo incondicional no solo durante el desarrollo de la maestría sino en el transcurso de toda mi vida.

Igualmente doy gracias al profesor Adhikari por sus útiles consejos y recomendaciones, pero sobre todo agradezco la oportunidad que me dio para dar un nuevo paso en mi desarrollo como Físico.

También doy un especial agradecimiento al IFT por acogerme durante estos dos años y a mis compañeros Luis Y., Segundo, Cristian, Fernando y Jhosep.

Finalmente, doy gracias a CAPES por el apoyo financiero que hizo posible el desarrollo de este trabajo.

Abstract

The ultracold atomic gases have provided an important environment for studying quantum many-particle systems in the last two decades. In 2005 the experimental realization of a ^{52}Cr Bose-Einstein condensate with inter-atomic magnetic dipole dipole interaction opened the door to a new level in the research of degenerate quantum gases. As opposed to the usual contact interaction, this new interaction is long-range and anisotropic being partially repulsive or attractive. In the mean-field approximation initially are introduced the main issues about non-dipolar condensates with particular interest in the attractive regime ($a < 0$) where is possible the formation of bright solitons and the existence of instability by collapse beyond a certain critical value. The study is carried out mainly using a numerical method and a variational one. Later, the dipolar Bose-Einstein condensate is depicted by means of the non-local Gross-Pitaevskii equation. From the non-dipolar scenario by means of the extension in the numerical and the variational method is determined the formation of bright solitons in the GPE in the three-dimensional model and the quasi-one-dimensional to three different dipolar condensates of experimental relevance, namely ^{52}Cr, ^{168}Er and ^{164}Dy. Plots of chemical potential and rms sizes of solitons are obtained. Finally, it is studied collision dynamics of two bright solitons in the quasi-1D dipolar model of every condensate above.

Keywords: dipolar Bose-Einstein condensate, dipolar Gross-Pitaevskii equation, dimensional reduction, variational approximation, bright soliton, collapse.

Resumo

Os gases atômicos ultrafrios têm proporcionado um importante ambiente no estudo de sistemas quânticos de muitas partículas nas duas últimas décadas. Em 2005, a realização experimental dum condensado de Bose-Einstein de ^{52}Cr com interação magnética dipolo dipolo inter-atômica abriu a porta para um novo nível na pesquisa de gases quânticos degenerados. Ao contrário da interacção de contacto, esta nova interação é de longo alcance e anisotrópica sendo em parte repulsiva ou atrativa. Na aproximação de campo-meio, inicialmente, são introduzidas as principais questões sobre condesados com especial interesse no regime atrativo ($a < 0$) onde é possível a formação de solitons brilhantes e a existência da instabilidade por colapso além de um certo valor crítico. O estudo é realizado, principalmente, usando um método numérico e um variacional. Posteriormente, o condensado de Bose-Einstein dipolar é descrito através da equação não-local de Gross-Pitaevskii. A partir do cenário não-dipolar, por meio da extensão no método numérico e no método variacional é determinada a formação de solitons brilhantes na equação de Gross-Pitaevskii nos modelos tridimensional e quasi-unidimensional para três diferentes condensados dipolares de relevância experimental, isto é ^{52}Cr, ^{168}Er e ^{164}Dy. Gráficos do potencial químico e a raiz quadrática média (rms) dos solitons são obtidos. Finalmente, estuda-se a dinâmica da colisão de dois solitons brilhantes no modelo dipolar quasi-1D de cada condensado acima.

Palavras-chave: Condensado de Bose-Einstein dipolar, equação de Gross-Pitaevskii dipolar, redução dimensional, aproximação variacional, soliton brilhante, colapso.

Introduction

The theoretical description of Bose-Einstein condensation (BEC) dates back to 1925 based on previous work of S. N. Bose (1924) when Einstein in a gas of noninteracting massive atoms predicted the presence of a phase transition below a critical temperature T_c. This new phenomenon is reflected by the fact that a fraction of the total number of particles would occupy the lowest energy single particle state as consequence of quantum statistical effects (for more details see [1, 2, 3, 4]). However, the short technological development of this time delayed the experimental observation of a BEC, which it was only achieved until 1995 combining different cooling techiques mostly developed since 70s. Cornell and Wieman *et al.* (Colorado University) in July of 1995, Bradley *et al.* (Rice University) in July of 1995 and Ketterle *et al.* (MIT) in november of 1995, reached the density and temperature required to observe a BEC in ^{87}Rb [5], ^{7}Li [6] and ^{23}Na [7] respectively.* In the last two decades, due to this important experimental progress has been shown that ultracold atomic gases provide an excellent environment for studying quantum many-particle systems.

So what is a BEC? [8] at room-temperature the behavior of the atoms in a gas is described in a classical sense. At lower temperatures however the de Broglie wavelength turns comparable to the distance between atoms and the quantum nature of the particles becomes important. In the quantum scenario using the spin is possible to define two kind of physical systems, fermions and bosons. In this dissertation only will be treated the bosonic particles. Thus, for bosons close and below to a critical temperature T_c the single wave packets begin to overlap until a zero temperature, where all of these occupy the same quantum ground state and it is represented for a singular macroscopic wave function. This phenomenon is called Bose-Einstein condensation (Figure 1). It is worth noting in addition to low temperatures, the formation of a condensate needs a dilute gas to reduce the three body collisions, because these create a high kinetic energy giving rise to a heating and hence losses which depend on the atomic density. Thus in a dilute gas only collisions between two particles are relevant. In other words, the dilution condition

*Bradley *et al.,* besides the BEC formation they also show the collapse evidence in a BEC. Curiously only Cornell, Wieman and Ketterle are awarded with the Nobel Prize in 2001.

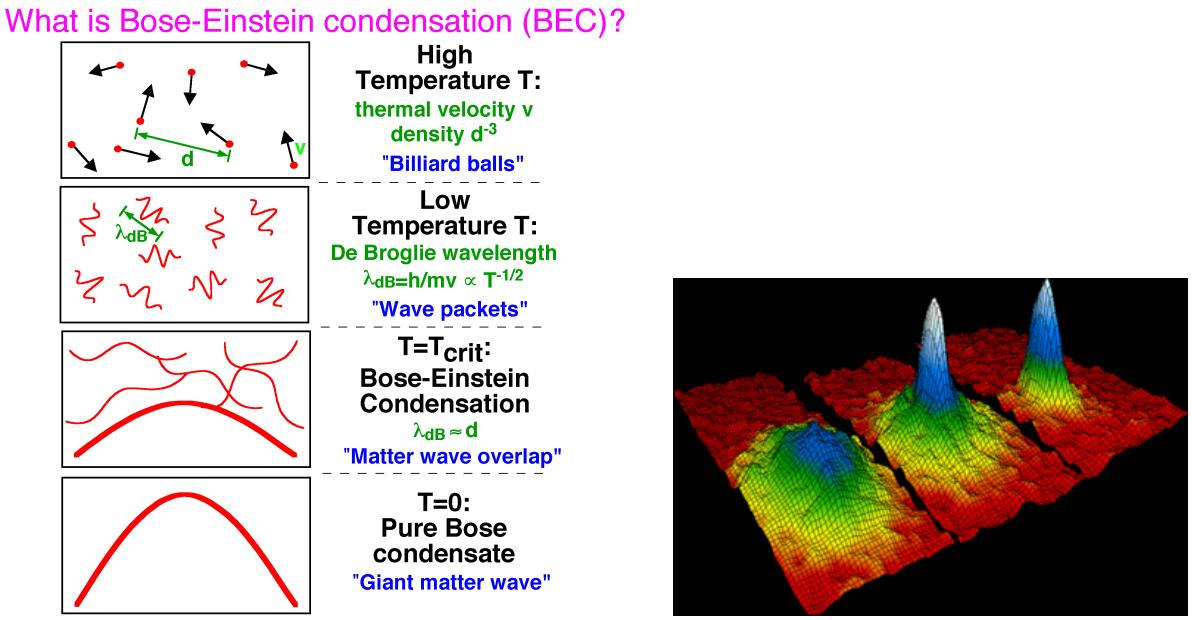

Figure 1: On the left side is shown the phase transition from an ideal gas to a BEC (http://cua.mit.edu/ketterle_group/intro/whatbec/whtisbec.html). The right side shows the velocity distribution of ^{87}Rb with a field of view $200\mu m \times 270\mu m$. The images are at $400nK$ (just above condensation), $200nK$ (after the condensation) and $50nK$ (after further evaporation leaves a sample of nearly pure condensate) respectively from left to rigth. The red color corresponds to the least amount of atoms but the fastest and so on until the white color to the largest number of atoms and the slowest (http://jila.colorado.edu/bec/CornellGroup/gallery/images/BEC_peaks.jpg).

at low energies could be interpreted such that the effective interaction between particles may be characterized by a single quantity, the scattering length a [2], thus the gases are dilute in the sense that the scattering length is much less than the interparticle spacing.

An approximate theoretical description of a condensate and agreement with the experimental results is given in terms of a mean-field theory or using the Hartree approximation in a similar way as for atoms. These methods lead to the time-dependent Gross-Pitaevskii equation (GPE), which describes the zero-temperature properties of a non-uniform dilute gas of Bose, both in attractive ($a < 0$) as repulsive ($a > 0$) regime with the number of particles N being much larger than 1. The GPE is a nonlinear Schrödinger equation (NLSE) where the nonlinear term corresponds to the interaction between two particles or called contact interaction too. This equation under special conditions enables the existence of analytical solutions called soliton solutions [2, 4], but in general, doesn't have an solution, hence is necessary to use numerical tools and approximations (e.g. variational and Thomas-Fermi). Sometimes deal with the time-dependent GPE is not the most suitable, particularly in the studying of properties related to the superfluid behavior of the BEC, such as collective modes and the expansion of the cloud when released from a trap. Therefore, is more helpful to use the hydrodynamic viewpoint because it leads to equivalent equations in terms of the density and superfluid velocity of the condensate [2, 4, 9].

The huge interest in the ultracold gases field allowed in 2005 the experimental realization of a ^{52}Cr Bose-Einstein condensate with inter-atomic magnetic dipole dipole interaction [10], opening the door to a new level in the degenerate quantum gases research. The richness of the new interaction is accompanied by a more complicated theoretical treatment as opposed to the contact interaction, this is because of its two new features, the long-range character and the anisotropy[†] (being partially repulsive or attractive). Those new properties attracted much interest, both theoretically and experimentally in the last 10 years ([11, 12, 13] and references therein), providing the possibility of controlling interparticle interactions either by tuning external fields or else by adjusting the trap anisotropy [11, 12, 14, 15, 16]. An interesting phenomenon and in analogy with the collapse in a non-dipolar condensate it was observed in a dipolar BEC (DBEC) with Chromium called the d-wave Bose-nova [17] where the theoretical description using simulations of the full GPE including the three-body losses agrees with the experimental results [16, 17].

This dissertation presents a basic description about of the most relevant features of a dipolar condensate. As part of the study is included the non-dipolar condensate to compare these results with those produced by the dipolar one. For a dipolar condensate are described the main ideas about the long-range character and the anisotropy of the interaction, the non-local mean-field GPE [11, 12], the TF approximation [2, 11, 13], and an overview of the hydrodynamic viewpoint [13] (contains a broad development about the hydrodynamics in a dipolar condensate). The main subject is focused in the numerical and variational study of the existence of bright solitons in a quasi-one-dimensional dipolar condensate. The results achieved are compared with those produced by the three-dimensional condensate.

The dissertation is organized as follows. The first Chapter shows a review of basic elements of Hartree approximation and the mean-field theory to get the Gross-Pitaevskii equation. Likewise as method to solving the GPE is applied the conventional Gaussian variational ansatz for a spherical symmetry in both regimes attractive and repulsive. The most relevant information is given for the repulsive interaction because here it is possible to find the critical parameter below which the condensate should collapse. The Thomas-Fermi (TF) approximation is included too. This is physically justified for sufficiently large clouds in which the interaction and the trap energy are larger than the kinetic energy, thus this latest contribution can be neglect in the GPE. The next Chapter leads the hydrodynamic viewpoint of a BEC, with a general but complete deduction of the density equation and superfluid velocity along with the physical implications established for the quantum nature of the condensation reflected in the appearance of the quantum pressure as opposed with the classical treatment of a fluid. The last part of Chapter includes a simple example of elementary excitations in a uniform gas in order to observe the effect of the contact

[†]By exploring this feature, the Stuttgart group was able to characterize the presence of the dipole dipole interaction because the alignment of dipoles respect to the trap axes changes the aspect ratio ω_z/ω_x or ω_z/ω_y (where ω_x, ω_y and ω_z are the harmonic trap frequencies) as a function of time after the trap release.

interaction in the energy spectrum of the condensate. In particular, it is shown that the attractive interaction constrains the existence of the spectrum. The third Chapter is designed to the dipole dipole interaction emphasizing its main features, the anisotropy and the long-range character. Again by means of a mean-field theory is described a dipolar condensate with the non-local GPE or dipolar GPE (DGPE). The effect of the dipolar interaction also is analized in the TF approximation. In a same way from the hydrodynamic theory are shown the different intervals of existence in the spectrum of energy of a homogeneous dipolar condensate some of which contrasting with the non-dipolar case. The fourth Chapter introduces the soliton theory in a BEC. As first insight of the possible existence of the soliton in a condensate is used the modulational instability in the quasi-one-dimensional model. This equation is achieved using dimensional reduction from the three- to one-dimension in the full GPE. The theory of differential equations allows the existence of analytical solutions of the quasi-1D GPE without trap, called dark and bright solitons for repulsive ($a > 0$) and attractive ($a < 0$) interactions respectively. The present dissertation is focused in bright solitons. The end of Chapter is devoted to the collapse in a three-dimensional BEC with attractive interactions without trap in the z direction. It is used a variational approximation for two different ansatz, a Gaussian function and a bright soliton-like function. In this study were found analytical expressions to the variational parameters as function of the product of the number of particles and the scattering length Na. Those analytical results agree with the numerical calculations. The last Chapter is a compilation of the different tools developed along the dissertation applied to three dipolar condensates of experimental interest, ^{52}Cr, ^{168}Er and ^{164}Dy. The study is performed to the three- and quasi-one-dimensional condensates under harmonic transverse confinement. In analogy with the non-dipolar stage it is introduced the dimensional reduction from 3D to 1D. The solution of these mean-field equations is carried out numerical and variational. The results obtained are plotted as stability diagrams, profiles of the wave function, physical observables like the chemical potential and the root mean square sizes. At the end of Chapter the dynamics collision for two bright solitons is analyzed in the quasi-1D dipolar model of every condensate above. In the last part of the dissertation the conclusions and perspectives are discussed. The dissertation also includes some appendices with additional material.

Contents

Chapter 1

The Gross–Pitaevskii equation

This Chapter introduces the Gross-Pitaevskii equation (GPE) to describe a Bose-Einstein condensate (BEC) confined in a trap to zero temperature [2, 3, 4, 9]. The gas is considered highly diluted allowing approximate the interaction potential between particles like an effective contact term [18, 19]. Will be featured the most relevant aspects to the GPE deduction in both the Hartree and the mean-field approximation. In a same way by means of a variational approximation and using the Thomas-Fermi regime are shown the first insights about the approximate solutions of the mean-field GPE.

1.1 A dilute quantum gas

The dilute quantum gases [2] differ from ordinary gases, liquids and solids in different ways. The density of molecules in the air at room temperature and atmospheric pressure is about 10^{19}cm^{-3}, in liquids and solids the density of atoms is of order 10^{22}cm^{-3}, and at center of the condensate the particle density is typically $(10^{13} - 10^{15})\,\text{cm}^{-3}$. To observe quantum phenomena at low density the temperature must be 10^{-5}K or less. This contrasted with the temperatures at which quantum phenomena occur in solids and liquids. For electrons in metals the quantum effects become strong below the Fermi temperature, which is typically $(10^4 - 10^5)\,\text{K}$, and for phonons these are appreciable below the Debye temperature, which is of order 10^2K.

Many of the interesting properties of atomic gases at low energies are derivates from the fact that the effective interaction between particles may be characterized by a single quantity, the scattering length "a" [2, 4, 20]. The gases are often dilute in the sense that the scattering length is much less than the interparticle separation. As a consequence, the effects of atomic interactions may be calculated using an effective interaction proportional to the scattering length. Some suitable candidates filling this condition are the alkali atoms [3] in which the scattering length is large compared with atomic dimensions and it is small compared with atomic separations in the gas clouds. The dimensionless parameter controlling the validity of the dilute gas approximation, is the number of par-

ticles N in a volume $|a|^3$ [3]. This can be written as $n|a|^3$, with n the average density of the gas. Experimentally the atomic scattering lengths used in the first BECs are: $a = 5.77$nm for ^{87}Rb, $a = -1.45$nm for ^{7}Li and $a = 2.75$nm for ^{23}Na. The density range is $(10^{13} - 10^{15})\,\mathrm{cm}^{-3}$ then $n|a|^3 < 10^{-3}$. So, since $n|a|^3 \ll 1$, the system is called dilute or weakly interacting. However, this quantity doesn't imply necessarily that the interaction effects are small, because these have to be compared with the kinetic energy of the atoms in the trap. The parameter that allows this comparison is given by $N|a|/a_{osc}$ such that this can be larger than 1 even if $n|a|^3 \ll 1$ and thus the gas behavior can be non ideal.

The two body effective interaction

In an identical bosons gas at very low temperature and dilute the only open scattering channel is the s-wave channel, this means that the relevant two body collisions have relative angular momentum between atoms equal to zero [20].

The experimental relevance achieved by the alkali atoms in the condensation is based in the interaction potential. The exact description of the interaction potential has a repulsive hard core, it is very deep with a minimum at a distance r and it contains many bound states corresponding to molecular states for two alkali atoms which aren't typically confined by the trap due to the total spin 0. Thus, the leading disadvantages to use the exact interaction potential are [18]:

- The potential is very difficult to calculate and a small error in this may result in a large error on the scattering length.
- The potential cannot be treated in the Born aproximation because it is very strongly repulsive at short distances and it has many bound states (for a potential as soft as a square well of radius r, the Born approach applies when the zero point energy for confinement $\hbar^2/2Mr^2$ (M the reduced mass), is much larger than the potential depth, which implies the nonexistence of bound state in the well).

In summary when the correlations between particles are neglected due to the interactions (mean-field approximation), the exact interaction potential cannot be used. The goal is replace this potential by a model having the same scattering length at low energy which can be treated in the Born approximation. For very low scattering energies, the effect of the scattering of a pair of particles with the centre of mass frame is dominated by the s-wave contribution to the wave function [1, 2, 20, 21]. The relative wave function has the form $\psi(r) = (1 - a/r)$. a is the scattering length and $\psi(r)$ is valid only outside the range of atomic potential because for smaller distances the wave function depends on details of the interatomic potential. To the Born approximation in the coordinate space [2].

$$a_{Born} = \frac{M}{2\pi\hbar^2}\int d\mathbf{r}\, V(\mathbf{r}) \tag{1.1}$$

From this expression, the low energy scattering behavior may be obtained by using of an effective interaction V_{eff}. So

$$\frac{2\pi\hbar^2}{M}a_{Born} = \int d\mathbf{r}\, V_{eff}(\mathbf{r}) \equiv g \tag{1.2}$$

for particles with the same mass m, this result becomes

$$g = \frac{4\pi\hbar^2 a}{m} \tag{1.3}$$

Thus the effective interaction between two particles at low energies in coordinate space corresponds to a pseudopotential [22] or contact interaction $V_{contact}(\mathbf{r}) = g\delta(\mathbf{r}-\mathbf{r}')$, where $\mathbf{r}$ and $\mathbf{r}'$ are the positions of the two particles.

Oscillator scale length a_{osc}

One relevant feature of the trapped Bose gases is its inhomogeneity and its finite size, where the number of atoms varies from a few thousands to several millions. As in most cases the confining traps are approximated by harmonic potentials, the trapping frequency ω_0 provides a natural scale of the system, and the oscillator length $a_0 = (\hbar/m\omega_0)^{1/2}$ is a natural length scale. This is of the order of a few microns in the available samples and can be used to simplify the problem. The unidimensional time-independent Schrödinger equation for the harmonic oscillator in terms of the new variable $x \longrightarrow x/a_0$ can be written as the dimensionless Schrödinger equation

$$\frac{1}{2}\left[-\frac{d^2}{dx^2} + x^2\right]\psi(x) = \frac{E}{\hbar\omega}\psi(x) \tag{1.4}$$

In general for three dimensions the oscillator scale length is given by

$$a_{osc} = \left(\frac{\hbar}{m\omega_{osc}}\right)^{1/2} \tag{1.5}$$

Defining the geometric average of the oscillator frequencies as $\omega_{osc} = (\omega_x\omega_y\omega_z)^{1/3}$ [3].

1.2 The GPE from the Hartree Approximation

As a consequence of the diluteness of the gas is possible in first approximation ignore correlations produced by the interaction among two atoms which are close to each other and use the Hartree's approach to investigate in a simple way the system of many-body, considering that the wave function is a symmetrized product of single-particle wave functions. In the condensed state, all bosons are in the same normalized single-particle state

$\phi(\mathbf{r},t)$ and thereby the wave function of the N particles system $\Psi(\mathbf{r}_1,\mathbf{r}_2,...,\mathbf{r}_N,t)$ may be written like [2, 4]

$$\Psi(\mathbf{r}_1,\mathbf{r}_2,...,\mathbf{r}_N,t) = \prod_{i=1}^{N}\phi(\mathbf{r}_i,t) \tag{1.6}$$

with the single-particle wave function normalization such that

$$\int d\mathbf{r}\,|\phi(\mathbf{r},t)|^2 = 1 \tag{1.7}$$

The other hand, the effective Hamiltonian of a N particles system with the same mass is

$$H = \sum_{i=1}^{N}\left[\frac{\mathbf{p}_i^2}{2m} + V(\mathbf{r}_i)\right] + g\sum_{i<j}^{N}\delta(\mathbf{r}_i-\mathbf{r}_j) \tag{1.8}$$

Where $\mathbf{p}_i$ is the momentum of a particle in the position $\mathbf{r}_i$. $V(\mathbf{r}_i)$ is an external potential. The last term corresponds to the contact interaction between two particles. One of the ways to get the motion equation implies the product of the Schrödinger equation by $N-1$ single-particle wave functions and the integration over these $N-1$ functions. Thus,

$$i\hbar\frac{\partial}{\partial t}\prod_{i=1}^{N}\phi(\mathbf{r}_i,t) = H\prod_{i=1}^{N}\phi(\mathbf{r}_i,t) \tag{1.9}$$

$$i\hbar\prod_{j=1}^{N-1}\int d\mathbf{r}_j\phi^*(\mathbf{r}_j,t)\frac{\partial}{\partial t}\prod_{i=1}^{N}\phi(\mathbf{r}_i,t) = \prod_{j=1}^{N-1}\int d\mathbf{r}_j\phi^*(\mathbf{r}_j,t)\,H\prod_{i=1}^{N}\phi(\mathbf{r}_i,t) \tag{1.10}$$

The result is the non-linear Schrödinger equation for a single-particle wave function (for more details see the Appendix A.1)

$$i\hbar\frac{\partial}{\partial t}\phi(\mathbf{r}_j,t) = -\frac{\hbar^2}{2m}\nabla^2\phi(\mathbf{r}_j,t) + V(\mathbf{r}_j)\phi(\mathbf{r}_j,t) + g(N-1)|\phi(\mathbf{r}_j,t)|^2\phi(\mathbf{r}_j,t) \tag{1.11}$$

Now, defining the condensate wave function like $\Psi(\mathbf{r},t) = N^{1/2}\phi(\mathbf{r},t)$, the density of particles is given by

$$n(\mathbf{r}) = |\Psi(\mathbf{r},t)|^2 \tag{1.12}$$

and the condition for the total number of particles turns into

$$N = \int d\mathbf{r}\;|\Psi(\mathbf{r},t)|^2 \tag{1.13}$$

So with the wave function $\Psi(\mathbf{r},t)$ and the approximation $N \gg 1$, the non-linear Schrödinger equation for the condensate (1.11) becomes [2, 3, 4]

$$i\hbar\frac{\partial\Psi(\mathbf{r},t)}{\partial t} = -\frac{\hbar^2}{2m}\nabla^2\Psi(\mathbf{r},t) + V(\mathbf{r})\Psi(\mathbf{r},t) + g|\Psi(\mathbf{r},t)|^2\Psi(\mathbf{r},t) \tag{1.14}$$

This equation is known as the time-dependent Gross-Pitaevskii equation (GPE) and it

describes the zero-temperature properties of a non-uniform Bose gas whereas the number of atoms in the condensate N is much larger than 1 and the scattering length a is much less than the average distance between atoms or also called weak-coupling limit $\left(n\left|a\right|^3 \ll 1\right)$. In the strong-coupling regime $\left(n\left|a\right|^3 \gg 1\right)$ the GPE highly overestimates the atomic contact interaction and leads to unphysical results (references therein [23]). An important feature in the GPE is given by the sign of scattering length a, while $a > 0$ it corresponds to an effective repulsion and if $a < 0$ it corresponds to an effective attraction. This dissertation gives more attention to the attractive case.

From theoretical viewpoint is easier dealing with a dimensionless model. So, taking the GPE with dimensions in terms of variables $\Phi\left(\tilde{\mathbf{r}},\tau\right)$, $\tilde{\mathbf{r}}$ and τ

$$i\hbar\frac{\partial\Phi\left(\tilde{\mathbf{r}},\tau\right)}{\partial\tau} = -\frac{\hbar^2}{2m}\nabla^2\Phi\left(\tilde{\mathbf{r}},\tau\right) + V\left(\tilde{\mathbf{r}}\right)\Phi\left(\tilde{\mathbf{r}},\tau\right) + gN\left|\Phi\left(\tilde{\mathbf{r}},\tau\right)\right|^2\Phi\left(\tilde{\mathbf{r}},\tau\right) \tag{1.15}$$

where the normalization and the density of particles number respectively are

$$\int d\tilde{\mathbf{r}}\ \left|\Phi\left(\tilde{\mathbf{r}},\tau\right)\right|^2 = 1 \tag{1.16}$$

$$n\left(\tilde{\mathbf{r}}\right) = N\left|\Phi\left(\tilde{\mathbf{r}},\tau\right)\right|^2 \tag{1.17}$$

Likewise in theoretical works is conventional to use a harmonic potential as

$$V\left(\tilde{\mathbf{r}}\right) = \frac{1}{2}m\left(\tilde{\omega}_x^2\tilde{x}^2 + \tilde{\omega}_y^2\tilde{y}^2 + \tilde{\omega}_z^2\tilde{z}^2\right) \tag{1.18}$$

To obtain a dimensionless GPE [24] is defined the variables change $\mathbf{r} = \tilde{\mathbf{r}}/a_{osc}$, or $x = \tilde{x}/a_{osc}$, $y = \tilde{y}/a_{osc}$, $z = \tilde{z}/a_{osc}$. In a same way $\omega_x^2 = \tilde{\omega}_x^2/\omega_{osc}^2$, $\omega_y^2 = \tilde{\omega}_y^2/\omega_{osc}^2$, $\omega_z^2 = \tilde{\omega}_z^2/\omega_{osc}^2$, with $a_{osc} = \left(\hbar/m\omega_{osc}\right)^{1/2}$. Also $t = \tau\omega_{osc}$, and $\Psi\left(\mathbf{r},t\right) = a_{osc}^{3/2}\Phi\left(\tilde{\mathbf{r}},\tau\right)$, thus

$$\frac{\partial\Phi\left(\tilde{\mathbf{r}},\tau\right)}{\partial\tau} = \frac{\omega_{osc}}{a_{osc}^{3/2}}\frac{\partial\Psi\left(\mathbf{r},t\right)}{\partial t} \qquad and \qquad \nabla^2\Phi\left(\tilde{\mathbf{r}},\tau\right) = \frac{1}{a_{osc}^{3/2}}\left[\frac{1}{a_{osc}^2}\nabla^2\Psi\left(\mathbf{r},t\right)\right] \tag{1.19}$$

Hence the GPE (1.15) takes the form

$$\begin{aligned}\frac{i\hbar\omega_{osc}}{a_{osc}^{3/2}}\frac{\partial\Psi\left(\mathbf{r},t\right)}{\partial t} &= \left[-\frac{\hbar^2}{2ma_{osc}^2}\nabla^2 + \frac{1}{2}ma_{osc}^2\omega_{osc}^2\left(\omega_x^2x^2 + \omega_y^2y^2 + \omega_z^2z^2\right)\right.\\ &+ \left.\frac{4\pi\hbar^2N\tilde{a}}{ma_{osc}^3}\left|\Psi\left(\mathbf{r},t\right)\right|^2\right]\frac{\Psi\left(\mathbf{r},t\right)}{a_{osc}^{3/2}}\end{aligned} \tag{1.20}$$

Or simple way

$$i\frac{\partial\Psi\left(\mathbf{r},t\right)}{\partial t} = \left[-\frac{1}{2}\nabla^2 + V\left(\mathbf{r}\right) + 4\pi aN\left|\Psi\left(\mathbf{r},t\right)\right|^2\right]\Psi\left(\mathbf{r},t\right) \tag{1.21}$$

with $a = \tilde{a}/a_{osc}$ and the potential

$$V(\mathbf{r}) = \frac{1}{2}\left(\omega_x^2 x^2 + \omega_y^2 y^2 + \omega_z^2 z^2\right) \tag{1.22}$$

Is common to express the potential in a cylindrical symmetry as follows

$$V(\mathbf{r}) = \frac{1}{2}\omega_\perp^2\left(\rho^2 + \lambda^2 z^2\right) \tag{1.23}$$

with $\omega_\perp^2 = \omega_x^2 = \omega_y^2$, $\rho^2 = x^2 + y^2$ and $\lambda = \omega_z/\omega_\perp$. This parameter defines three types of condensates. For $\lambda = 1$ the condensate is spherical. For $\lambda > 1$ it is referred as disk- or pancake-shaped where the width in z smaller than width along ρ. For $\lambda < 1$ the condensate is cigar-shaped and it is more larger in the z direction than in the radial. In a same way the normalization of the wave function and the condensed density respectively are

$$\int d\mathbf{r}\,|\Psi(\mathbf{r},t)|^2 = 1 \tag{1.24}$$

$$n(\mathbf{r}) = N\,|\Psi(\mathbf{r},t)|^2 \tag{1.25}$$

In a first insight the GPE (1.21) looks like an eigenvalue equation, where the eigenvalue could be the energy given by the expectation value for H'

$$i\frac{\partial\Psi(\mathbf{r},t)}{\partial t} = \underbrace{\left[-\frac{1}{2}\nabla^2 + V(\mathbf{r}) + 4\pi a N\,|\Psi(\mathbf{r},t)|^2\right]}_{H'}\Psi(\mathbf{r},t) \tag{1.26}$$

However it is not completely correct because of the presence of the interaction energy which it is counted twice. The energy asocciated to the interaction term is the chemical potential according to the thermodynamic relation $\mu = \Delta E/\Delta N$. Thus,

$$i\frac{\partial\Psi(\mathbf{r},t)}{\partial t} = H'\Psi(\mathbf{r},t) = \mu\Psi(\mathbf{r},t) \tag{1.27}$$

with the solution

$$\Psi(\mathbf{r},t) = \Psi(\mathbf{r})\exp(-i\mu t) \tag{1.28}$$

Then the chemical potential is the eigenvalue to the GPE do not the energy per particle like this it is for the Schrödinger linear equation. Using the solution $\Psi(\mathbf{r},t)$ in the GPE (1.21) the time-independent behavior of the condensate is given by

$$\mu\Psi(\mathbf{r}) = \left[-\frac{1}{2}\nabla^2 + V(\mathbf{r}) + 4\pi a N\,|\Psi(\mathbf{r})|^2\right]\Psi(\mathbf{r}) \tag{1.29}$$

From the wave function normalization $\int d\mathbf{r}\,|\Psi(\mathbf{r})|^2 = 1$ the chemical potential of a BEC can be calculated as

$$\mu = \int d\mathbf{r}\,\Psi^*(\mathbf{r})\left[-\frac{1}{2}\nabla^2 + V(\mathbf{r}) + 4\pi a N\,|\Psi(\mathbf{r})|^2\right]\Psi(\mathbf{r}) \tag{1.30}$$

So, the correct way to obtain the energy of a particle on the condensate is given by the hamiltonian H such that

$$H = H' - 2\pi aN \left|\Psi\left(\mathbf{r},t\right)\right|^2 = -\frac{1}{2}\nabla^2 + V\left(\mathbf{r}\right) + 2\pi aN \left|\Psi\left(\mathbf{r},t\right)\right|^2 \tag{1.31}$$

and using the condensed wave function (1.28) the accurate hamiltonian to obtain the energy is

$$H \quad = \quad -\frac{1}{2}\nabla^2 + V\left(\mathbf{r}\right) + 2\pi aN \left|\Psi\left(\mathbf{r}\right)\right|^2 \tag{1.32}$$

The Hamiltonian expectation value corresponds to the energy of a particle and the total energy of the condensate can be written as

$$E\left(\Psi\right) = \int d\mathbf{r}\left[\frac{1}{2}N\left|\nabla\Psi\left(\mathbf{r}\right)\right|^2 + V\left(\mathbf{r}\right)N\left|\Psi\left(\mathbf{r}\right)\right|^2 + 2\pi aN^2\left|\Psi\left(\mathbf{r}\right)\right|^4\right] \tag{1.33}$$

with the respective energies on the condensate

$$E_{kin} = \frac{1}{2}\int d\mathbf{r}\, N\left|\nabla\Psi\left(\mathbf{r}\right)\right|^2 \tag{1.34}$$

$$E_{int} = 2\pi\int d\mathbf{r}\, aN^2\left|\mathbf{\Psi}\left(\mathbf{r}\right)\right|^4 \tag{1.35}$$

$$E_{trap} = \int d\mathbf{r}\, V\left(\mathbf{r}\right)N\left|\mathbf{\Psi}\left(\mathbf{r}\right)\right|^2 \tag{1.36}$$

The chemical potential (1.30) may also be obtained from the energy (1.33) using the thermodynamic relation $\mu = \partial E/\partial N$. Or alternatively as

$$\mu = \frac{1}{N}\left(E_{kin} + E_{trap} + 2E_{int}\right) \tag{1.37}$$

Thus for non-interacting particles all in the same state the chemical potential has the same value that the energy per particle. A further important relationship can be found by means of the virial theorem (Appendix C.1). This allows to testing the accuracy of a numerical algorithm. So

$$2E_{kin} + 3E_{int} - 2E_{trap} \quad = \quad 0 \tag{1.38}$$

1.3 The GPE in the mean-field approximation

Another way to get the GPE implies the use of second quantization and the Bogoliubov approach for a system of many interacting bosons, i.e. taking the Heisenberg equation with the boson fields operators and the Bogoliubov consideration [3]. The many-body Hamiltonian in second quantization describing N interacting bosons confined by an external potential is given by

$$\hat{H} = \int d\mathbf{r}\,\hat{\Psi}^\dagger\left(\mathbf{r},t\right)\hat{H}_0\hat{\Psi}\left(\mathbf{r},t\right) + \frac{1}{2}\int d\mathbf{r}d\mathbf{r}'\hat{\Psi}^\dagger\left(\mathbf{r},t\right)\hat{\Psi}^\dagger\left(\mathbf{r}',t\right)V\left(\mathbf{r}-\mathbf{r}'\right)\hat{\Psi}\left(\mathbf{r}',t\right)\hat{\Psi}\left(\mathbf{r},t\right) \tag{1.39}$$

With the single particle operator

$$\hat{H}_0 = -\frac{\hbar^2}{2m}\nabla^2 + V(\mathbf{r}) \tag{1.40}$$

the two-body interatomic potential $V(\mathbf{r}-\mathbf{r}')$ and the creation and annihilation boson fields operators $\hat{\Psi}^\dagger(\mathbf{r})$ and $\hat{\Psi}(\mathbf{r})$ respectively. These obey the usual commutation relations

$$\left[\hat{\Psi}(\mathbf{r},t), \hat{\Psi}^\dagger(\mathbf{r}',t)\right] = \delta(\mathbf{r}-\mathbf{r}') \tag{1.41}$$

$$\left[\hat{\Psi}(\mathbf{r},t), \hat{\Psi}(\mathbf{r}',t)\right] = 0 \tag{1.42}$$

$$\left[\hat{\Psi}^\dagger(\mathbf{r},t), \hat{\Psi}^\dagger(\mathbf{r}',t)\right] = 0 \tag{1.43}$$

To the effective interaction between two particles the hamiltonian takes the form

$$\begin{aligned}\hat{H} &= \int d\mathbf{r}\, \hat{\Psi}^\dagger(\mathbf{r},t)\, \hat{H}_0 \hat{\Psi}(\mathbf{r},t) + \frac{g}{2}\int d\mathbf{r} d\mathbf{r}' \hat{\Psi}^\dagger(\mathbf{r},t)\, \hat{\Psi}^\dagger(\mathbf{r}',t)\, \delta(\mathbf{r}-\mathbf{r}')\, \hat{\Psi}(\mathbf{r}',t)\, \hat{\Psi}(\mathbf{r},t) \\ &= \int d\mathbf{r}\, \hat{\Psi}^\dagger(\mathbf{r},t)\, \hat{H}_0 \hat{\Psi}(\mathbf{r},t) + \frac{g}{2}\int d\mathbf{r}\, \hat{\Psi}^\dagger(\mathbf{r},t)\, \hat{\Psi}^\dagger(\mathbf{r},t)\, \hat{\Psi}(\mathbf{r},t)\, \hat{\Psi}(\mathbf{r},t)\end{aligned} \tag{1.44}$$

in the Heisenberg picture the dynamics of the system is given by

$$i\hbar\frac{\partial}{\partial t}\hat{\Psi}(\mathbf{r}',t) = \left[\hat{\Psi}(\mathbf{r}',t), \hat{H}\right] \tag{1.45}$$

Therefore, the result is a field operators equation (for more details see (A.2))

$$i\hbar\frac{\partial}{\partial t}\hat{\Psi}(\mathbf{r}',t) = \left[-\frac{\hbar^2}{2m}\nabla^2 + V(\mathbf{r}') + g\hat{\Psi}^\dagger(\mathbf{r}',t)\,\hat{\Psi}(\mathbf{r}',t)\right]\hat{\Psi}(\mathbf{r}',t) \tag{1.46}$$

Finally, using the Bogoliubov approach [2, 4] according to which since the condensate state involves the macroscopic occupation of a single state it is appropriate to decompose the Bose field operator in terms of a macroscopically populated mean field term $\left\langle\hat{\Psi}(\mathbf{r}',t)\right\rangle = \Psi(\mathbf{r}',t)$ and taking into account small fluctuations (quantum or thermal) about the condensate state $\delta\hat{\Psi}(\mathbf{r}',t)$. Thus,

$$\hat{\Psi}(\mathbf{r}',t) = \Psi(\mathbf{r}',t) + \delta\hat{\Psi}(\mathbf{r}',t) \tag{1.47}$$

Taking only the leading order terms in $\Psi(\mathbf{r}',t)^*$ the time-dependent GPE is given by

$$i\hbar\frac{\partial}{\partial t}\Psi(\mathbf{r},t) = \left[-\frac{\hbar^2}{2m}\nabla^2 + V(\mathbf{r}) + g\left|\Psi(\mathbf{r},t)\right|^2\right]\Psi(\mathbf{r},t) \tag{1.48}$$

*It would be wrong to replace $\hat{\Psi}(\mathbf{r},t)$ with $\Psi(\mathbf{r})$ for a realistic potential [4]. However, the change is accurate if (i) the effective potential $V(\mathbf{r})$ is soft where the Born approximation is applicable. It is true when the scattering length is less than the thermal de Broglie wavelength $a \ll \lambda_B \approx \hbar/(mk_BT)^{1/2}$ with m the mass of the particle and k_B the Boltzmann's constant.(ii) The temperature is much less than the transition temperature for the onset of condensation.

For the stationary states in the GPE the wave function evolves in time in a same way like the ansatz $\Psi(\mathbf{r},t) = \Psi(\mathbf{r})\exp(-i\mu t/\hbar)$. The phase factor reflects the fact that microscopically $\Psi(\mathbf{r},t)$ is equal to the matrix elements of the annihilation operator $\hat{\Psi}(\mathbf{r},t)$ in Heisenberg picture between the ground state with N particles and that with $N-1$ particles [2]

$$\left\langle \hat{\Psi} \right\rangle = \Psi(\mathbf{r},t) = \left\langle N-1 \left| \hat{\Psi}(\mathbf{r}) \right| N \right\rangle \tag{1.49}$$

$$\Psi(\mathbf{r},t) = \left\langle N-1 \left| e^{i\hat{H}t/\hbar}\hat{\Psi}(\mathbf{r})\, e^{-i\hat{H}t/\hbar} \right| N \right\rangle \propto e^{-i(E_N - E_{N-1})t/\hbar} \tag{1.50}$$

For a large particle numbers N, it is possible to perform the approximation $E_N - E_{N-1} \sim \partial E/\partial N$ which is equal to the chemical potential μ. So, in a same way like it was done above with the dimensionless GPE (1.21), the chemical potencial and the total energy of the condensate correspond with (1.30) and (1.33) respectively.

1.4 Approximate solutions to the time-independent GPE

Now will be examined some solutions of the GPE for bosons in a trap [2, 3, 4]. Due to the experimental relevance will be considered harmonic traps $V(\mathbf{r})$, but the formalism may be applied to more general traps.

1.4.1 Variational solution

The variational method is one way of find approximations to the lowest energy eigenstate or ground state. The idea consists in take a trial function with a fixed shape but some free parameters and finding the values of these parameters for which the expectation value of the energy is the lowest possible. The expectation value of the energy in the new state is an upper bound to the ground state energy. If the shape of the actual solution is close to the trial function, the results obtained with the variational method will be in good agreement with the real solutions, but in other cases the method can be very rough or even fail.

In the weak coupling limit ($Na \to 0$) the interaction contribution is small and it may be neglected, thus the system matches with a harmonic oscillator like (1.4). In three dimensions, the lowest single-particle state to the harmonic oscillator has a Gaussian form as

$$\phi_0(\mathbf{r}) = \frac{1}{\pi^{3/4}}\, e^{-r^2/2} \tag{1.51}$$

where $r^2 = x^2 + y^2 + z^2$. Now, will be taken as normalized trial function the same gaussian form for the condensate wave function $\Psi(\mathbf{r})$, such that

$$\Psi(\mathbf{r}) = \left(\frac{1}{w^3\pi^{3/2}}\right)^{1/2} e^{-r^2/2w^2} \tag{1.52}$$

As the presence of the interatomic interactions change the dimensions of the cloud then is useful to take as dimensionless variational parameter the length w which fixes the width of the condensate [25]. A variational solution with a more general wave function to the time-dependent GPE is presented by Salasnich [26].

The substitution from normalized trial function (1.52) into the condensate energy (1.33) yields the contributions†

$$|\mathbf{\Psi}(\mathbf{r})|^2 = \frac{1}{w^3\pi^{3/2}}\, e^{-r^2/w^2} \tag{1.53}$$

$$|\mathbf{\Psi}(\mathbf{r})|^4 = \frac{1}{w^6\pi^3}\, e^{-2r^2/w^2} \tag{1.54}$$

$$|\nabla\mathbf{\Psi}(\mathbf{r})|^2 = \frac{1}{w^3\pi^{3/2}}\left(\frac{r}{w^2}\right)^2 e^{-r^2/w^2} \tag{1.55}$$

For a spherical trap $V(\mathbf{r})$ ($\lambda = 1$ in (1.23) and for easily taking $\omega_\perp = 1$), the potential is given by

$$V(\mathbf{r}) = \frac{1}{2}r^2 \tag{1.56}$$

Thus the total energy of the condensate takes the form

$$\begin{aligned} E &= N\int d\mathbf{r}\left[\frac{1}{2}\frac{1}{w^3\pi^{3/2}}\, e^{-r^2/w^2}\left(\frac{r}{w^2}\right)^2 + \frac{1}{2}r^2\frac{1}{w^3\pi^{3/2}}\, e^{-r^2/w^2} + 2\pi aN\frac{1}{w^6\pi^3}\, e^{-2r^2/w^2}\right] \\ &= \frac{N}{2w^3\pi^{3/2}}\left(\frac{1}{w^4}+1\right)\int d\mathbf{r}\, r^2 e^{-r^2/w^2} + \frac{2\pi aN^2}{w^6\pi^3}\left(\frac{\pi}{2}\right)^{3/2} w^3 \\ &= \frac{3}{4}\frac{N}{w^3\pi^{3/2}}\left(\pi w^6\right)^{1/2}\left(\pi w^2\right)\left(\frac{1}{w^4}+1\right) + \frac{2\pi aN^2}{w^3}\left(\frac{1}{2\pi}\right)^{3/2} \\ &= \frac{3}{4}N\left(\frac{1}{w^2}+w^2\right) + \frac{aN^2}{(2\pi)^{1/2}\, w^3} \end{aligned} \tag{1.57}$$

The chemical potential can be obtained from $\mu = \partial E/\partial N$

$$\mu(w) = \frac{3}{4}\left(w^2 + \frac{1}{w^2}\right) + \left(\frac{2}{\pi}\right)^{1/2}\frac{Na}{w^3} \tag{1.58}$$

and the total energy per particle turns into [2, 3, 4]

$$\frac{E(w)}{N} = \frac{3}{4}\left(w^2 + \frac{1}{w^2}\right) + \frac{1}{\sqrt{2\pi}}\frac{Na}{w^3} \tag{1.59}$$

Na is a measure of the strength of the atom-atom interaction expressing its importance

†Useful integrals

$\int_{-\infty}^{\infty} e^{-bx^2}dx = \sqrt{\frac{\pi}{b}}$ $\quad b>0$ $\qquad$ $\int_{-\infty}^{\infty} x^2 e^{-bx^2}dx = \frac{1}{2}\sqrt{\frac{\pi}{b^3}}$ $\quad b>0$

compared to the kinetic energy. In most experiments on atoms with repulsive interactions, Na is much larger than unity [3]. In the first experiments with rubidium atoms at JILA (1995) the ratio $|a| \sim 7\times10^{-3}$ with N a few thousands, then $N|a| > 1$. In the experiments with ^{7}Li at Rice University (1995) the number of particles is of the order of 1000 and $|a| \sim 0.5 \times 10^{-3}$ and $N|a| > 1$. In the experiments with sodium at MIT (1995) the number of atoms in the condensate is very large $10^6 - 10^7$ and $N|a| \sim 10^3 - 10^4$.

The Figure (1.1) illustrates the energy per particle E/N (1.59) in the variational treatment of a condensate like function of the variational parameter w for different values of the parameter Na. The curve $Na = 0$ shows the behavior of the ground state of the system without interactions which is equivalent with a three-dimensional isotropic harmonic oscillator and the corresponding energy per particle is equal to 3/2. For repulsive interacions ($a > 0$) the energy per particle always has a minimum indicating the existence of a stable ground state. The other hand, a local minimum exists for attractive interactions when N is less than some critical value of particle number N_c [2, 3, 4, 27], but for larger values of N the cloud will collapse, this is the case of the ^{7}Li [6]. The N_c satisfies that both the first and second derivative of E/N with respect to the variational parameter w are equal to zero. So using the energy per particle (1.59) for attactive interactions ($a < 0$)

$$\frac{E}{N} = \frac{3}{4}\left(\frac{1}{w^2} + w^2\right) - \frac{1}{\sqrt{2\pi}}\frac{N|a|}{w^3} \tag{1.60}$$

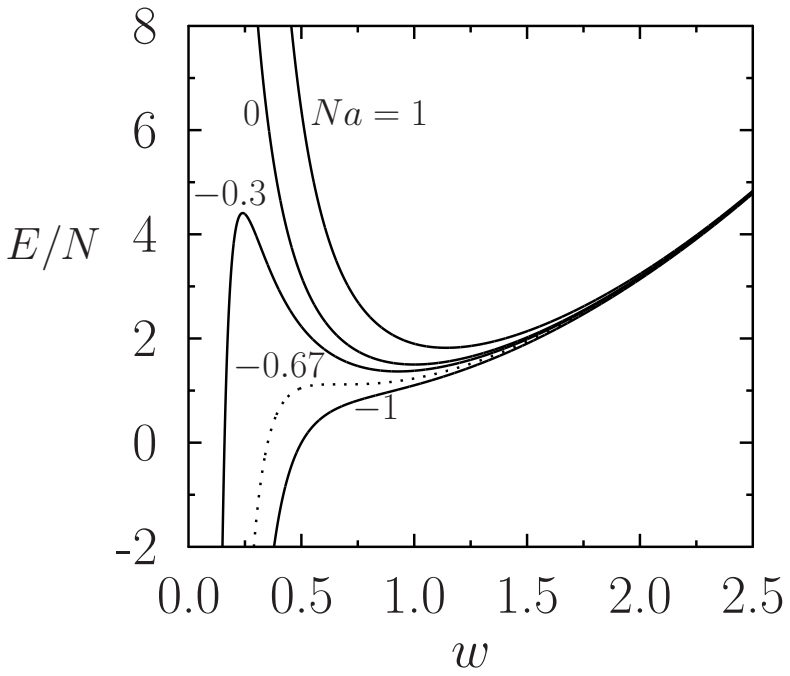

Figure 1.1: Energy per particle of a condensate in an isotropic harmonic trap as a function of the variational parameter w, for different values of the parameter Na. The dotted curve corresponds to the critical value at which the cloud becomes unstable.

Deriving E/N respect to the variational parameter w and equaling to zero

$$\frac{3}{4}\left(2w - \frac{2}{w^3}\right) + \frac{3}{\sqrt{2\pi}}\frac{N|a|}{w^4} = 0 \tag{1.61}$$

$$\sqrt{\frac{2}{\pi}}N|a| = w - w^5 \tag{1.62}$$

To the second one derivate and again equaling to zero

$$\frac{3}{4}\left(2 + \frac{6}{w^4}\right) - \frac{12}{\sqrt{2\pi}}\frac{N|a|}{w^5} = 0 \tag{1.63}$$

$$w^5 + 3w = 4\sqrt{\frac{2}{\pi}}N|a| \tag{1.64}$$

When the equations to the first and the second derivate (1.62) and (1.64) are equal to each other, the critical variational parameter is

$$w_c = \left(\frac{1}{5}\right)^{1/4} \tag{1.65}$$

Using this critical parameter in (1.64) the critical value of particle number is given by

$$N_c|a| = \frac{1}{4}\sqrt{\frac{\pi}{2}}\left[\left(\frac{1}{5}\right)^{5/4} + 3\left(\frac{1}{5}\right)^{1/4}\right] \tag{1.66}$$

Thus, [2, 3, 25]

$$N_c|a| = \frac{(8\pi)^{1/2}}{5^{5/4}} \approx 0.671 \tag{1.67}$$

A numerical integration of the GPE gives $N_c|a| = 0.575$ [28, 29]. The other hand, when the spherical trap frequency is different to 1, the critical parameter is given by $N_c|a| \approx 0.671/\omega_\perp^{1/2}$.

1.4.2 The Thomas–Fermi approximation

For a harmonic trap with large number of atoms (or for sufficiently large clouds) and repulsive interactions the atoms are pushed outwards, the central density becomes rather flat and the radius grows. As a consequence, the term in the GPE proportional to $N|\nabla\Psi(\mathbf{r})|^2$, i.e. the kinetic energy of the condensate takes a significant contribution only near the boundary and becomes less important with respect to the interaction energy inside the atomic cloud where the gradients of the wave function are small, in other words, the kinetic energy is small compared with other energies and thus an analytical wave function to the condensate may be obtained by solving the GPE without this term. This regime is called the Thomas-Fermi approximation (TF) [2, 3, 4]. Now the time independent GPE (1.29) has the solution

$$n(\mathbf{r}) = N|\Psi(\mathbf{r})|^2 = \frac{\mu - V(\mathbf{r})}{4\pi a} \tag{1.68}$$

This equation is valid when $n(\mathbf{r}) > 0$ and it gives the size of the cloud if $\mu = V(\mathbf{r})$. Therefore the energy to add a particle at any point in the cloud is the same everywhere and the density profile is completely determined by the trapping potential.

In the TF approximation for a spherical trap, the energy can be calculated as follows. In this approximation the radius of the condensate is defined by R and it is obtained using the harmonic potential (1.56) and the condition $\mu = V(\mathbf{r})$, so

$$R^2 = 2\mu \tag{1.69}$$

According to the normalization condition of the wave function (1.24) the chemical potential is fixed and it is relationed with the total number of particles

$$\begin{aligned} N &= \int d\mathbf{r}\, N|\Psi(\mathbf{r})|^2 \\ &= \frac{\mu}{4\pi a}\int d\mathbf{r}\left(1 - \frac{V}{\mu}\right) \\ &= \frac{\mu}{4\pi a}\int d\mathbf{r}\left[1 - \frac{r^2}{R^2}\right] \end{aligned}$$

Integrating inside a sphere of radius R

$$1 = \frac{\mu}{4\pi a N}\left[\frac{4}{3}\pi R^3 - \frac{4}{5}\pi R^3\right] = \frac{2}{15}\frac{\mu}{aN}R^3 \tag{1.70}$$

and using (1.69)

$$1 = \frac{2}{15}\frac{\mu}{aN}(2\mu)^{3/2} \tag{1.71}$$

the chemical potential is

$$\mu = \frac{15^{2/5}}{2}(Na)^{2/5} \tag{1.72}$$

The Figure (1.2) compares the trial wave function in the variational study (1.52) for a variational parameter equal to 1, with the TF solution (1.68) for a spherical trap (1.56) and using the chemical potential given by (1.72). In the TF regime the condensate has well defined edges and from the chemical potential (1.72), the radius of the condensate (1.69) can be given in terms of the strength of the atom-atom interaction Na as

$$R = (15Na)^{1/5} \tag{1.73}$$

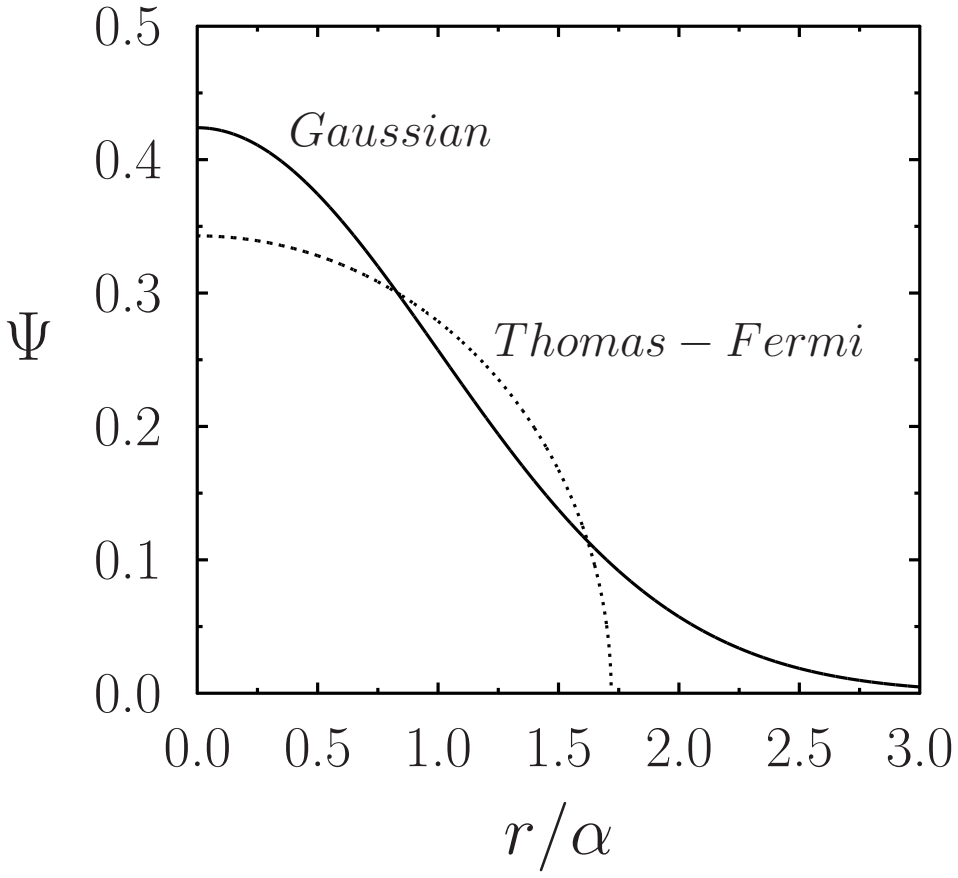

Figure 1.2: The full line is the ground state wave function for the Gaussian variational solution and the dotted line is the TF approximation to an isotropic harmonic oscillator potential. The wave functions are in units $\alpha = (Na)^{1/5}$, thus the variable change is $\Psi\alpha^{3/2} \to \Psi$.

The energy of the condensate in the TF approximation can be calculated according to the usual thermodynamic relation $\mu = \partial E/\partial N$ from (1.72)

$$E = \frac{(15a)^{2/5}}{2}\int_0^N dN'\, N'^{2/5} = \frac{5}{7}\frac{(15a)^{2/5}}{2}N^{7/5} \tag{1.74}$$

The energy per particle can be written like

$$\frac{E}{N} = \frac{5}{7}\frac{(15)^{2/5}}{2}\,(Na)^{2/5} \tag{1.75}$$

So in terms of the chemical potential (1.72) the energy per particle in the TF regime has the form [2]

$$\frac{E}{N} = \frac{5}{7}\mu \tag{1.76}$$

Now is compared the TF energy (1.75) with the TF energy calculated using the variational approximation. From variational approach the TF energy is obtained neglecting the kinetic term (proportional to $1/w^2$) in the energy (1.59) and minimizing this energy

respect to the variational parameter. The minimization is given in the same way as the equation (1.62), thus

$$w^5 = \sqrt{\frac{2}{\pi}} Na \tag{1.77}$$

Then, the energy per particle for the TF approximation turns into

$$\frac{E}{N} = \frac{3}{4}\left(\frac{2}{\pi}\right)^{1/5}(Na)^{2/5} + \frac{1}{2}\left(\frac{2}{\pi}\right)^{1/5}(Na)^{2/5} \tag{1.78}$$

$$\frac{E}{N} = \frac{5}{4}\left(\frac{2}{\pi}\right)^{1/5}(Na)^{2/5} \tag{1.79}$$

In the Figure (1.3) the minimum energy per particle in the TF regime obtained from the variational approximation (1.79) within the range of stability $Na \geq -0{,}67$ is compared with the TF approximation (1.75). From these results, the TF energy per particle in the variational treatment is greater than the TF energy (1.75) as expected. The rate is given by a factor $7/\left(3600\pi\right)^{1/5} \approx 1{,}08$.

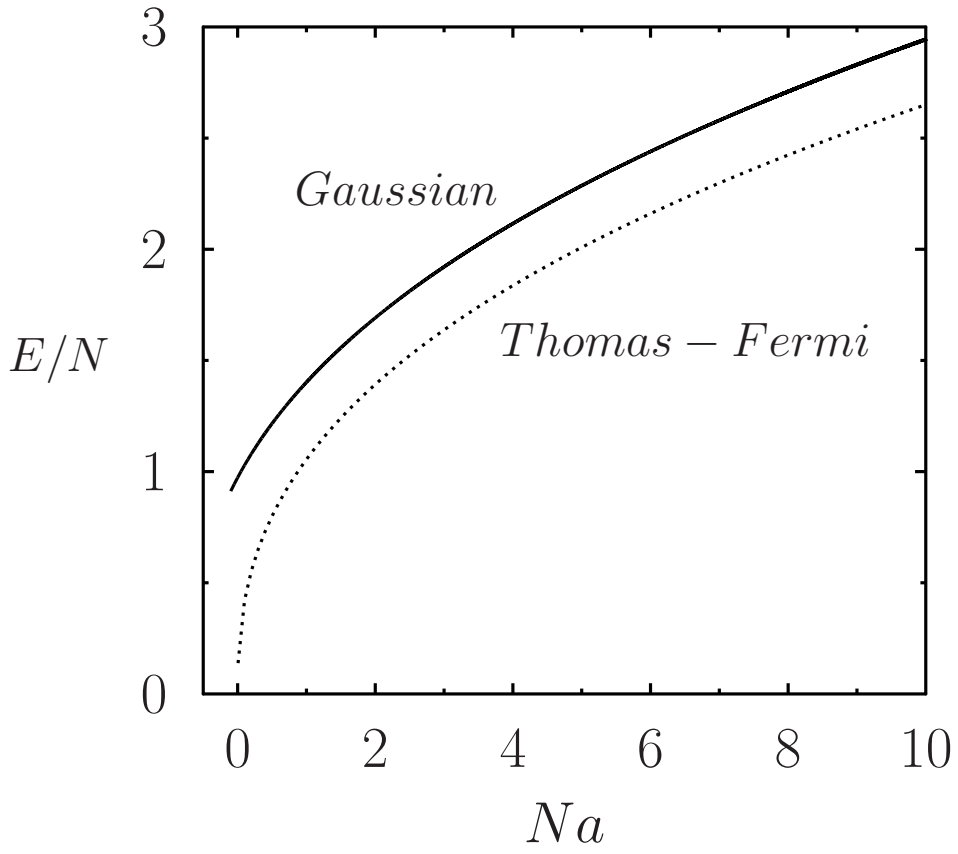

Figure 1.3: Energy per particle in the TF approximation obtained from the variational treatment (1.79) and the dotted line corresponds to the TF approximation (1.75).

The TF approximation lets see how the total energy is distributed between potential and interaction energies. For this is necesary insert the TF solution (1.68) with a spherical potential (1.56) into the energies in (1.35) and (1.36), neglecting the kinetic contribution (1.34). So

$$E_{int} = 2\pi a \int d\mathbf{r}\, N^2 \left|\Psi\left(\mathbf{r}\right)\right|^4 = \frac{1}{8\pi a}\int d\mathbf{r}\, \left(\mu^2 - 2\mu V + V^2\right) \tag{1.80}$$

Using the volume integral in a spherical coordinates with radius R. To the first term

$$\mu^2 \int d\mathbf{r}\, = \frac{4\pi}{3}\mu^2 R^3 \tag{1.81}$$

To the second one

$$2\mu \int d\mathbf{r}\, V = 4\pi\mu \int dr\, r^4 = \frac{8\pi}{5}\mu^2 R^3 \tag{1.82}$$

To the third one

$$\int d\mathbf{r}\, V^2 = \pi \int dr\, r^6 = \frac{\pi}{7}R^7 = \frac{4}{7}\pi\mu^2 R^3 \tag{1.83}$$

Adding those three contributions the resulting interaction energy per particle is

$$E_{int} = \frac{4}{105}\left(\frac{\mu^2 R^3}{a}\right) \tag{1.84}$$

In a same way the trap energy or the oscillator energy per particle is

$$E_{trap} = \int d\mathbf{r}\, V\left(\mathbf{r}\right) N \left|\Psi\left(\mathbf{r}\right)\right|^2 = \int d\mathbf{r}\, V\left(\mathbf{r}\right)\left[\frac{\mu - V\left(\mathbf{r}\right)}{4\pi a}\right] = \frac{2}{35}\left(\frac{\mu^2 R^3}{a}\right) \tag{1.85}$$

The ratio between these energies is given by

$$\frac{E_{int}}{E_{trap}} = \frac{2}{3} \tag{1.86}$$

Since the total energy in the TF approximation is $E = 5\mu/7$ (1.76) and

$$E = E_{int} + E_{trap} \tag{1.87}$$

Furthermore, using the ratio between interaction and trap energy (1.86) the energy distribution in the TF approximation is

$$E_{int} = \frac{2}{7}\mu \qquad\qquad E_{trap} = \frac{3}{7}\mu \tag{1.88}$$

Chapter 2

The hydrodynamic theory of a BEC

The collective modes and the expansion of the condensed cloud when released from a trap are important sources of physical information for a better description of the BEC. The behavior of these phenomena is investigated by means of the time-dependent GPE [2, 4]. Using this mean-field equation (1.21) may be derived useful equations very similar to those of classical hydrodynamics that represent the conservation laws for the number of particles and the total momentum (an extensive description about the hydrodynamic in a condensate may be found in [13]).

2.1 The hydrodynamic equations

The hydrodynamic as macroscopic theory can be used to studying the superfluid behavior at zero temperature of a BEC. The link between a superfluid and a condensate is given by means of the definition of the superfluid velocity [19]. Nevertheless, in the hydrodynamic description it is not appropriate to deal with the time-dependent GPE to research the superfluid macroscopic state, instead it is better to use equivalent equations for the density and the gradient phase [9].

The mean-field GPE has like a conserved quantity the total number of particles such that $dN/dt = 0$, therefore it is possible considering a continuity equation reflecting this fact. Thus performing the product of the time-dependent GPE (1.21) by $N\Psi^*(\mathbf{r}, t)$ and subtracting the complex conjugate of the new equation it is obtained the continuity equation

$$\frac{\partial}{\partial t}\left(N\left|\Psi\right|^2\right) - \frac{i}{2}\nabla\cdot\left[N\left(\Psi^*\nabla\Psi - \Psi\nabla\Psi^*\right)\right] \;=\; 0 \tag{2.1}$$

with the particles density $n = N\left|\Psi\right|^2$. Defining the local velocity as

$$\mathbf{v} \;=\; -\frac{i}{2}\frac{\left(\Psi^*\nabla\Psi - \Psi\nabla\Psi^*\right)}{\left|\Psi\right|^2} \tag{2.2}$$

and the particle current density $\mathbf{j} = n\mathbf{v}$, the continuity equation turns into

$$\frac{\partial n}{\partial t} + \nabla \cdot \mathbf{j} = 0 \tag{2.3}$$

The density may be obtained using the ansatz $\Psi(\mathbf{r},t) = [n(\mathbf{r},t)/N]^{1/2} \exp[i\phi(\mathbf{r},t)]$ (the phase $\phi(\mathbf{r},t)$ is a real quantity) on the GPE (1.21) such that

$$\begin{aligned} i\left[\frac{\partial\sqrt{n}}{\partial t}e^{i\phi} + i\sqrt{n}\frac{\partial\phi}{\partial t}e^{i\phi}\right] &= -\frac{1}{2}\left\{\nabla\left[\left(\nabla\sqrt{n}\right)e^{i\phi} + i\sqrt{n}\left(\nabla\phi\right)e^{i\phi}\right]\right\} + \left(V + 4\pi an\right)\sqrt{n}e^{i\phi} \\ &= -\frac{1}{2}\left\{\left(\nabla^2\sqrt{n}\right)e^{i\phi} + i\left(\nabla\phi\nabla\sqrt{n}\right)e^{i\phi} + i\left[\left(\nabla\phi\nabla\sqrt{n}\right)e^{i\phi}\right.\right. \\ &\quad \left.\left. + \sqrt{n}\left(\nabla^2\phi + i\left(\nabla\phi\right)^2\right)e^{i\phi}\right]\right\} + \left(V + 4\pi an\right)\sqrt{n}e^{i\phi} \end{aligned} \tag{2.4}$$

As the GPE is a complex equation it can be separated in a real and an imaginary part. The real contribution is given by

$$-\frac{\partial\phi}{\partial t} = -\frac{1}{2\sqrt{n}}\nabla^2\sqrt{n} + \frac{1}{2}\left(\nabla\phi\right)^2 + V + 4\pi an \tag{2.5}$$

Introducing the ansatz $\Psi(\mathbf{r},t) = (n(\mathbf{r},t)/N)^{1/2} \exp[i\phi(\mathbf{r},t)]$ in the momentum density $\mathbf{j} = n\mathbf{v}$ the condensed velocity can be defined like

$$\mathbf{v}(\mathbf{r},t) = \nabla\phi(\mathbf{r},t) \tag{2.6}$$

This velocity characterizes the behavior of a macroscopic number of particles (the condensate) and it can thus be regarded as a classical quantity. So the real contribution becomes [2]

$$-\frac{\partial\phi}{\partial t} = -\frac{1}{2\sqrt{n}}\nabla^2\sqrt{n} + \frac{1}{2}v^2 + V + 4\pi an \tag{2.7}$$

According to the velocity (2.6), the motion of the condensate can be interpreted like a potential flow*. If the condensed phase $\phi(\mathbf{r},t)$ is not singular (this condition is not fulfilled for the core of a vortex line) the motion of the condensate is irrotational

$$\nabla \times \mathbf{v} = \nabla \times \nabla\phi = 0 \tag{2.8}$$

Now, the imaginary part in the GPE turns into

$$\frac{\partial\sqrt{n}}{\partial t} = -\frac{1}{2}\left(2\nabla\sqrt{n}\,\nabla\phi + \sqrt{n}\nabla^2\phi\right) \tag{2.9}$$

Multiplicand both side by $\sqrt{n}$, then

$$\frac{1}{2}\frac{\partial n}{\partial t} = -\frac{1}{2}\left[\nabla n\,\nabla\phi + n\nabla^2\phi\right] \tag{2.10}$$

*Since the velocity is the gradient of a scalar quantity, which is referred to as the velocity potential.

and with the property $\nabla n\,\nabla\phi = \nabla\left(n\nabla\phi\right) - n\nabla^2\phi$ the imaginary part in the GPE is [2]

$$\frac{\partial n}{\partial t} = -\nabla\left(n\nabla\phi\right) \tag{2.11}$$

The motion equation for the velocity is obtained taking the gradient to the real part (2.7) and using the velocity definition (2.6). So

$$\frac{\partial \mathbf{v}}{\partial t} = -\nabla\left[\frac{1}{2}v^2 + V + 4\pi a n - \frac{1}{2\sqrt{n}}\nabla^2\sqrt{n}\right] \tag{2.12}$$

It is more useful converting the hydrodynamics equations of the condensate as follows, with the purpose of contrasting these with the classical hydrodynamic equations. So from the thermodynamic Gibbs–Duhem relation $dp = nd\mu$ in an uniform Bose gas with chemical potential $\mu = 4\pi a n$ the pressure is $p = 2\pi a n^2$. Thus, $4\pi a\nabla n = \nabla p/n$ and the equation (2.12) takes the form

$$\frac{\partial \mathbf{v}}{\partial t} = -\frac{1}{n}\nabla p - \nabla\left(\frac{v^2}{2}\right) + \nabla\left(\frac{1}{2\sqrt{n}}\nabla^2\sqrt{n}\right) - \nabla V \tag{2.13}$$

The continuity equation (2.3) has the same form that for an ideal fluid, while the equation (2.13) is analogue to Euler equation

$$\frac{\partial \mathbf{v}}{\partial t} + \left(\mathbf{v}\cdot\nabla\right)\mathbf{v} + \frac{1}{n}\nabla p = -\nabla V \tag{2.14}$$

Or using the vector identity

$$\nabla\left(\mathbf{A}\cdot\mathbf{B}\right) = \left(\mathbf{A}\cdot\nabla\right)\mathbf{B} + \left(\mathbf{B}\cdot\nabla\right)\mathbf{A} + \mathbf{A}\times\left(\nabla\times\mathbf{B}\right) + \mathbf{B}\times\left(\nabla\times\mathbf{A}\right) \tag{2.15}$$

when $\mathbf{A} = \mathbf{B} = \mathbf{v}$

$$\mathbf{v}\times\left(\nabla\times\mathbf{v}\right) = \nabla\left(\frac{v^2}{2}\right) - \left(\mathbf{v}\cdot\nabla\right)\mathbf{v} \tag{2.16}$$

So the Euler equation takes the form

$$\frac{\partial \mathbf{v}}{\partial t} - \mathbf{v}\times\left(\nabla\times\mathbf{v}\right) = -\frac{1}{n}\nabla p - \nabla\left(\frac{v^2}{2}\right) - \nabla V \tag{2.17}$$

There exist two differences between the condensate velocity equation (2.13) and the Euler equation for an ideal fluid (2.17) [2]. The first one is that the potential flow to BEC is zero. In second place, the third term in the right hand of (2.13) is referred as the quantum pressure. This term describes forces due to spatial variations in the magnitude of the wave function for the condensed state i.e., it is arising from inhomogeneities in the density and vanishes in the limit of BECs containing a large number of atoms or TF regime. Its origin is the kinetic energy term in the GPE like happens to $\nabla\left(v^2/2\right)$ but with physical meaning

different. The quantum pressure $\left(\nabla\sqrt{n}\right)^2/2$ is refered to 'zero-point motion', which it is not produced because of the particle currents, and $\nabla\left(v^2/2\right)$ is referred to the kinetic energy of the particles motion. Definining the spatial scale of variations for the wave function like l, in the motion equation (2.13) the quantum pressure is of order $1/l^3$, and the pressure term is of order $4\pi an/l$. So the usual pressure dominates on larger scales and the dynamics of the condensate can be described by the classical hydrodynamic equation. The quantum pressure dominates when the spatial variations of the density occur on length scales l less than order of the coherence length† $\xi = (8\pi an)^{-1/2}$. As it was described above, at zero temperature the motion of the condensate may be specified in terms of a local density and a local velocity. The equations of motion are very similar to those of a ideal fluid expressing thus the conservation of the particle number and the total momentum.

2.2 Elementary excitations

The properties of elementary excitations may be investigated using the hydrodynamic formulation [2, 4]. Writing the density as $n \longrightarrow n_0 + \delta n$, where n_0 is the equilibrium density and δn is the deviation value of this equilibrium. Similarly the velocity potential becomes $\phi \longrightarrow \phi_0 + \delta\phi$. Dealing the velocity and the variation δn as small quantities and linearizing the density in the continuity equation (2.3) and in the Euler equation (2.12), it is possible to get that the continuity equation becomes (2.3)

$$\frac{\partial n_0}{\partial t} + \frac{\partial \delta n}{\partial t} = -\nabla\cdot\left[\left(n_0+\delta n\right)\nabla\left(\phi_0+\delta\phi\right)\right] \tag{2.18}$$

Here $\partial n_0/\partial t = -\nabla\cdot\left(n_0\nabla\phi_0\right)$ and the term $-\nabla\cdot\left[\delta n\,\nabla\left(\phi_0+\delta\phi\right)\right]$ does not contribute in the linearization. So the new continuity equation is

$$\frac{\partial \delta n}{\partial t} = -\nabla\cdot\left(n_0\nabla\delta\phi\right) \tag{2.19}$$

and for the Euler equation (2.12) the phase ϕ_0 is time constant and the velocity squared does not contribute, so

$$\frac{\partial}{\partial t}\left(\nabla\delta\phi\right) = -\nabla\delta\tilde{\mu} \tag{2.20}$$

where $\delta\tilde{\mu}$ is achieved by the linearization of $\tilde{\mu}$ [9] with

$$\tilde{\mu} = V + 4\pi an - \frac{1}{2\sqrt{n}}\nabla^2\sqrt{n} \tag{2.21}$$

†If a uniform Bose gas is pertudrbed locally, ξ is the length over which the gas heals back to its equilibrium density, and it can be written as $1/\left(2\xi^2\right) = 4\pi an$. In the dilute limit $na^3 \ll 1$, the healing length ξ is large compared to the interparticle spacing $n^{-1/3}$[2, 9, 19].

The motion equation is obtained taking the time derivate in (2.19) and using the Euler equation (2.20). Thus, the equation describing the excitations of a Bose gas in an arbitrary potential is

$$\frac{\partial^2 \delta n}{\partial t^2} = \nabla \cdot (n_0 \nabla \delta\tilde{\mu}) \tag{2.22}$$

A uniform gas

In this section, it will be investigated the spectrum energy of a homogeneous BEC where the external potential is constant. The solutions sought are travelling wave such that $\delta n \rightarrow \delta n\, exp\,(i\mathbf{q}.\mathbf{r} - i\omega t)$ where $\mathbf{q}$ is the wave vector and ω the frequency. Henceforth neglecting the zero-temperature depletion and to keeping the notation simple will be denoting the density of the equilibrium by n [2]. For the motion equation the term $\delta\tilde{\mu}$ can be written like

$$\begin{aligned} \delta\tilde{\mu} &= 4\pi a\delta n - \frac{1}{2}\left[\delta\left(\frac{1}{\sqrt{n}}\right)\nabla^2\sqrt{n} + \frac{1}{\sqrt{n}}\delta\left(\nabla^2\sqrt{n}\right)\right] \\ &= 4\pi a\delta n - \frac{1}{2}\left[-\frac{\nabla^2\sqrt{n}}{2n^{3/2}}\delta n + \frac{1}{\sqrt{n}}\nabla^2\left(\frac{\delta n}{2\sqrt{n}}\right)\right] \end{aligned} \tag{2.23}$$

Where $\sqrt{n}$ is constant because in the unperturbed state the density is the same everywhere. From the solution to δn then $\nabla^2(\delta n) = (iq)^2\,\delta n$, thus

$$\delta\tilde{\mu} = 4\pi a\delta n - \frac{1}{2}\left[\frac{1}{2n}\nabla^2(\delta n)\right] = 4\pi a\delta n - \frac{1}{2}\left[\frac{(iq)^2}{2n}\delta n\right] \tag{2.24}$$

$$\delta\tilde{\mu} = \left(4\pi a + \frac{q^2}{4n}\right)\delta n \tag{2.25}$$

and the equation of motion (2.22) takes the form

$$\frac{\partial^2 \delta n}{\partial t^2} = n\nabla^2(\delta\tilde{\mu}) \tag{2.26}$$

or

$$\omega^2 = \left(4\pi a n q^2 + \frac{q^4}{4}\right) \tag{2.27}$$

With possible solutions only if $\omega = \pm\epsilon_q$. Taking just the positive values and defining $\epsilon_q^0 = q^2/2$ as the free particle energy, the energy spectrum is [2, 9]

$$\epsilon_q = \sqrt{8\pi a n \epsilon_q^0 + \left(\epsilon_q^0\right)^2} \tag{2.28}$$

The Figure (2.1) illustrates the excitation spectrum (2.28) for repulsive interactions ($a > 0$) and the respective approach for long (2.29) and short (2.30) wavelengths. For small wave number q, the spectrum is sound-like

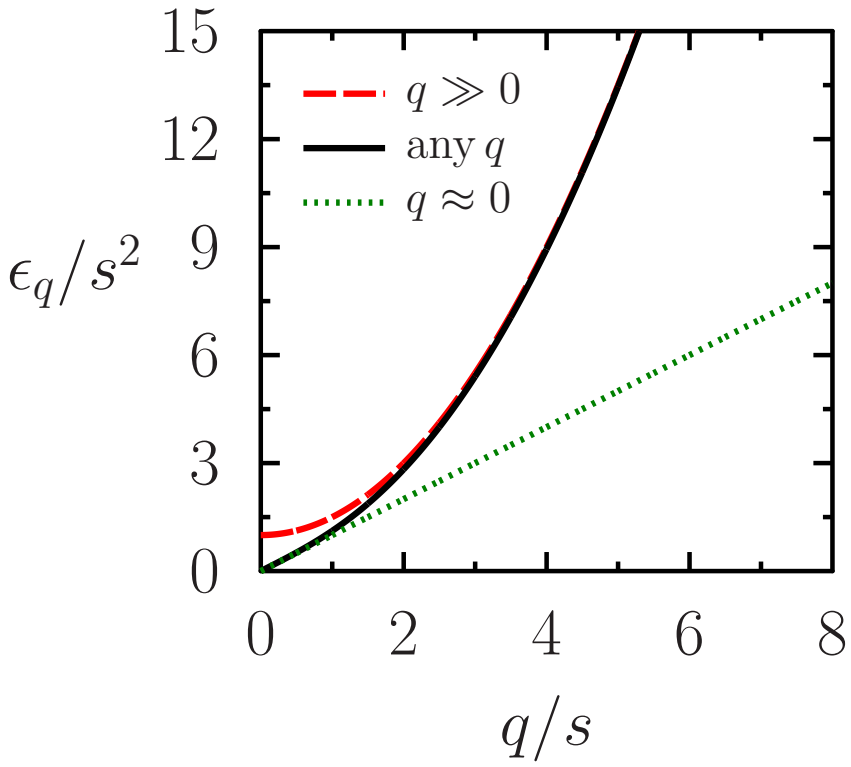

Figure 2.1: Dispersion of elementary excitations for repulsive interactions. The black line (solid curve) corresponds to the excitation spectrum of a homogeneous Bose gas as function of the dimensionless wave number q/s. The red line (dashed curve) shows the espectrum for long wave number. The green line (dotted curve) is the approach to short wave number.

$$\epsilon_q \approx sq \tag{2.29}$$

with the sound velocity $s = \sqrt{4\pi an}$ [‡], which matches with the Bogoliubov results [30]. According to the above results the energy spectrum at long wavelengths is quadratic in q for free particles and lineal when the repulsive interaction is present, agreement with experimental observations in liquid ^{4}He. The transition between the linear and the quadratic spectrum occurs when the two pressures are very close, in other words, the kinetic energy is approximately equal to the interaction term, so $q^2/2 \sim 4\pi an$, or $q = (8\pi an)^{1/2} = \sqrt{2}\xi^{-1}$. For length scales longer than ξ atoms move collectively and for shorter length scales these behave as free particles [2].

In the short wavelengths approximation the contribution at the energy spectrum is given by the free-particle spectrum plus a mean field shift.

$$\epsilon_q = \epsilon_q^0 \left(1 + \frac{8\pi an}{\epsilon_q^0}\right)^{1/2} \approx \epsilon_q^0 \left[1 + \frac{1}{2}\left(\frac{8\pi an}{\epsilon_q^0}\right) + ...\right] = \epsilon_q^0 + 4\pi an \tag{2.30}$$

Or in terms of the sound velocity is

[‡]The speed of sound becomes purely imaginary for attractive interaction and it implies instability. A condensate with attractive interaction is stable by balancing the kinetic energy with the interaction.

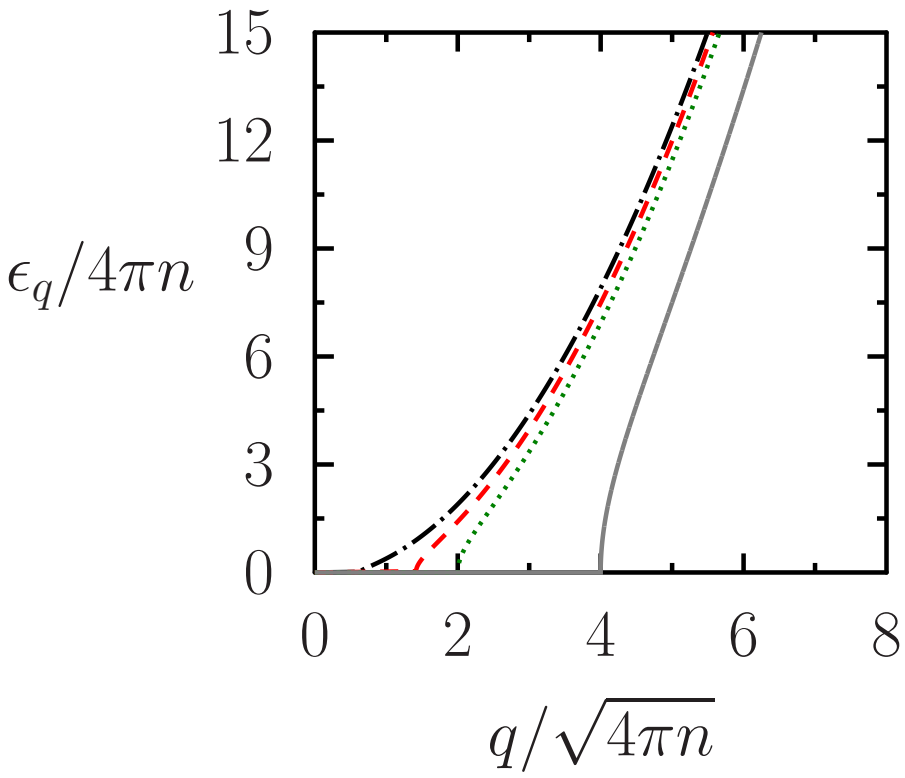

Figure 2.2: Excitation spectrum of a homogeneous Bose gas with attractive interactions $a < 0$. The black dashed and dotted line corresponds to the $|a| = 0,1$ value. The red dashed line is for $|a| = 0,5$. The green dotted line is for $|a| = 1,0$. The gray solid line is for $|a| = 4,0$.

$$\epsilon_q \approx \epsilon_q^0 + s^2 \tag{2.31}$$

A relevant feature for large wavenumbers and attractive stage ($a < 0$) is the possibility of having a real energy. So the modes are stable, since the free particle kinetic energy term dominates in the dispersion relation [2] fulfilling the condition.

$$q \geq \sqrt{8\pi n\,|a|} \tag{2.32}$$

or

$$q \geq \sqrt{2}\,|s| \tag{2.33}$$

and the new spectrum is

$$\epsilon_q \approx \epsilon_q^0 - 4\pi\,|a|\,n \tag{2.34}$$

The other hand, the general spectrum (2.28) with attractive interactions ($a < 0$) is real (Figure 2.2) fulfilling the same condition (2.32).

Chapter 3

Dipolar Bose-Einstein condensate

At short distances the interaction between atoms in a condensate is characterized essentially by a single parameter, the scattering length a. Nevertheless, the dilute quantum degenerate gases with dipole dipole interaction (mainly with magnetic dipole moment in atomic systems and recently molecular systems proposed with electric dipole moment) have attracted much attention in the last decade [11, 12, 13, 31, 32, 33, 34, 35, 36, 37] due to the possibility to handling systems of many particles with long-range anisotropic interactions, in both weak and strong regime. Whereas the dipole moments are sufficiently large, the resulting interaction may even completely change the properties of the condensate. The first experimental studies of dipolar effects in a BEC were carried out in ^{52}Cr [10] which has a large intrinsic magnetic dipole moment $m = 6\mu_B$, (μ_B is the Bohr magneton) six times larger than the alkali atoms. Later, Lev and co-workers achieved a dipolar condensate of ^{164}Dy with a dipole moment $m = 10\mu_B$ [38]. Recently, power-

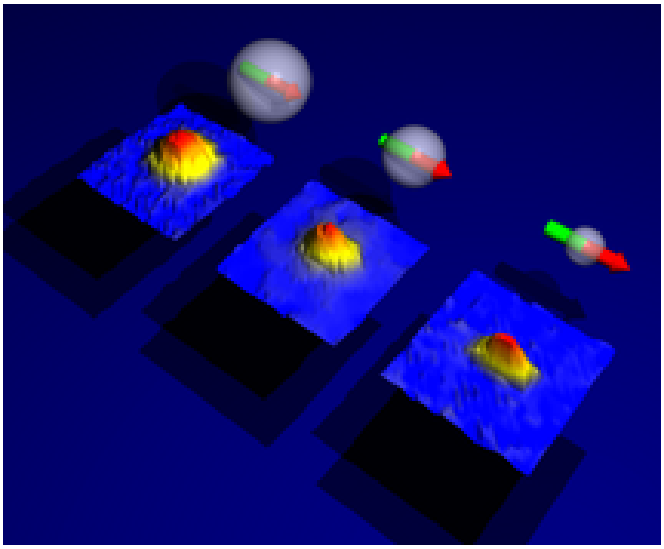

Figure 3.1: Effect observed on a BEC due to the anisotropy of the dipole dipole interaction (http://www.pi5.uni-stuttgart.de/en/research/projects.php/A/#6). While the magnetic dipole moment (arrow) remains constant and the contact interaction (sphere) is reduced, the condensate undergoes an elongation along the magnetization direction. (The color is not real in the experimental images bottom).

ful laser techniques have created bosonic heteronuclear polar molecules such as $^{40}K^{87}Rb$ [39, 40] with large electric dipole moments. The physical effect observed in the BEC with dipolar interaction elongates the cloud along the direction in which the dipoles are aligned (Figure 3.1). This Chapter introduces the two main features of the dipolar interaction, the long-range character and the anisotropy. Likewise is analyzed the effect of the new interaction in the TF approximation with a spherical trap by means of the dipolar GPE. The last part of the Chapter is devoted to the hydrodynamic description of a dipolar condensate displaying that some of the different intervals existence in the spectrum of energy of a homogeneous dipolar condensate contrasting with the non-dipolar stage.

3.1 Magnetic and Electric dipole dipole interaction

The dipole dipole interaction can be obtained like a generalization of magnetic and electric dipolar interaction.

3.1.1 Magnetic dipole dipole interaction.

The dipolar contribution to the magnetic case is determined in the expansion of the vector potential as [41, 42]

$$\mathbf{A}(\mathbf{r}) = \frac{\mu_0}{4\pi}\frac{\mathbf{m}\times\hat{\mathbf{r}}}{r^2} \tag{3.1}$$

where μ_0 is the permeability of vacuum and $\mathbf{m}$ is the magnetic dipole moment. The ideal magnetic field for a dipole is easiest to calculate when $\mathbf{m}$ is at the origin in the z direction (Figure 3.2). Then, the vector potential at point (r, θ, φ) is

$$\mathbf{A}(\mathbf{r}) = \frac{\mu_0}{4\pi}\frac{m\sin\theta}{r^2}\hat{\boldsymbol{\varphi}} \tag{3.2}$$

and hence in spherical coordinates the magnetic field becomes

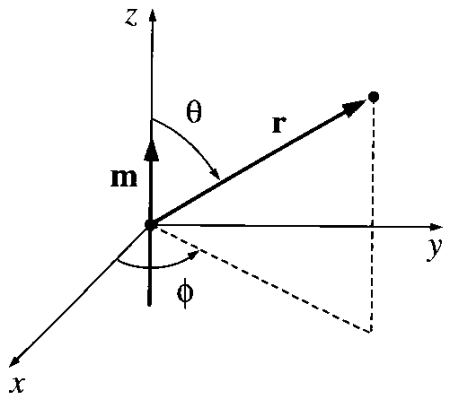

Figure 3.2: Magnetic dipole moment in the z axis [41].

$$\mathbf{B}(\mathbf{r}) = \nabla \times \mathbf{A}(\mathbf{r}) = \frac{\mu_0 m}{4\pi r^3}\left(2\cos\theta\hat{\mathbf{r}} + \sin\theta\hat{\boldsymbol{\theta}}\right) \tag{3.3}$$

For a coordinate free system the magnetic field can be read as

$$\mathbf{B}(\mathbf{r}) = \frac{\mu_0}{4\pi}\left[\frac{3(\mathbf{m}.\hat{\mathbf{r}})\,\hat{\mathbf{r}} - \mathbf{m}}{r^3}\right] \tag{3.4}$$

Here, was used the geometry of Figure (3.2) where the decomposition of the magnetic dipole moment $\mathbf{m}$ on radial $\hat{\mathbf{r}}$ and angular $\hat{\boldsymbol{\theta}}$ axes is

$$\mathbf{m} = m\left(\cos\theta\hat{\mathbf{r}} - \sin\theta\hat{\boldsymbol{\theta}}\right) \tag{3.5}$$

so the term $m\left(2\cos\theta\hat{\mathbf{r}} + \sin\theta\hat{\boldsymbol{\theta}}\right) = 3(\mathbf{m}.\hat{\mathbf{r}})\,\hat{\mathbf{r}} - \mathbf{m}$. In this way the interaction energy between two magnetic dipoles $U_m = -\mathbf{m}.\mathbf{B}(\mathbf{r})$ obeys the equation

$$U_m = \frac{\mu_0}{4\pi}\left[\frac{\mathbf{m}_1.\mathbf{m}_2 - 3(\mathbf{m}_1.\hat{\mathbf{r}}_{12})(\mathbf{m}_2.\hat{\mathbf{r}}_{12})}{r_{12}^3}\right] \tag{3.6}$$

with $\mathbf{r}_{12} = \mathbf{r}_1 - \mathbf{r}_2$ the vector joining the two dipoles.

3.1.2 Electric dipole dipole interaction.

In SI units, the dipolar term in the expansion for the electrostatic potential in rectangular coordinates is given by [9, 41, 42]

$$\phi(\mathbf{r}) = \frac{\mathbf{p}.\mathbf{r}}{4\pi\varepsilon_0\mathbf{r}^3} \tag{3.7}$$

with ε_0 the permittivity of vacuum and $\mathbf{p}$ the electric dipole moment. Now, taking the momentum lies at the origin and in the z axis (Figure 3.3)

$$\phi(r,\theta) = \frac{\mathbf{p}.\hat{\mathbf{r}}}{4\pi\varepsilon_0\mathbf{r}^3} = \frac{p\cos\theta}{4\pi\varepsilon_0 r^2} \tag{3.8}$$

and the corresponding electric field in spherical coordinates is

$$\mathbf{E} = E_r\hat{\mathbf{r}} + E_\theta\hat{\boldsymbol{\theta}} + E_\varphi\hat{\boldsymbol{\varphi}} \tag{3.9}$$

with components

$$E_r = -\frac{\partial\phi}{\partial r} = \frac{2p\cos\theta}{4\pi\varepsilon_0 r^3} \qquad E_\theta = -\frac{1}{r}\frac{\partial\phi}{\partial\theta} = \frac{p\sin\theta}{4\pi\varepsilon_0 r^3} \qquad E_\varphi = -\frac{1}{r\sin\theta}\frac{\partial\phi}{\partial\varphi} = 0 \tag{3.10}$$

Thereby the electric field turns out

$$\mathbf{E} = \frac{2p\cos\theta\hat{\mathbf{r}} + p\sin\theta\hat{\boldsymbol{\theta}}}{4\pi\varepsilon_0 r^3} \tag{3.11}$$

It is worth noting that this electric field is an approach to the physical dipolar electric field only if $\mathbf{r} \ggg \mathbf{d}$ with the $\mathbf{d}$ the separation between charges [41].

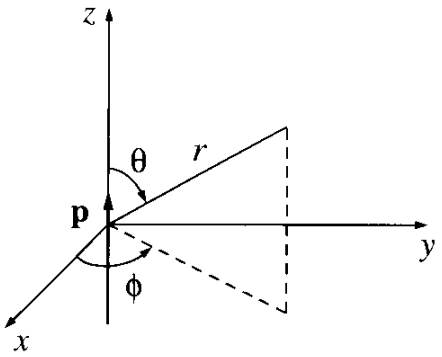

Figure 3.3: Electric dipole moment in the z axis [41].

This equation is identical in structure to the field of a magntetic dipole (3.3). In a same way like was done to the dipolar magnetic field, from the geometry of the Figure (3.3) the dipolar electric field can be generalized as

$$\mathbf{E}(\mathbf{r}) = \frac{3(\mathbf{p}.\hat{\mathbf{r}})\,\hat{\mathbf{r}} - \mathbf{p}}{4\pi\varepsilon_0 r^3} \tag{3.12}$$

and the corresponding energy between two electric dipoles $U_e = -\mathbf{p}.\mathbf{E}(\mathbf{r})$ obeys the equation

$$U_e = \frac{\mathbf{p}_1.\mathbf{p}_2 - 3(\mathbf{p}_1.\hat{\mathbf{r}}_{12})(\mathbf{p}_2.\hat{\mathbf{r}}_{12})}{4\pi\varepsilon_0 r_{12}^3} \tag{3.13}$$

with $\mathbf{r}_{12} = \mathbf{r}_1 - \mathbf{r}_2$ the vector joining the two dipoles.

3.2 Dipolar interaction

According both energies, the dipolar magnetic (3.6) and the dipolar electric (3.13), for two particles 1 and 2 with dipole moments along the unit vectors $\mathbf{e}_i = \mathbf{r}_i/r_i$ $(i = 1, 2)$ and whose relative position is $\mathbf{r} = |\mathbf{r}_1 - \mathbf{r}_2|$ (Figure 3.4 (a)) the dipole dipole interaction energy is read as [9, 11, 13]

$$U_{dd}(\mathbf{r}) = \frac{C_{dd}}{4\pi}\left[\frac{(\boldsymbol{e}_1.\boldsymbol{e}_2)\,r^2 - 3(\boldsymbol{e}_1.\mathbf{r})(\boldsymbol{e}_2.\mathbf{r})}{r^5}\right] \tag{3.14}$$

where $C_{dd} = \mu_0 m^2$ for particles having a permanent magnetic dipole moment m and p^2/ε_0 for particles having a permanent electric dipole moment p. To simplify this interaction energy is common to work with a polarized sample where all dipoles point in the same direction z. Thus $\boldsymbol{e}_1.\boldsymbol{e}_2 = 1$ and $\boldsymbol{e}_1.\mathbf{r} = \boldsymbol{e}_2.\mathbf{r} = r\cos\theta$, so the dipole dipole interaction energy takes the form

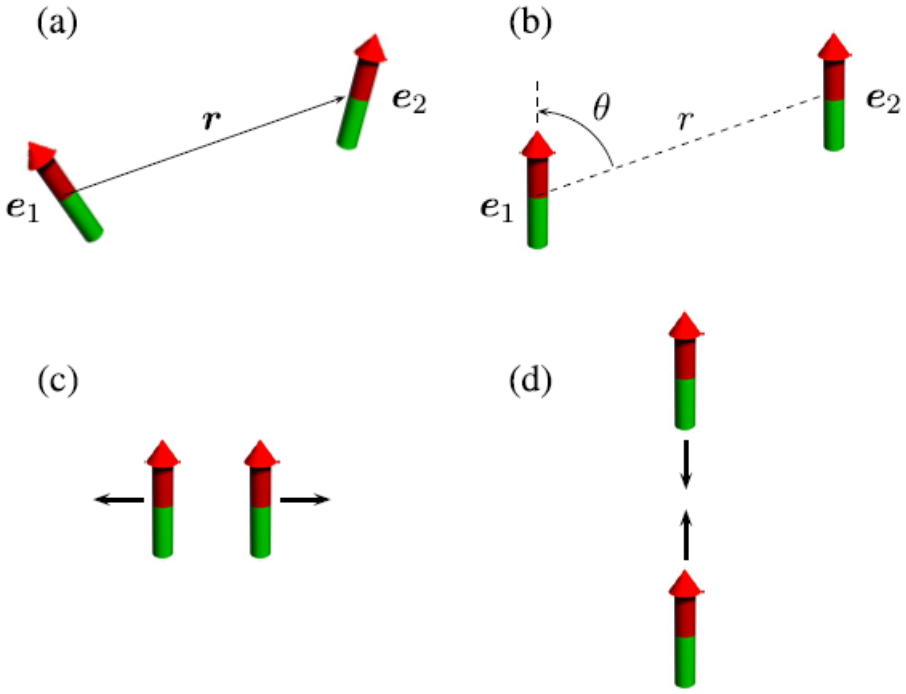

Figure 3.4: Dipole dipole interaction. (a) Non-polarized case. (b) Polarized case. (c) Two polarized dipoles side by side repel each other (black arrows). (d) Two polarized dipoles in a 'head-to-tail' attracting each other (black arrows) [11].

$$U_{dd}(\mathbf{r}) = \frac{C_{dd}}{4\pi}\frac{1-3\cos^2\theta}{r^3} \tag{3.15}$$

with θ the angle between the direction of polarization and the relative position of the particles $\mathbf{r}$ (Figure 3.4 (b)).

The dipole dipole interaction has two main properties, the long-range character r^{-3} and the anisotropy reflected by the angle dependence. Contrasting strongly with the short-range and isotropic behavior from contact interaction $U_{contact}(\mathbf{r}) = g\delta(\mathbf{r}-\mathbf{r}')$.

Long-range character. A way to classify the potential as long or short-range depends on whether the chemical potential is extensive or intensive [11, 43, 44]. Whereas a large system the homogeneous properties can be defined only in terms of the density n, the chemical potential $\mu(n)$ is extensive, thus the potential is short-range. In systems with long-range interactions the energy per particle depends on the density and strongly the total number of particles (such that it is divergent) with $\mu(n, N)$. The convergence of the interaction potential $U(\mathbf{r})$ at larges distances can be verified from the integral

$$I = \int_{r_0}^{\infty} d^D r\, U(\mathbf{r}) = \Omega_{D-1}\int_{r_0}^{\infty} dr\, r^{D-1} U(\mathbf{r}) \tag{3.16}$$

Where D is the dimensionality of the system and r_0 some small cut-off which converges

at large distances. In the present case is necessary to using interactions decaying at long distances as r^{-n}. To consider this kind of interactions as short range, i.e. when the integral I converges, these must decay faster than r^{D-1}, in other words, must be satisfied the condition $D < n$. Therefore, the dipole dipole interaction (3.15) with $n = 3$ is long-range in three dimensions and short-range in one and two dimensions. Alternatively, other method determining the behaviour of a potential implies the solution of the two-body scattering problem for a potential r^{-3} [44]. The short-range potentials can be defined as potentials of range R which can be described at large distances ($r \gg R$) by a free wave with an appropriate phase shift (the s-wave scattering length a). So the explicit solution of the scattering problem for one, two and three dimensions is compared with the solution in terms of a wave plane to the corresponding number of dimensions. The results show that in two dimensions the r^{-3} potential can be treated as a short-range one. In contrast for one and three dimensions the potential can be treated like a long-range one. The two methods lead to different answers for one dimension.

Anisotropy. The dipole dipole interaction (3.15) has the angular symmetry of the Legendre polynomial of second order $P_2(\cos\theta)$ with $0 \leq \theta \leq \pi/2$. Whether $\theta = \pi/2$ so $U_{dd}(\mathbf{r}) > 0$ and if $\theta = 0$ then $U_{dd}(\mathbf{r}) < 0$. Hence the dipole dipole interaction is repulsive for particles sitting side by side, while this is attractive (twice the strength of the previous case, i.e. $|U_{dd}(\theta = 0)| = 2\,|U_{dd}(\theta = \pi/2)|$) for dipoles in a 'head-to-tail' configuration (Figure 3.4 (c) y (d)) respectively [11]. So in a trapped dipolar BEC (DBEC), for the dipoles is energetically more favourable to be aligned. For the special value $\theta = \cos^{-1}\left(1/\sqrt{3}\right)$ the dipole dipole interaction vanishes. Therefore in a real physical system the dipolar interaction elongates the cloud along the direction in which the dipoles are aligned. According to the above a cigar-shaped pure DBEC (Figure 3.5 (a)) undergoes instability and should collapse because of the main effect of the interaction is attractive. Whereas in a disk-shaped pure dipolar condensate the interaction is repulsive and the system should be stable [9, 11] (Figure 3.5 (b)). However, recently a complete numerical solution of the dynamics of a dipolar condensate shows that it is possible the collapse of a strongly disk-shaped due to the long-range anisotropic dipolar interaction [15].

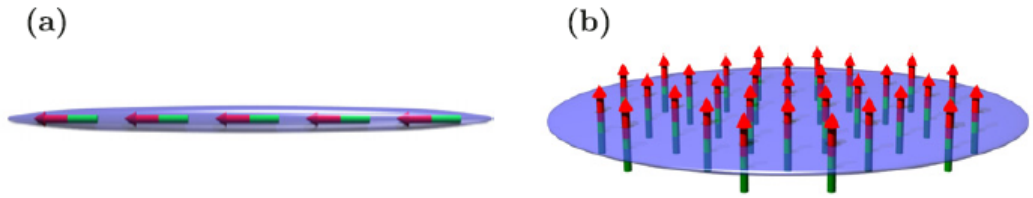

Figure 3.5: Geometric dependence of the stability of a trapped pure dipolar condensate [11]. (a) In a cigar-shaped condensate the dipoles are aligned along the axis of the trap and the effect of the dipole dipole interaction is attractive which leads to an instability. (b) In a pancake-shaped condensate the dipoles are oriented perpendicularly to the confinement axis. In this case with the repulsive dipole dipole interaction the condensate is stable.

3.3 Dipolar Gross-Pitaevski equation

Based on the dipolar interaction (3.15) the hamiltonian operator in second quantization turns out

$$\hat{H}_{dd} = \frac{1}{2}\int d\mathbf{r}d\mathbf{r}'\hat{\Psi}^{\dagger}(\mathbf{r},t)\,\hat{\Psi}^{\dagger}(\mathbf{r}',t)\,U_{dd}(\mathbf{r}-\mathbf{r}')\,\hat{\Psi}(\mathbf{r}',t)\,\hat{\Psi}(\mathbf{r},t) \tag{3.17}$$

with $\mathbf{r}-\mathbf{r}'$ the relative position of the dipoles and

$$U_{dd}(\mathbf{r}-\mathbf{r}') = \frac{C_{dd}}{4\pi}\frac{1-3\cos^2\theta}{|\mathbf{r}-\mathbf{r}'|^3} \tag{3.18}$$

So in a similar way like was obtained the GPE (1.48), the Heisenberg equation (1.45) in the mean-field approximation leads to the corresponding time-dependent GPE with dipolar interaction or DGPE ([2, 9, 11, 13] and references therein)

$$\begin{aligned} i\hbar\frac{\partial\Phi(\tilde{\mathbf{r}},\tau)}{\partial\tau} &= -\frac{\hbar^2}{2m}\nabla^2\Phi(\tilde{\mathbf{r}},\tau) + V(\tilde{\mathbf{r}})\,\Phi(\tilde{\mathbf{r}},\tau) + gN\left|\Phi(\tilde{\mathbf{r}},\tau)\right|^2\Phi(\tilde{\mathbf{r}},\tau) \\ &+ \frac{N\widetilde{C}_{dd}}{4\pi}\int d\tilde{\mathbf{r}}'\left(\frac{1-3\cos^2\theta}{|\tilde{\mathbf{r}}-\tilde{\mathbf{r}}'|^3}\right)\left|\Phi(\tilde{\mathbf{r}}',\tau)\right|^2\Phi(\tilde{\mathbf{r}},\tau) \end{aligned} \tag{3.19}$$

As in the non-dipolar condensate with the variables change $\mathbf{r} = \tilde{\mathbf{r}}/a_{osc}$, $\omega_x^2 = \tilde{\omega}_x^2/\omega_{osc}^2$, $\omega_y^2 = \tilde{\omega}_y^2/\omega_{osc}^2$, $\omega_z^2 = \tilde{\omega}_z^2/\omega_{osc}^2$, with $a_{osc} = (\hbar/m\omega_{osc})^{1/2}$. Also $t = \tau\omega_{osc}$, and $\Psi(\mathbf{r},t) = a_{osc}^{3/2}\Phi(\tilde{\mathbf{r}},\tau)$, the dimensionless DGPE is

$$\begin{aligned} i\frac{\partial\Psi(\mathbf{r},t)}{\partial t} &= \left[-\frac{1}{2}\nabla^2 + V(\mathbf{r}) + 4\pi aN\left|\Psi(\mathbf{r},t)\right|^2\right. \\ &+ \left.\frac{NC_{dd}}{4\pi}\int d\mathbf{r}'\left(\frac{1-3\cos^2\theta}{|\mathbf{r}-\mathbf{r}'|^3}\right)\left|\Psi(\mathbf{r}',t)\right|^2\right]\Psi(\mathbf{r},t) \end{aligned} \tag{3.20}$$

with $a = \tilde{a}/a_{osc}$ and

$$C_{dd} = m\,\widetilde{C}_{dd}/a_{osc}^2\hbar^2$$

. Here m is the oscillator mass. The normalization of the wave function and the density of the condensate can be read respectively as

$$\int d\mathbf{r}\left|\Psi(\mathbf{r},t)\right|^2 = 1 \tag{3.21}$$

$$n(\mathbf{r}) = N\left|\Psi(\mathbf{r},t)\right|^2 \tag{3.22}$$

The dimensionless dipolar interaction is

$$U_{dd}\left(\mathbf{r}-\mathbf{r}'\right) = \frac{C_{dd}}{4\pi}\frac{1-3\cos^2\theta}{\left|\mathbf{r}-\mathbf{r}'\right|^3} \tag{3.23}$$

In the weak-coupling limit $\left(n\left|a\right|^3 \ll 1\right)$ the mean-field DGPE gives a good description of a trapped dipolar BEC. In the strong-coupling regime $\left(n\left|a\right|^3 \gg 1\right)$ this model is not valid and beyond mean-field corrections become important [23].

The ansatz (1.28) $\Psi\left(\mathbf{r},t\right) = \Psi\left(\mathbf{r}\right)\exp\left(-i\mu t\right)$ allows obtaining of the time-independent dipolar GPE

$$\mu\Psi\left(\mathbf{r}\right) = \left[-\frac{1}{2}\nabla^2 + V\left(\mathbf{r}\right) + 4\pi aN\left|\Psi\left(\mathbf{r}\right)\right|^2 + NV_{dd}\left(\mathbf{r}\right)\right]\Psi\left(\mathbf{r}\right) \tag{3.24}$$

with the definition

$$V_{dd}\left(\mathbf{r}\right) = \int d\mathbf{r}'\, U_{dd}\left(\mathbf{r}-\mathbf{r}'\right)\left|\Psi\left(\mathbf{r}'\right)\right|^2 \tag{3.25}$$

It is worth noting that $V_{dd}\left(\mathbf{r}\right)$ is non-local, i.e. its value for $\mathbf{r}$ depends on total density of the condensate, reflecting the long-range nature of the interaction.

From (3.24) the chemical potential is

$$\mu = \int d\mathbf{r}\,\Psi^*\left(\mathbf{r}\right)\left[-\frac{1}{2}\nabla^2 + V\left(\mathbf{r}\right) + 4\pi aN\left|\Psi\left(\mathbf{r}\right)\right|^2 + NV_{dd}\left(\mathbf{r}\right)\right]\Psi\left(\mathbf{r}\right) \tag{3.26}$$

The corresponding energy per particle with dipolar contribution can be obtained from the contact interaction hamiltonian (1.32) modified

$$H = -\frac{1}{2}\nabla^2 + V\left(\mathbf{r}\right) + 2\pi aN\left|\Psi\left(\mathbf{r}\right)\right|^2 + \frac{N}{2}V_{dd}\left(\mathbf{r}\right) \tag{3.27}$$

leading to the dipolar condensate energy

$$E\left(\Psi\right) = \int d\mathbf{r}\left[\frac{N}{2}\left|\nabla\Psi\left(\mathbf{r}\right)\right|^2 + V\left(\mathbf{r}\right)N\left|\Psi\left(\mathbf{r}\right)\right|^2 + 2\pi aN^2\left|\Psi\left(\mathbf{r}\right)\right|^4 + \frac{N^2}{2}V_{dd}\left(\mathbf{r}\right)\left|\Psi\left(\mathbf{r}\right)\right|^2\right] \tag{3.28}$$

Likewise from the thermodynamic relation $\mu = \partial E/\partial N$ and with the energy (3.28) the chemical potential (3.26) arises. Maintaining the relation among the energy and the chemical potential (1.37), add the new interaction. Thus

$$\mu = \frac{1}{N}\left[E_{kin} + E_{ho} + 2\left(E_{contact} + E_{dipolar}\right)\right] \tag{3.29}$$

A important relationship between the energies in a dipolar condensate can be found using the virial theorem (Appendix C.2). This theorem takes into account that the energy must be independent of a scaling transformation of the coordinates and besides that it imposes

that the energy must be a minimum. The theorem allows to testing the accuracy of a numerical algorithm. Thus,

$$2E_{kin} + 3E_{int} - 2E_{trap} = 0 \tag{3.30}$$

3.4 Thomas-Fermi approximation for the DGPE

In the TF approach the generlization of (1.68) according to (3.24) is given by [2, 9, 11, 13]

$$\mu = V(\mathbf{r}) + 4\pi a N |\Psi(\mathbf{r})|^2 + N V_{dd}(\mathbf{r}) \tag{3.31}$$

Solving (3.31) in general is not easy [35, 36, 45] due to dipolar term. Nonetheless, a parabolic density profile can be found in a simple way considering an isotropic harmonic trap with spherical symmetry $V(r) = r^2/2$ and the dipolar interaction like an anisotropic perturbation which distorts the cloud [2] (the perturbation treatment may be extended to anisotropic traps). When the dipolar interaction is not present, the solution to (3.31) becomes in

$$N |\Psi_0(\mathbf{r})|^2 = \frac{1}{4\pi a}\left(\mu - \frac{r^2}{2}\right) \tag{3.32}$$

Inserting this solution in the last term of (3.31) leads to

$$V_{dd}^{(0)}(\mathbf{r}) = \int d\mathbf{r}'\, U_{dd}(\mathbf{r} - \mathbf{r}') |\Psi_0(\mathbf{r}')|^2 \tag{3.33}$$

So the solution to the dipolar density in TF approximation (3.31) may take the form

$$N |\Psi(\mathbf{r})|^2 = \frac{1}{4\pi a}\left[\mu - V(\mathbf{r}) - N V_{dd}^{(0)}(\mathbf{r})\right] \tag{3.34}$$

Rewriting the dipolar interaction (3.23) as [2]

$$U_{dd}(\mathbf{r} - \mathbf{r}') = \frac{C_{dd}}{4\pi} \frac{1}{|\mathbf{r} - \mathbf{r}'|^3}\left[1 - \frac{3(z - z')^2}{|\mathbf{r} - \mathbf{r}'|^2}\right] \tag{3.35}$$

and simpliflying this using the property

$$\begin{aligned} \frac{1}{|\mathbf{r} - \mathbf{r}'|^3} - 3\frac{(z - z')^2}{|\mathbf{r} - \mathbf{r}'|^5} &= -\frac{\partial^2}{\partial z^2}\left(\frac{1}{|\mathbf{r} - \mathbf{r}'|}\right) + \frac{1}{3}\nabla_{\mathbf{r}}^2\left(\frac{1}{|\mathbf{r} - \mathbf{r}'|}\right) \\ &= -\frac{\partial^2}{\partial z^2}\left(\frac{1}{|\mathbf{r} - \mathbf{r}'|}\right) - \frac{4\pi}{3}\delta(\mathbf{r} - \mathbf{r}') \end{aligned} \tag{3.36}$$

the dipolar interaction becomes

$$V_{dd}^{(0)}(\mathbf{r}) = \frac{C_{dd}}{4\pi}\int d\mathbf{r}'\left[-\frac{\partial^2}{\partial z^2}\left(\frac{1}{|\mathbf{r}-\mathbf{r}'|}\right)-\frac{4\pi}{3}\delta(\mathbf{r}-\mathbf{r}')\right]|\Psi_0(\mathbf{r}')|^2 \tag{3.37}$$

Deriving by parts the first term can be written as

$$-\left[\frac{\partial^2}{\partial z^2}\left(\frac{1}{|\mathbf{r}-\mathbf{r}'|}\right)\right]|\Psi_0(\mathbf{r}')|^2 = -\frac{\partial^2}{\partial z^2}\left(\frac{|\Psi_0(\mathbf{r}')|^2}{|\mathbf{r}-\mathbf{r}'|}\right) \tag{3.38}$$

Thus, the dipolar contribution is given by

$$\begin{aligned} NV_{dd}^{(0)}(\mathbf{r}) &= -\frac{C_{dd}}{4\pi}\int d\mathbf{r}'\left[\frac{\partial^2}{\partial z^2}\left(\frac{N|\Psi_0(\mathbf{r}')|^2}{|\mathbf{r}-\mathbf{r}'|}\right)+\frac{4\pi}{3}\delta(\mathbf{r}-\mathbf{r}')N|\Psi_0(\mathbf{r}')|^2\right] \\ &= -C_{dd}\left[\frac{\partial^2}{\partial z^2}\left(\frac{1}{4\pi}\int d\mathbf{r}'\frac{N|\Psi_0(\mathbf{r}')|^2}{|\mathbf{r}-\mathbf{r}'|}\right)+\frac{1}{3}N|\Psi_0(\mathbf{r})|^2\right] \\ &= -C_{dd}\left[\frac{\partial^2\phi(\mathbf{r})}{\partial z^2}+\frac{1}{3}N|\Psi_0(\mathbf{r})|^2\right] \end{aligned} \tag{3.39}$$

Here ϕ satisfies the Poisson equation $\nabla^2\phi = -N|\Psi_0(\mathbf{r})|^{2*}$ [42] and looks like an electrostatic potential due to a charge distribution $N|\Psi_0(\mathbf{r})|^2$. So the dipolar interaction is split into a long-range term which is $\phi-$function and a local term proportional to the density $N|\Psi_0(\mathbf{r})|^2$.

From the size of the cloud R in spherically symmetry to the TF approach (1.69), the non-dipolar density reads as

$$N|\Psi_0(\mathbf{r})|^2 = n_0\left(1-\frac{r^2}{R^2}\right) \tag{3.40}$$

with the density in the central point ($\mathbf{r}=0$) written like $n_0 = N|\Psi_0(\mathbf{r}=0)|^2 = \mu/4\pi a$ and $N|\Psi_0(\mathbf{r})|^2 > 0$ for r less than the Thomas–Fermi radius R and $N|\Psi_0(\mathbf{r})|^2 = 0$ in the otherwise.

The potential ϕ can be determined by splitting up the system into two regions, $r' < r$ and $r' > r$. The potential from a spherical shell with radius $r' > r$ and thickness dr' is $1/r$ times the total charge contained in the shell. Therefore the potential is

- For $r > R$ with $|\mathbf{r}-\mathbf{r}'| \sim r$

$$\phi(r) = \frac{1}{4\pi}\int d\mathbf{r}'\frac{N|\Psi_0(\mathbf{r}')|^2}{|\mathbf{r}-\mathbf{r}'|} = \frac{1}{4\pi r}\int d\mathbf{r}' N|\Psi_0(\mathbf{r}')|^2 \tag{3.41}$$

From the wave function normalization (3.21) and for a constant number of particles, the

*Like $\nabla_r^2\left(\frac{1}{|\mathbf{r}-\mathbf{r}'|}\right) = -4\pi\delta(\mathbf{r}-\mathbf{r}')$, then $\int d\mathbf{r}'\,\nabla_r^2\left(\frac{N|\Psi_0(\mathbf{r}')|^2}{|\mathbf{r}-\mathbf{r}'|}\right) = -4\pi N|\Psi_0(\mathbf{r})|^2$

potential is

$$\phi(r) = \frac{N}{4\pi r} \tag{3.42}$$

- For $r < R$

$$|\mathbf{r} - \mathbf{r}'| \sim \begin{cases} r & r' < r \\ r' & r' > r \end{cases}$$

Solving the integral for the potential

$$\begin{aligned} \phi(r) &= \frac{1}{4\pi} \int d\mathbf{r}' \frac{N |\Psi_0(\mathbf{r}')|^2}{|\mathbf{r} - \mathbf{r}'|} \\ &= \frac{1}{r} \int_0^r dr' (r')^2 N |\Psi_0(\mathbf{r}')|^2 + \int_r^R dr' (r')^2 \frac{N}{r'} |\Psi_0(\mathbf{r}')|^2 \\ &= \frac{1}{r} \int_0^r dr' r'^2 \left[n_0 \left(1 - \frac{r'^2}{R^2} \right) \right] + \int_r^R dr' r'^2 \frac{1}{r'} \left[n_0 \left(1 - \frac{r'^2}{R^2} \right) \right] \\ &= n_0 \left\{ \frac{1}{r} \left[\frac{r^3}{3} - \frac{r^5}{5R^2} \right] + \frac{1}{2} \left(R^2 - r^2 \right) - \frac{1}{4R^2} \left(R^4 - r^4 \right) \right\} \end{aligned} \tag{3.43}$$

Finally,

$$\phi(r) = n_0 \left[\frac{R^2}{4} + \frac{r^4}{20R^2} - \frac{r^2}{6} \right] \tag{3.44}$$

Using the potential for $r < R$ the energy contribution to the dipolar interaction (3.39) can be calculated like

$$\frac{\partial^2 \phi(\mathbf{r})}{\partial z^2} = n_0 \frac{\partial}{\partial z} \left[\frac{4r^2 z}{20R^2} - \frac{2z}{6} \right] = n_0 \left[\frac{r^2 + 2z^2}{5R^2} - \frac{1}{3} \right] \tag{3.45}$$

so

$$NV_{dd}^{(0)}(\mathbf{r}) = \frac{2}{15} C_{dd} n_0 \left[\frac{r^2 - 3z^2}{R^2} \right] \tag{3.46}$$

Or by substituting the radius $r^2 = x^2 + y^2 + z^2$ and the chemical potential in terms of the extension of the cloud in the TF approach (1.69) the density in the central point

$$n_0 = \frac{\mu}{4\pi a} = \frac{R^2}{8\pi a} \tag{3.47}$$

leads to

$$NV_{dd}^{(0)}(\mathbf{r}) = \frac{C_{dd}}{60\pi a} \left(x^2 + y^2 - 2z^2 \right) \tag{3.48}$$

Hence the density distribution with dipolar interaction in the TF approach (3.34) is given

by

$$N\left|\Psi\left(\mathbf{r}\right)\right|^{2} = \frac{\mu}{4\pi a}\left[1-\frac{r^{2}}{R^{2}}-\frac{C_{dd}}{30\pi aR^{2}}\left(x^{2}+y^{2}-2z^{2}\right)\right]$$
$$= n_{0}\left[1-\left(1+\frac{C_{dd}}{30\pi a}\right)\left(\frac{x^{2}+y^{2}}{R^{2}}\right)-\left(1-\frac{C_{dd}}{15\pi a}\right)\frac{z^{2}}{R^{2}}\right] \tag{3.49}$$

In a dipolar BEC is useful to define the dimensionless quantity $\epsilon_{dd} = C_{dd}/12\pi a$ which measures the strength of the dipole dipole interaction relative to the s-wave scattering one. Hence the density for the TF limit with dipolar interaction is [2, 9]

$$N\left|\Psi\left(\mathbf{r}\right)\right|^{2} = n_{0}\left[1-\frac{x^{2}}{R_{x}^{2}}-\frac{y^{2}}{R_{y}^{2}}-\frac{z^{2}}{R_{z}^{2}}\right] \tag{3.50}$$

defining the radii R_x, R_y and R_z as

$$R_{\perp} = R_{x} = R_{y} = R\left(1+\frac{2}{5}\epsilon_{dd}\right)^{-1/2} \tag{3.51}$$

$$R_{z} = R\left(1-\frac{4}{5}\epsilon_{dd}\right)^{-1/2} \tag{3.52}$$

and for a trap with cylindrical symmetry, such that $\rho^2 = x^2 + y^2$, the TF density takes the form [11, 35, 36, 45]

$$N\left|\Psi\left(\mathbf{r}\right)\right|^{2} = n_{0}\left[1-\frac{\rho^{2}}{R_{\perp}^{2}}-\frac{z^{2}}{R_{z}^{2}}\right] \tag{3.53}$$

From the density definition (3.22), the number of particle N can be given by

$$N = \int d\mathbf{r}\, N\left|\Psi\left(\mathbf{r}\right)\right|^{2} \tag{3.54}$$

thus the usual normalization constant n_0 can be written like

$$n_{0} = \frac{15N}{8\pi R_{\perp}^{2}R_{z}} \tag{3.55}$$

Therefore the density in the TF approximation of a DBEC with cylindrical symmetry is

$$N\left|\Psi\left(\mathbf{r}\right)\right|^{2} = \frac{15N}{8\pi R_{\perp}^{2}R_{z}}\left[1-\frac{\rho^{2}}{R_{\perp}^{2}}-\frac{z^{2}}{R_{z}^{2}}\right] \tag{3.56}$$

3.5 The hydrodynamic equations

In the same way as the hydrodynamic in a non-dipolar condensate was studied in the previous Chapter, for a dipolar BEC [11, 13, 33] is possible taking a solution like $\Psi\left(\mathbf{r},t\right) = \left(n\left(\mathbf{r},t\right)/N\right)^{1/2}\exp\left[i\phi\left(\mathbf{r},t\right)\right]$ (with the phase of the order parameter $\phi\left(\mathbf{r},t\right)$ as a real quantity). Thus, the continuity equation is given by

$$\frac{\partial n}{\partial t} + \nabla \cdot \mathbf{j} = 0 \tag{3.57}$$

with the respective condensate density $n = N\left|\Psi\right|^2$, the particle current density $\mathbf{j} = n\mathbf{v}$, and the velocity

$$\mathbf{v} = -\frac{i}{2}\frac{\left(\Psi^*\nabla\Psi - \Psi\nabla\Psi^*\right)}{\left|\Psi\right|^2} \tag{3.58}$$

or in terms of phase $\phi\left(\mathbf{r},t\right)$

$$\mathbf{v}\left(\mathbf{r},t\right) = \nabla\phi\left(\mathbf{r},t\right) \tag{3.59}$$

and the Euler equation

$$\frac{\partial \mathbf{v}}{\partial t} = -\nabla\left[\frac{1}{2}v^2 + V + 4\pi an + NV_{dd}\left(\mathbf{r}\right) - \frac{1}{2\sqrt{n}}\nabla^2\sqrt{n}\right] \tag{3.60}$$

3.5.1 Homogeneous gas: phonon instability

In the Chapter 1 was shown that a homogeneous condensate with attractive contact interactions ($a < 0$) is unstable. In the Chapter 2 from the hydrodynamic viewpoint this effect can also be appreciated by the critical wavenumber ($q_c = \sqrt{2}/\xi$) below which the condensate becomes unstable i.e., the excitation frequencies are imaginary. Now, it will be considered a homogeneous dipolar condensate with an equilibrium density n, small density and velocity perturbations (with frequency ω and wave vector q). Linearizing the continuity equation (3.57) and the Euler equation (3.60) around equilibrium, the excitation spectrum is determined in a same way as for the Bose uniform gas with solutions $\delta n \longrightarrow \delta n\, exp\left[-i\left(\mathbf{q}.\mathbf{r} - \omega t\right)\right]$. The dipolar contribution to the spectrum corresponds with the Fourier transform for $V_{dd}\left(\mathbf{r}\right)$ [11, 46, 47, 48] (Appendix B) such that

$$\epsilon_q = \omega = \left\{q^2\left[4\pi an + n\widetilde{U}_{dd}\left(\mathbf{q}\right)\right] + \frac{q^4}{4}\right\}^{1/2} \tag{3.61}$$

with

$$\widetilde{U}_{dd}\left(\mathbf{q}\right) = \frac{C_{dd}}{3}\left(3\frac{q_z^2}{\mathbf{q}^2} - 1\right) = \frac{C_{dd}}{3}\left(3\cos^2\theta_q - 1\right) \tag{3.62}$$

where θ_q is the angle between $\mathbf{q}$ and the polarization direction (Figure 3.6). For the case $\theta_q = \cos^{-1}\left(1/\sqrt{3}\right)$ the dipolar contribution vanishes and the spectrum matches the condensate with contact interaction (2.27). Therefore, the excitation spectrum for a homogeneous dipolar BEC should be [11, 12, 13, 32]

$$\epsilon_q = \omega = \left\{4\pi anq^2\left[1 + \epsilon_{dd}\left(3\cos^2\theta_q - 1\right)\right] + \left(\frac{q^2}{2}\right)^2\right\}^{1/2} \tag{3.63}$$

where the dimensionless quantity $\epsilon_{dd} = C_{dd}/12\pi a$. Defining $\alpha = \left[1 + \epsilon_{dd}\left(3\cos^2\theta_q - 1\right)\right]$ and in analogy with the non-dipolar condensate, when $a > 0$ and $\alpha < 0$ or $a < 0$ and $\alpha > 0$, the energy is real only as $q \geq \left(16\pi n\left|a\right|\left|\alpha\right|\right)^{1/2}$. However, considering a constant

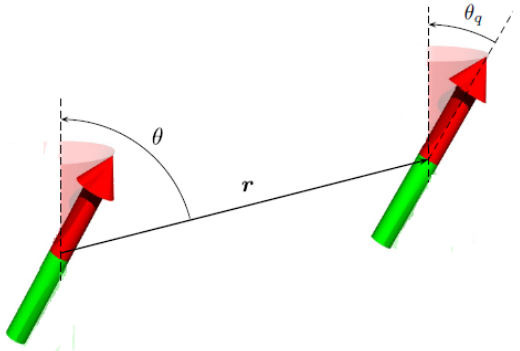

Figure 3.6: θ_q angle in the dipole dipole system [11].

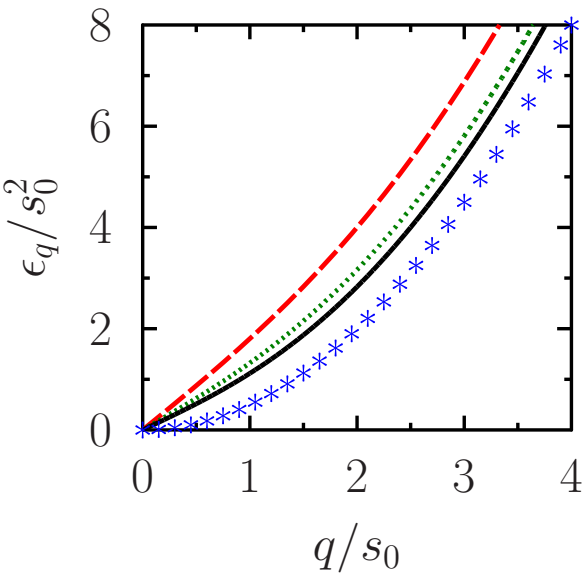

Figure 3.7: Spectrum of elementary excitations (3.63) in units of the s_0^2 (with repulsive interaction $a > 0$), $\epsilon_{dd} = 1$ and different values of the angle θ_q. Such that $\theta_q = 0$ (red dashed line), $\theta_q = \pi/4$ (green dotted line), $\theta_q = \cos^{-1}\left(1/\sqrt{3}\right)$ (black solid line), and $\theta_q = \pi/2$ (blue asterisk).

density, the energy (3.63) can be imaginary depending of the parameters such as ϵ_{dd}, the scattering length a and the angle θ_q. A simple way to see this energy as a wave number function in both repulsive and attractive interactions is given by the Figures (3.7) and (3.8) respectively, both with $|\epsilon_{dd}| = 1$ and $0 \leq \theta_q \leq \pi/2$. However, the richness of the dipole dipole interaction leads at more interesting properties, e.g. in the sound velocity behavior. The sound velocity s is obtained by considering the limit of the spectrum at small wave vector $|q|$ and is defined by

$$s = \lim_{|q|\to 0} \frac{\epsilon_q}{|q|} = \lim_{|q|\to 0} \frac{\omega}{|q|} \tag{3.64}$$

this leads to

$$s = s_0 \left[1 + \epsilon_{dd}\left(3\cos^2\theta_q - 1\right)\right]^{1/2} \tag{3.65}$$

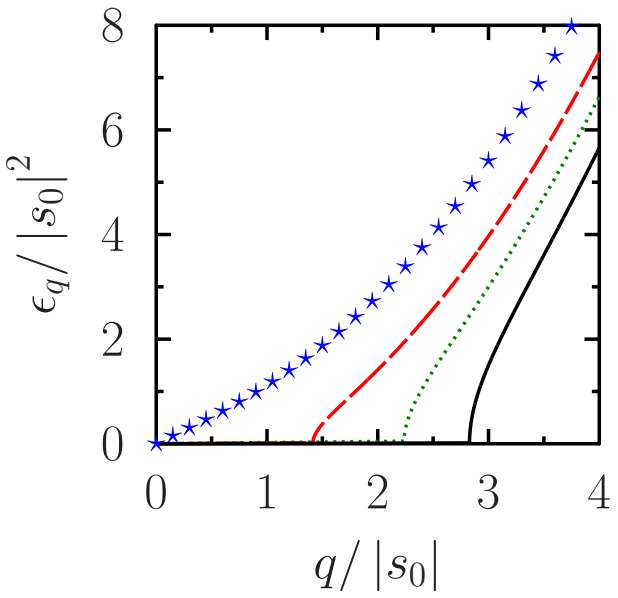

Figure 3.8: Spectrum of elementary excitations (3.63) in units of the $|s_0|^2$ (with attractive interaction $a<0$), $|\epsilon_{dd}|=1$ and different values of the angle θ_q. Such that $\theta_q=0$ (blue asterisk), $\theta_q=\pi/4$ (red dashed line), $\theta_q=\pi/3$ (green dotted line), and $\theta_q=\pi/2$ (black solid line).

with the sound velocity $s_0=\sqrt{4\pi an}$ in the non-dipolar condensate. Notice that the sound velocity can be real or imaginary. For a constant density there are two possible cases

- For $a>0$ (implies $\epsilon_{dd}>0$) then

$$\cos^2\theta_q \geq \frac{1}{3}\left(1-\frac{1}{\epsilon_{dd}}\right) \tag{3.66}$$

When the parameter ϵ_{dd} is within the interval $0<\epsilon_{dd}\leq 1$ the above condition is satisfied for any angle within $0\leq\theta_q\leq\pi/2$ and the sound velocity is real (Figure 3.9). Moreover, to maintain the sound velocitity real when $\epsilon_{dd}>1$, it is necessary the condition

$$\theta_q < \cos^{-1}\left[\frac{1}{3}\left(1-\frac{1}{\epsilon_{dd}}\right)\right]^{1/2} \tag{3.67}$$

Here when $\epsilon_{dd}\to 1$ then $\theta_q\to\pi/2$ and when $\epsilon_{dd}\gg 1$ then $\theta_q\to\cos^{-1}\left(1/\sqrt{3}\right)$. The above condition is a sign of the general instability present in homogeneous dipolar gases (Figure 3.10). In the particular situation $\epsilon_{dd}>1$ and $\theta_q=\pi/2$ being the wave vector q perpendicular to the orientation of the dipoles, the dipolar gas is unstable.

- For $a<0$ (implies $\epsilon_{dd}<0$) then

$$\cos^2\theta_q > \frac{1}{3}\left(1+\frac{1}{|\epsilon_{dd}|}\right) \tag{3.68}$$

Or in the form

$$\theta_q \leq \cos^{-1}\left[\frac{1}{3}\left(1+\frac{1}{|\epsilon_{dd}|}\right)\right]^{1/2} \tag{3.69}$$

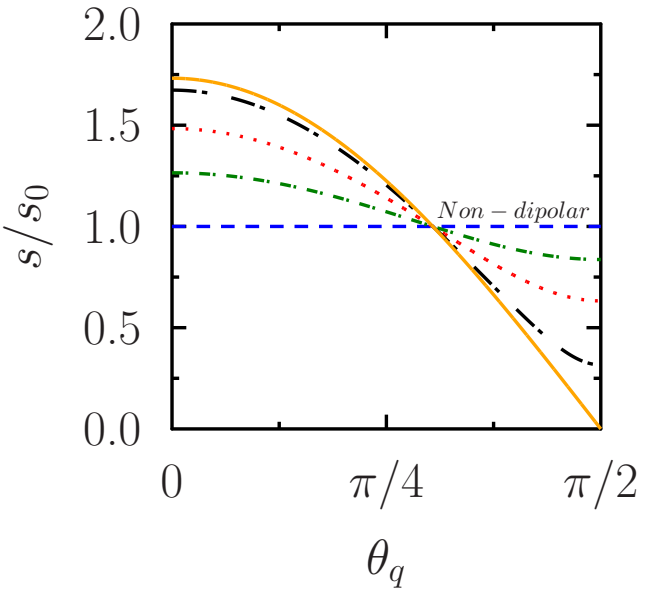

Figure 3.9: Sound velocity in units of the s_0 (with $a > 0$) as a function of the angle θ_q (in radians) within the interval $0 \leq \epsilon_{dd} \leq 1$. The non-dipolar case $\epsilon_{dd} = 0$ (blue dashed line), $\epsilon_{dd} = 0.3$ (green short line and dot), $\epsilon_{dd} = 0.6$ (red dotted line), $\epsilon_{dd} = 0.9$ (black large line and dot), and $\epsilon_{dd} = 1$ (orange solid line).

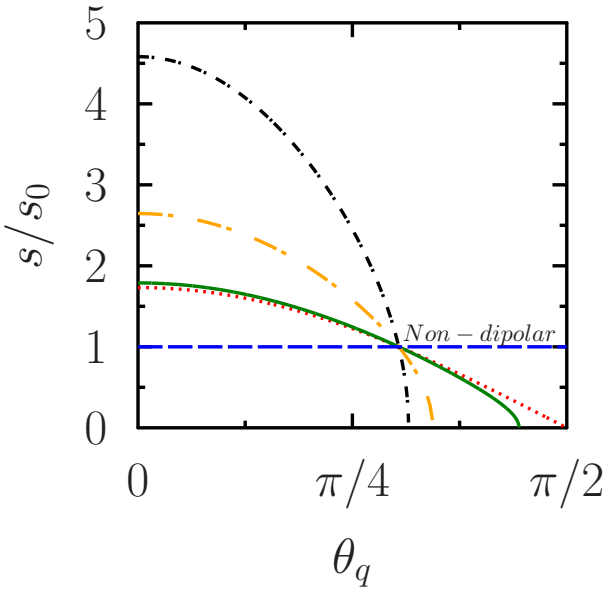

Figure 3.10: Sound velocity in units of the s_0 (with $a > 0$) as a function of the angle θ_q (in radians) for $\epsilon_{dd} > 1$. The non-dipolar case $\epsilon_{dd} = 0$ (blue dashed line), $\epsilon_{dd} = 1$ (red dotted line), $\epsilon_{dd} = 1.1$ (green solid line), $\epsilon_{dd} = 3$ (orange large line and dot), and $\epsilon_{dd} = 10$ (black short line and dot).

so when $|\epsilon_{dd}| \geq 1/2$ the condition is fulfilled and the sound velocity is real. In this region when $|\epsilon_{dd}| \to \infty$ then $\theta_q \to \cos^{-1}\left(1/\sqrt{3}\right)$ (Figure 3.11). The angle varies within the interval $0 \leq \theta_q < \cos^{-1}\left(1/\sqrt{3}\right)$. The existence of the sound velocity to $a < 0$ contrasts with the non-dipolar case where it doesn't exist.

Just like in the non-dipolar condensate, the dipolar excitation spectrum (3.63) has two approaches, the first one to short wavenumbers and the second one to long wavenumbers. So to short wavenumbers $q \to 0$ and repulsive interactions $a > 0$, the spectrum is linear in q, such that $\epsilon_q \approx sq$. To long wavenumbers $q \gg 0$ and repulsive interactions $a > 0$, the spectrum has a free particle contribution ($\epsilon_q^0 = q^2/2$) plus a shift.

$$\epsilon_q \approx \epsilon_q^0 + s^2 \tag{3.70}$$

In the attractive stage $a < 0$ and short wave numbers $q \to 0$ the spectrum (3.63) becomes linear in q contradicting the non-dipolar condensate where the spectrum doesn't exist. Thus,

$$\epsilon_q = q\left\{4\pi n\,|a|\left[|\epsilon_{dd}|\left(3\cos^2\theta_q - 1\right) - 1\right]\right\}^{1/2} \tag{3.71}$$

To long wavenumbers $q \gg 0$ and $a < 0$ the spectrum becomes

$$\epsilon_q \approx \epsilon_q^0 + 4\pi\,|a|\,n\left[|\epsilon_{dd}|\left(3\cos^2\theta_q - 1\right) - 1\right] \tag{3.72}$$

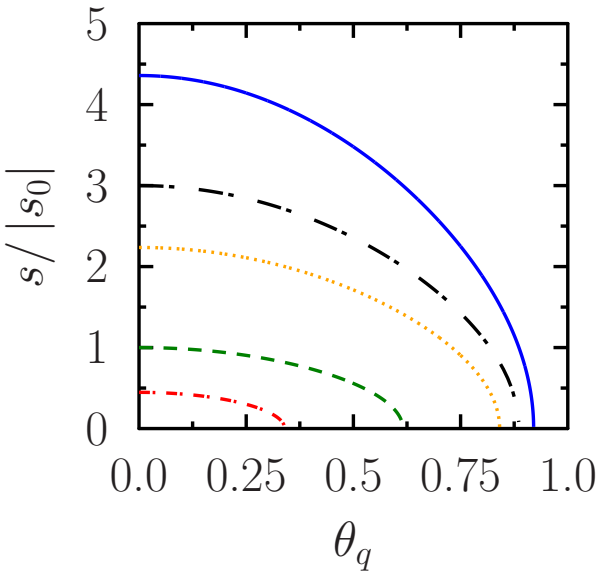

Figure 3.11: Sound velocity in units of the $|s_0|$ (with $a < 0$) as a function of the angle θ_q (in radians) for $|\epsilon_{dd}| \geqslant 1/2$. $|\epsilon_{dd}| = 3/5$ (red short line and dot), $|\epsilon_{dd}| = 1$ (green dashed line), $|\epsilon_{dd}| = 3$ (orange dotted line), $|\epsilon_{dd}| = 5$ (black large line and dot), and $|\epsilon_{dd}| = 10$ (blue solid line).

Chapter 4

Solitons in a BEC

In a BEC the fundamental excitations at zero-temperature are divided into collective [2, 13] and topological ones [2, 3]. The collective excitations are related to the density perturbations depending on the excitation wavelength λ_e, relative to the size of the condensate R, thus when $\lambda_e < R$, the excitations are phonons (sound waves) and for $\lambda_e > R$, the excitations represent large-scale oscillations (breathing and quadrupole modes). The topological excitations are solitons (bright and dark) and vortices (single vortices, vortex rings and vortex lattices) [2, 3, 4]. The solitons are the main subject in this Chapter.

The Thomas-Fermi regime and the variational approximation are very useful research methods to describe some properties of a condensate as was seen in Chapter 1. However the mean-field equation (1.21) in a one dimension and without trap has a special kind of analytical solutions called solitons [2, 4]. The solitons are generated in both repulsive (dark soliton) and attractive (bright soliton) condensates as will be illustrated in this Chapter. The last part of the Chapter is devoted to found solitons in a three dimensional condensate without trap in the z direction by means of a Gaussian variational approximation and the numerical calculation using the split-step Crank–Nicolson method [24].

4.1 The soliton

A solitary wave or soliton is defined as a localised nonlinear wave arises from a balance between dispersive and nonlinear effects [49, 50, 51]. Besides for a conservative system the soliton behaves like a "particle" i.e.

- It must maintain its shape when it travels at constant speed, reflecting a characteristic of the so-called solitary wave.
- When a soliton interacts with another soliton, it emerges from the "collision" unchanged except for a possibly phase shift, in other words, the amplitude, shape and velocity are conserved after the collision. This soliton property shows the particle-like interaction behavior*.

*From which the name soliton was coined in 1965 by Norman Zabusky and Martin Kruskal.

The solitons arise in both continuous systems such as the Korteweg–de Vries equation equation and discrete systems such as the Toda lattice and in both one and multiple spatial dimensions [49, 51].

Brief historical development of solitons

A useful and simple introduction about the soliton is found in [49, 50] (and references therein). The birth of the soliton was first recorded by John Scott Russell (1834) when he was investigating how improve the efficiency of designs for barges in canals. After about 50 years being ignored this interesting discovery, Diederik Korteweg and his PhD student, Hendrik de Vries derived a nonlinear partial differential equation confirming mathematically the existence of Scott's solitary waves. They show that the change of the wave's height in time is determined by nonlinear and dispersive effects. However, they did not find a general solution. In 1955, by means of the Los Alamos MANIAC computing machine, Enrico Fermi, John Pasta and Stanislaw Ulam (FPU) were exploring the energy equipartition in a slightly nonlinear mechanical system. It was expected that if all the energy was initially introduced in a single mode, the small nonlinearity would cause energy redistribution among all the modes, but this did not happen and the energy was periodically returning to the initially excited mode. Motivated to find an explanation for this phenomenon, Norman Zabusky and Martin Kruskal (1965) approximated the FPU system in the continuum limit using the KdV equation. They solved the equation numerically and reported that the solitary waves can pass through each other without change in their shape or speed, the only change found was a small phase shift after a collision. Zabusky and Kruskal then introduced for the first time the term soliton for this solitary waves, thus highlighting its particle-like behavior. In 1967 was discovered a method by Clifford Gardner, John Greene, Martin Kruskal and Robert Miura, to finding exact solutions (including soliton) of the KdV equation. At present this method is known as the inverse scattering method (ISM). It was later found that the ISM is more general and allows sought exact solitons in many others integrable nonlinear systems. In 1972 Vladimir Zakharov and Alexei Borisovich Shabat generalized the inverse scattering method and solved the nonlinear Schrödinger equation (NLSE). They demonstrated both integrability and existence of soliton solutions. The NLSE was found as a fundamental model in many important applications, in hydrodynamics, nonlinear optics, nonlinear acoustics, plasma waves, Bose-Eistein condensate, inter alia. Next, in 1973, Mark Ablowitz, David Kaup, Alan Newell and Harvey Segur also applied ISM finding the solitons in the sine-Gordon (SG) equation which admits kink and anti-kink solitons. The SG equation also appears in many physical applications, including the propagation of crystal defects and the propagation of fluxons (quantum units of magnetic flux) on long Josephson transmission lines.

In addition to the discovery of the integrable nonlinear continuous systems, appear some integrable discrete systems admitting exact discrete solitons. Morikazu Toda becomes

the first to discover a soliton in a discrete integrable system (called the Toda lattice). Later, arises the Ablowitz-Ladik (AL) equation which is an important discretization of the continuous NLSE. Although the AL equation is not physically relevant as if it is the usual discretization (the discrete nonlinear Schrödinger equation or DNLSE), its advantage lies in that it preserves the integrability of its continuous counterpart and is theoretically useful as a starting point in perturbative studies. Other researchers have subsequently derived other integrable models (in one and multiple spatial dimensions) with soliton solutions. By contrast, studying solitary waves in nonintegrable equations becomes the analytical techniques in perturbative methods, asymptotic analysis or variational approximations. The above shows that the solitons are a huge research field in different scenarios of the science.

4.2 The nonlinear Schrödinger equation

The nonlinear Schrödinger equation (NLSE) ([52] contains some general aspects) is regarded a universal nonlinear model because of that it describes a large amount of physical nonlinear systems. The equation can be applied to hydrodynamics, nonlinear optics, nonlinear acoustics, Bose-Einstein condensates, heat pulses in solids and various other nonlinear instability phenomena.

4.2.1 The NLSE in a BEC

Until now the behavior of a condensate has been studied using different approximations like the TF approach and the variational solution. However the time-dependent GPE has exact analytical solutions in the nonlinear case. These have form of solitons, i.e. localized perturbations which propagate without change of form. These are physically created by the nonlinearity and dispersion compensation according to the dispersion relation given by (2.27) which has both, local density and wave number dependence. The GPE (1.14) can be considered like a NLS-like equation, which in turn is identical to that appearing in non-linear optics of Kerr media. Interesting resemblances have been observed between both fields, including four-wave mixing, BEC collapse and the creation of bright, dark and gap solitons (more information about those phenomena is found in references of [11]).

The solitons in the integrable NLSE are localised one-dimensional wavepackets and come in two distinct forms. For analogy with the optical solitons the intensity of the light can be equivalent of the condensate density. Thus, the dark solitons [2, 4, 51, 53] correspond to density depressions and these are generated in repulsive (or defocussing) nonlinear media. These solitons are divided into black ones, for which the minimum density is zero, and grey ones for which the density is greater than zero. The other hand, are the solitons with a density maximum referred as bright [2, 4, 51], i.e. the bright solitons are humps of positive density and these are supported in attractive (or self-focussing) media.

According to the above, the solitary waves are bright and dark depending on the nature of the nonlinearity in the system, and these are arise in many other areas of physics, such as shallow water waves, plasma systems, macromolecules, acoustic, optical fibres, photonics and possible applications in the future include interferometry, quantum entanglement and quantum information.

4.3 GPE reduction from 3D to 1D

In the Chapter 1, it was described that a variation of the parameter $\lambda = \omega_z/\omega_\perp$ can result in three kinds of condensates: $\lambda = 1$ spherical, $\lambda > 1$ disk- or pancake-shaped (quasi-two-dimensional condensate) and $\lambda < 1$ cigar-shaped (quasi-one-dimensional condensate). The 3D to 1D reduction will be done using the adiabatic approximation [54, 55, 56] which considers that in a cigar-shaped trap with tight radial binding the dynamics takes place along the axial direction and in the transverse direction the condensate wavefunction remains in the ground state and the opposite happens for the disc-shaped trap. Therefore in those two limits the scales are very different and it is possible separate the wave function in ρ and z variables [54, 55, 56, 57, 58, 59]. The first experimental realization of solitons in a BEC it was done in a quasi-1D model [60]. An approximate search of solitons in a BEC can be performed using the reduced 1D mean-field GPE. Theoretically, the literature offers several schemes to obtain a quasi-1D GPE. In this dissertation it will be used the reduction procedure proposed by [54, 55, 56, 57, 58] (and references therein), where the wave function $\Psi(\mathbf{r}, t)$ can be factorized as

$$\Psi(\mathbf{r}, t) = \phi(\rho)\,\kappa(z, t) \tag{4.1}$$

with $\rho^2 = x^2 + y^2$. This approximate wave function is valid whereas the main force on the transverse direction is caused by the trapping potential [57]. So, by substituting this wave function into the GPE (1.21) it leads to

$$i\phi\frac{\partial\kappa}{\partial t} = -\frac{1}{2}\phi\frac{\partial^2\kappa}{\partial z^2} - \frac{1}{2}\kappa\nabla_\rho^2\phi + V_\rho\phi\kappa + V_z\phi\kappa + 4\pi a_{3D}N\left|\phi\right|^2\left|\kappa\right|^2\phi\kappa \tag{4.2}$$

where the radial equation is read as

$$-\frac{1}{2}\nabla_\rho^2\phi + V_\rho\phi = \omega_\rho\phi \tag{4.3}$$

and corresponding to an eigenvalue problem for the two-dimensional isotropic harmonic oscillator with the ground state given by

$$\phi_0(\rho) = \frac{1}{\sqrt{\pi}}e^{-\rho^2/2} \tag{4.4}$$

Now, multiplying (4.2) by $\phi^*(\rho)$ and integrating over ρ using the normalization $\int d^2\rho\left|\phi\right|^2 = 1$, the new equation is

$$i\frac{\partial\kappa}{\partial t} = \int d^2\rho\,\phi^*\left[-\frac{1}{2}\left(\nabla_\rho^2 + \frac{\partial^2}{\partial z^2}\right) + V_\rho + V_z + 4\pi a_{3D} N\left|\phi\right|^2\left|\kappa\right|^2\right]\phi\kappa \tag{4.5}$$

Here

$$\int d^2\rho\,\phi^*\left(-\frac{1}{2}\nabla_\rho^2\phi + V_\rho\phi\right)\kappa = \int d^2\rho\,\phi^*\omega_\rho\phi\kappa = \omega_\rho\kappa \tag{4.6}$$

This expression it gives rise the axial equation

$$i\frac{\partial\kappa}{\partial t} = -\frac{1}{2}\frac{\partial^2\kappa}{\partial z^2} + V_z\kappa + 2a_{3D}N\left|\kappa\right|^2\kappa + \omega_\rho\kappa \tag{4.7}$$

the additional factor $1/2\pi$ in the nonlinear term comes from the solution (4.4) such that

$$\frac{\int_0^\infty \rho\,d\rho\,\left|\phi_0\right|^4}{\int_0^\infty \rho\,d\rho\,\left|\phi_0\right|^2} = \frac{1}{2\pi} \tag{4.8}$$

Finally, with the transformation [57]

$$\kappa\left(z,t\right) \;=\; \psi\left(z,t\right)\exp\left(i\omega_\rho t\right) \tag{4.9}$$

the time-dependent quasi-one-dimensional GPE is

$$i\frac{\partial\psi}{\partial t} = -\frac{1}{2}\frac{\partial^2\psi}{\partial z^2} + V_z\psi + 4\pi a_{1D}N\left|\psi\right|^2\psi \tag{4.10}$$

with $a_{1D} = a_{3D}/2\pi$ [61] and the usual harmonic potential $V_z = \omega_z^2 z^2/2$.

4.4 Modulational instability

The modulational instability represents a fundamental effect associated with wave propagation in nonlinear media, i.e. the aim is know the growth of a small perturbation in the amplitude or phase of the wave while it propagates [62, 63, 64]. Initially this phenomenon was predicted for electromagnetic waves in nonlinear media with cubic nonlinearity (1966) and for waves on deep water (1967). To date, it has been observed in nonlinear optics, plasma physics, condensed matter (fibers, magnetics, BEC, long Josephson junctions, etc.), fluids, discrete nonlinear systems such as molecular chains, inter alia. So the time-dependent quasi-one-dimensional GPE (4.10) with $V_z = 0$ is

$$i\frac{\partial\psi}{\partial t} + \frac{1}{2}\frac{\partial^2\psi}{\partial z^2} \pm 4\pi N\left|a_{1D}\right|\left|\psi\right|^2\psi = 0 \tag{4.11}$$

the sign sets the nonlinearity. The (+) sign is for an attractive system and the (-) sign is for a repulsive one. The GPE has the simplest solution in the form of a plane wave given e.g. by

$$\psi \;=\; \psi_0\exp\left[i\left(qz - \omega t\right)\right] \tag{4.12}$$

where q and ω satisfy the dispersion relation

$$\omega = \frac{1}{2}q^2 \mp 4\pi N |a_{1D}| \psi_0^2 \tag{4.13}$$

This solution shows that a plane wave propagates through the BEC unchanged except for a possible density-dependent phase. An important issue is to know whether this solution is stable against small perturbations or not. The answer is given by a linear stability analysis. The procedure consists in look for solutions describing small variations around the exact solution [51, 65]

$$\psi(z,t) = [\psi_0 + \varphi(z,t)] e^{i[qz-\omega t+\alpha(z,t)]} \tag{4.14}$$

where $\varphi(z,t)$ and $\alpha(z,t)$ are small perturbations. Substituting (4.14) into the GPE (4.11) and linearizing the resulting equations, is obtained a system of two coupled linear equations for φ and α. Looking for solutions to these functions in form of plane waves, e.g. $\varphi, \alpha \approx \exp(i\Omega t - iQz)$ the result is the dispersion relation (Appendix D)

$$(\Omega - qQ)^2 = Q^2 \left[\frac{1}{4}Q^2 \pm 4\pi N |a_{1D}| \psi_0^2\right] \tag{4.15}$$

This expression shows that the plane wave (4.12) is absolutely stable just in the repulsive interactions case (+ sign). Physically this means that the small amplitude waves can propagate along the background and these are characterized by a minimum velocity given by

$$v^2 = \lim_{|Q|\to 0}\left[\left.\frac{\Omega^2}{Q^2}\right|_{q=0}\right] = 4\pi N |a_{1D}| \psi_0^2 \tag{4.16}$$

this velocity should be identified with the sound velocity such that $v^2 = s^2 = 4\pi N |a_{1D}| \psi_0^2$ which it was found from the hydrodynamic viewpoint.

Moreover, the solution (4.12) becomes unstable in a BEC with attractive interactions whenever $Q^2 < 16\pi N |a_{1D}| \psi_0^2$. In this case

$$\Omega = qQ \pm i|Q| \left[4\pi N |a_{1D}| \psi_0^2 - \frac{1}{4}Q^2\right]^{1/2} \tag{4.17}$$

The modulation instability is reflected by the fact that in a unstable condensate the term $\exp(i\Omega)$ leads to an exponential growth of the perturbation. The growth rate of the perturation g or modulation instability gain is related to the imaginary part of Ω, such that

$$g(Q) = \mathrm{Im}[\Omega(Q)] = |Q| \left[4\pi N |a_{1D}| \psi_0^2 - \frac{1}{4}Q^2\right]^{1/2} \tag{4.18}$$

In the Figure (4.1) is plotted the instability gain as function of the perturbation wavevector Q for different values of $|s| = (4\pi N |a_{1D}| \psi_0^2)^{1/2}$. The gain exists in the range $|Q| < 2|s|$ with the maximum for $Q = \sqrt{2}|s|$ and value $g_{max} = |s|^2$. Thus, the modulational insta-

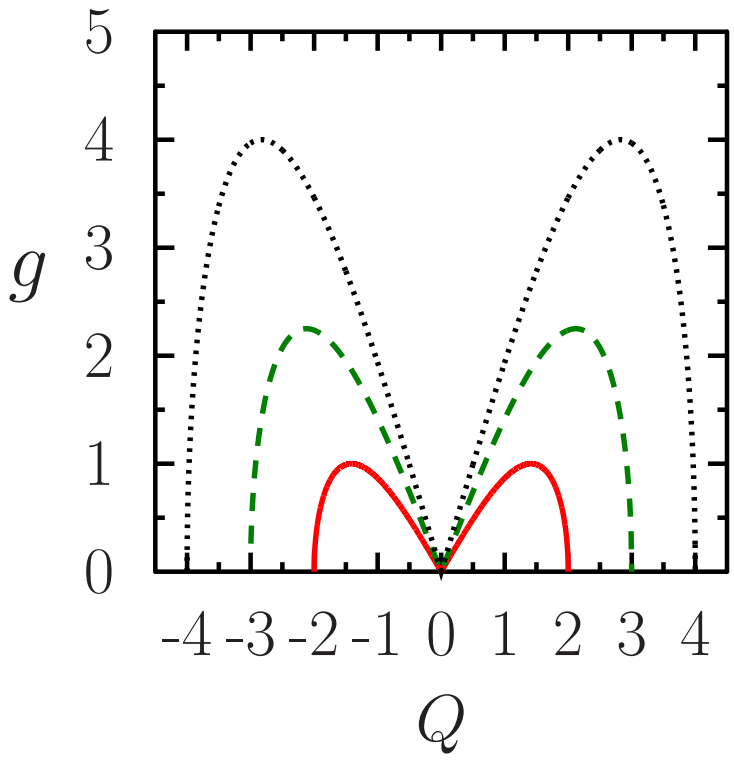

Figure 4.1: Gain spectrum $g\,(Q)$ of modulation instability for $|s| = 1$ (red solid line), $|s| = 1.5$ (green dashed line), and $|s| = 2$ (black dotted line).

bility corresponds to an energy localisation induced by the nonlinear term [66], because of the value g_{max} depends on nonlinear term in the GPE and the plane wave amplitude. It is worth noting that the growth rate of the instability is independent of the wavevector q and the frecuency ω of the plane wave (4.12). More specifically, the modulational instability is closely connected with the existence of solitary waves of the GPE with attactive interactions whose amplitude vanishes when $|z| \to \infty$. These kind of solutions are called bright solitons. These contrast with the dark solitons, which are formed in absence of modulational instability, i.e. in a repulsive system.

4.5 Dark and bright solitons in the quasi-one-dimensional GPE

The solitons in quasi-two or three dimensional GPE are not very easy to find, instead it is more useful begin with the most simple case in a quasi-one-dimension. In this regime for a homogeneous BEC, the GPE admits analytical nontrivial solutions in the form of dark[†] and bright solitons. The dark solitons can be regarded as strongly nonlinear excitations of the plane wave solution [67, 68, 69] (the first observation of quasi-one-dimensional dark solitons were in ^{87}Rb [70, 71], and later in ^{23}Na [72], employing quantum-phase engineering techniques or by dragging a moving impurity through the condensate). The

[†]In analogy to shallow water, the dark solitons in a BEC correspond to density depressions, whereas for waves in shallow water they correspond to elevations in the water level. The velocity of surface waves increases with the depth of the water, just like the speed of sound in a Bose increases with density.

bright solitons [57, 73, 74] are product of the modulational instability in a condensate with attractive interaction (the formation of quasi-one-dimensional bright solitons and bright soliton trains has been observed in ^{7}Li [75, 76] and ^{85}Rb [77] atoms tuning the interatomic interaction within the stable BEC from repulsive to attractive via Feshbach resonances [78] and releasing the BEC in an axially free or an expulsive trap).

4.5.1 Static dark solitons

According to the procedure outlined earlier, the study system coresponds to a quasi-one-dimensional homogeneous condensate (the ground state in the ρ direction is uniform), confined in the z direction. Thus, to the stationary regime on (4.10) with $V_z = 0$ the wave function can be taken as

$$\psi(z,t) \quad \rightarrow \quad \psi(z)\exp(-i\mu t) \tag{4.19}$$

this ansatz leads to the time-independent quasi-one-dimensional GPE

$$\mu\psi(z) = \left[-\frac{1}{2}\frac{d^2}{dz^2} + 4\pi a_{1D}N\left|\psi(z)\right|^2\right]\psi(z) \tag{4.20}$$

The chemical potential for the bulk can be approximated to the uniform Bose gas, in other words $\mu = 4\pi a_{1D}N\left|\psi_0\right|^2$ with ψ_0 the bulk wave function. Thus, the GPE becomes

$$\frac{d^2\psi(z)}{dz^2} = 8\pi a_{1D}N\left(\left|\psi\right|^2 - \left|\psi_0\right|^2\right)\psi \tag{4.21}$$

When ψ is a real function the GPE has the same form as a classical equation of motion of a particle in a potential $V(z)$

$$\frac{d^2\psi(z)}{dz^2} = -\frac{dV(z)}{d\psi} \tag{4.22}$$

Multiplicand the GPE (4.21) by $d\psi/dz$ and integrating over z

$$\int_{z_0}^{z} dz\frac{d\psi}{dz}\frac{d^2\psi}{dz^2} = \int_{z_0}^{z} dz\frac{d\psi}{dz}\frac{dU}{d\psi} \tag{4.23}$$

$$\frac{1}{2}\int_0^z dz\frac{d}{dz}\left(\frac{d\psi}{dz}\right)^2 = \int_{U_0}^{U} dU = 8\pi a_{1D}N\int_{\psi_0}^{\psi}\left(\psi^3 - \psi_0^2\psi\right)d\psi \tag{4.24}$$

$$\frac{1}{16\pi a_{1D}N}\left(\frac{d\psi}{dz}\right)^2 = \left[U(\psi) - U(\psi_0)\right] = \frac{1}{4}\left(\psi^2 - \psi_0^2\right)^2 \tag{4.25}$$

Taking the negative[‡] root and by separating variables, the solution is given by

$$\frac{1}{\psi_0}\tanh^{-1}\left(\frac{\psi}{\psi_0}\right) = (4\pi a_{1D}N)^{1/2}\ z \tag{4.26}$$

[‡]the possitive root corresponds to the anti-soliton or anti-kink $\psi(z) = -\psi_0\tanh\left(z/\sqrt{2}\xi\right)$

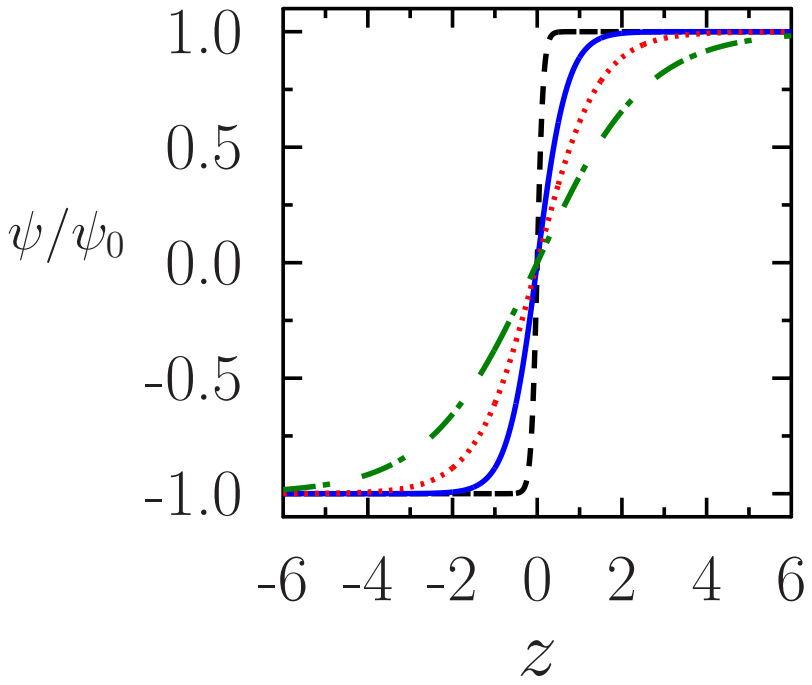

Figure 4.2: Kink soliton profile for different values of healing length. $\xi = 1.8$ (green line and dot), $\xi = 1$ (red dotted line), $\xi = 0.5$ (blue solid line) and $\xi = 0.1$ (black dashed line).

with the static solution or soliton with velocity zero $\psi(z)$, which is referred as a kink[§] (Figure 4.2) [2, 4]

$$\psi(z) = \psi_0 \tanh\left(\frac{z}{\sqrt{2}\xi}\right) \tag{4.27}$$

Here $(8\pi a_{1D} N \psi_0^2)^{-1} = (8n\pi a_{1D})^{-1} = \xi^2$. According this soliton, the wave function approaches its bulk value over the distance $\sim \xi$, in agreement with the healing length definition (Figure 4.3).

4.5.2 Moving dark solitons

For repulsive interactions the simplest example of a traveling soliton solution that propagate without distortion is obtained by extending to the whole of space the stationary solution to the GPE (4.20) [2, 4]. These solitons correspond to a localized modulation of the density profile characterized by a suppression of the density with respect to the bulk value (grey soliton). For convenience the typical length to describe the density modulation is given by the healing length ξ. It will be considered quasi-one-dimensional solutions where the wave function is z-dependent, through the combination $\tilde{z} = z - vt$ (with v the soliton velocity) and the condition $n = n_0$ when $z \to \pm\infty$. These considerations give rise

[§]"... since the phase of the wave function jumps discontinuously by π as z passes through zero..." [2].

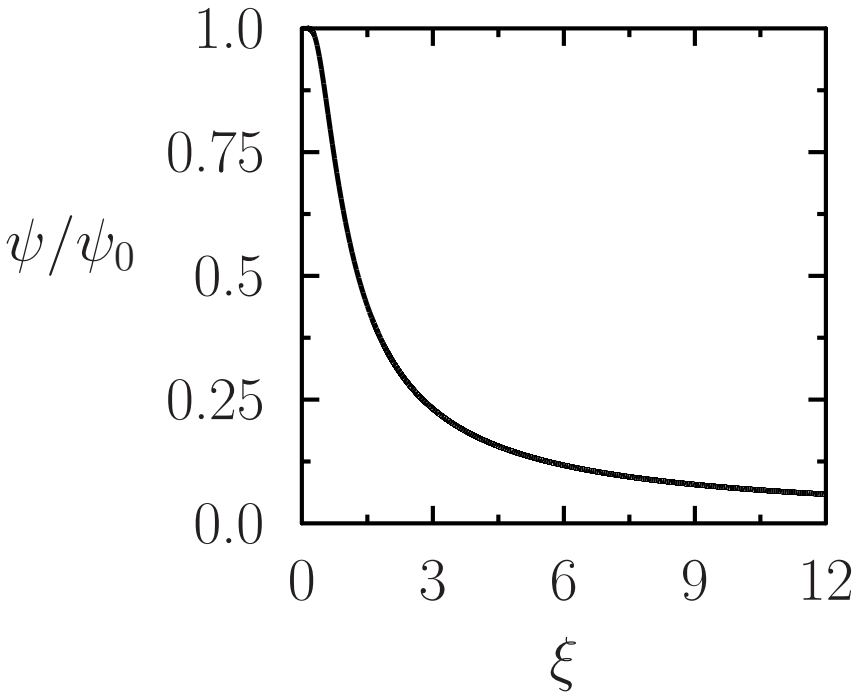

Figure 4.3: Effect of the healing length over the kink soliton. When $\xi \to 0$ the wave function tends its bulk. However, when the coherence length $\xi \to \infty$ the soliton can vanish.

to the wave function.

$$\psi(z,t) = f(\tilde{z}) \exp(-i\mu t) \tag{4.28}$$

Using this solution in the quasi-one-dimensional time-dependent GPE (4.10) with the external potential $V_z = 0$

$$i\frac{d\psi(z,t)}{dt} = \left[-\frac{1}{2}\frac{d^2}{dz^2} + 4\pi a_{1D} N |\psi(z,t)|^2\right] \psi(z,t) \tag{4.29}$$

so the corresponding derived respect to the time and the variable $\tilde{z} = z - vt$ are

$$\frac{d\psi}{dt} = \left(-v\frac{df}{d\tilde{z}} - i\mu f\right) \exp(-i\mu t) \qquad \frac{d^2\psi}{d\tilde{z}^2} = \frac{d^2 f}{d\tilde{z}^2} \exp(-i\mu t) \tag{4.30}$$

and defining $\tilde{z}/\xi = \zeta$ the equation (4.29) is

$$-\frac{iv}{\xi}\frac{df}{d\zeta} + \frac{1}{2\xi^2}\frac{d^2 f}{d\zeta^2} = \left(4\pi a_{1D} N |f|^2 - \mu\right) f \tag{4.31}$$

The product of this equation by f^* and subtracting the complex conjugated of the new equation allows obtaining

$$\frac{1}{2}\left(f^*\frac{d^2 f}{d\zeta^2} - f\frac{d^2 f^*}{d\zeta^2}\right) - iv\xi\left(f^*\frac{df}{d\zeta} + f\frac{df^*}{d\zeta}\right) = 0 \tag{4.32}$$

using derivation by parts and its complex conjugate, such that

$$\frac{d}{d\zeta}\left(f^*\frac{df}{d\zeta}\right) = f^*\frac{d^2f}{d\zeta^2} + \frac{df^*}{d\zeta}\frac{df}{d\zeta} \tag{4.33}$$

and integrating over ζ. The expression (4.32) becomes

$$f^*\frac{df}{d\zeta} - f\frac{df^*}{d\zeta} + c = 2iv\xi\left|f\right|^2 \tag{4.34}$$

where c is a constant. To construct a localized solution it is useful applying the conditions $|f| \to f_0$ (denotes the amplitude of the condensate wave function) and $df/d\zeta \to 0$ for $\zeta \to \pm\infty$, allowing get $c = 2iv\xi f_0^2$. So the final equation is

$$f^*\frac{df}{d\zeta} - f\frac{df^*}{d\zeta} = 2iv\xi\left(\left|f\right|^2 - f_0^2\right) \tag{4.35}$$

for the complex function $f = f_0\left(f_1 + if_2\right)$, the normalization $f_0 = \left(n_0/N\right)^{1/2}$ and with f_2 constant (to obtain an analytical solution) [2, 4], the imaginary part for the equation (4.35) is given by

$$f_2\frac{df_1}{d\zeta} = v\xi\left(1 - f_1^2 - f_2^2\right) \tag{4.36}$$

Moreover, using f on the equation (4.31) the corresponding imaginary part is

$$-v\xi f_0\frac{df_1}{d\zeta} = f_0 f_2\xi^2\left[4\pi a_{1D}Nf_0^2\left(f_1^2 + f_2^2\right) - \mu\right] \tag{4.37}$$

with the chemical potential for the bulk as $\mu = 4\pi a_{1D}Nf_0^2$. Thus, the equation is

$$\frac{df_1}{d\zeta} = \frac{4\pi a_{1D}N\xi f_0^2 f_2}{v}\left[1 - f_1^2 - f_2^2\right] \tag{4.38}$$

To ensure the consistency of the equations (4.36) and (4.38) is necessary

$$f_2^2 = \frac{v^2}{4\pi a_{1D}Nf_0^2} = \frac{v^2}{s^2} \tag{4.39}$$

with the sound velocity $s = \sqrt{4\pi a_{1D}n_0}$. Thereby substituting (4.39) in (4.38), the differential equation to f_1 is

$$\frac{df_1}{d\zeta} = \xi s\left[1 - f_1^2 - \frac{v^2}{s^2}\right] \tag{4.40}$$

with the respective solution

$$\frac{1}{\sqrt{1 - \frac{v^2}{s^2}}}\tanh^{-1}\left(\frac{f_1}{\sqrt{1 - \frac{v^2}{s^2}}}\right) = \xi s\zeta \tag{4.41}$$

or

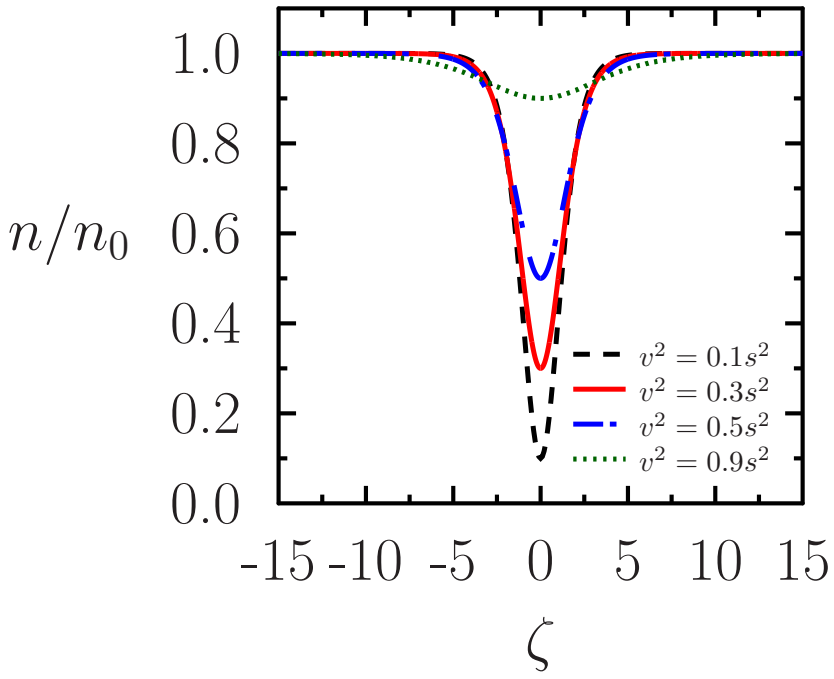

Figure 4.4: Density profile of a grey soliton. The width of the soliton increases as its velocity is close to the sound velocity according to the factor $\xi/\left(1-v^2/s^2\right)^{1/2}$.

$$f_1 = \sqrt{1-\frac{v^2}{s^2}}\tanh\left[\sqrt{1-\frac{v^2}{s^2}}\xi s\zeta\right] \tag{4.42}$$

with $\xi s\zeta = s\left(z-vt\right) = \left(z-vt\right)/\sqrt{2}\xi$ and $f_0 = \left(n_0/N\right)^{1/2}$ the wave function solution of the GPE (4.29) to repulsive interactions or defocusing cubic nonlinearity [2, 4, 65, 67] is a dark soliton which it corresponds to a moving hole on a background

$$\psi = \sqrt{\frac{n_0}{N}}\left\{i\frac{v}{s}+\sqrt{1-\frac{v^2}{s^2}}\tanh\left[\frac{z-vt}{\sqrt{2}\xi}\sqrt{1-\frac{v^2}{s^2}}\right]\right\}e^{-i\mu t} \tag{4.43}$$

with the associated density

$$n = n_0\left\{\frac{v^2}{s^2}+\left(1-\frac{v^2}{s^2}\right)\tanh^2\left[\frac{z-vt}{\sqrt{2}\xi}\sqrt{1-\frac{v^2}{s^2}}\right]\right\} \tag{4.44}$$

The density has a minimum in the center of the soliton (Figure 4.4) corresponding to

$$n_{min} = n_0\frac{v^2}{s^2} \tag{4.45}$$

this expression shows that the dark soliton velocity v is given by bulk sound velocity evaluated at the minimum density, i.e. as $s^2 = 4\pi a_{1D}n_0$ then $v = \left(4\pi a_{1D}n_{min}\right)^{1/2}$. When the dark soliton velocity is equal to zero the density profile corresponds with the static

solution profile obtained in (4.27) with minimum density equal to zero. This soliton is referred as black soliton [65]. In contrast, to $v \neq 0$ the minimum intensity doesn't drop to zero, such solitons are called gray. It is worth noting that the soliton width is determined by the factor $\xi/\left(1-v^2/s^2\right)^{1/2}$, according which the width increases as $v \to s$. Another important quantity to describe the system is the fluid velocity u [2, 58] which shows how changes the velocity of the condensate caused by the dark soliton motion. From the hydrodynamic relation (2.6) this velocity is given by $u = d\varphi/dz$ with

$$\tan\varphi = \frac{v}{s\gamma}\frac{1}{\tanh\left[\gamma\frac{\zeta}{\sqrt{2}}\right]} \tag{4.46}$$

defining $\gamma = \left(1-v^2/s^2\right)^{1/2}$ and $\zeta = (z-vt)/\xi$ such that $d\zeta = dz/\xi$, so.

$$u = v\frac{\tanh^2\left[\gamma\frac{z-vt}{\sqrt{2}\xi}\right]-1}{\tanh^2\left[\gamma\frac{z-vt}{\sqrt{2}\xi}\right]+\left(\frac{v}{s\gamma}\right)^2} \tag{4.47}$$

With some simple mathematical manipulations this velocity can be expressed like [2]

$$u = v\left(1-\frac{n_0}{n}\right) \tag{4.48}$$

Soliton energy. The energy of the dark soliton per unit surface perpendicular to the direction of propagation is defined as $\epsilon = E_{tot}/A$ and this can be evaluated taking the difference between the grand canonical energies in the presence $E_{with\,soliton}$ and in the absence of the soliton $E_{without\,soliton}$, in other words considering the quantity $E-\mu N$ instead of the energy itself. Thus the difference between energies $\triangle\left(E-\mu N\right) = E_{tot}$ is

$$\begin{aligned}
\triangle\left(E-\mu N\right) &= N\left[\left(E-\mu N\right)_{with\,soliton} - \left(E-\mu N\right)_{without\,soliton}\right] \\
&= AN\int_{-\infty}^{\infty} dz\left[\left(\frac{1}{2}\left|\frac{d\psi}{dz}\right|^2 + 2\pi a_{1D}N\left|\psi\right|^4 - \mu\left|\psi\right|^2\right)\right. \\
&- \left.\left(\frac{1}{2}\left|\frac{d\psi_0}{dz}\right|^2 + 2\pi a_{1D}N\left|\psi_0\right|^4 - \mu\left|\psi_0\right|^2\right)\right]
\end{aligned} \tag{4.49}$$

So

$$\epsilon = N\int_{-\infty}^{\infty} dz\left[\frac{1}{2}\left|\frac{d\psi}{dz}\right|^2 + 2\pi a_{1D}N\left(\left|\psi\right|^4 - \left|\psi_0\right|^4\right) - \mu\left(\left|\psi\right|^2 - \left|\psi_0\right|^2\right)\right]$$

or

$$\epsilon = N\int_{-\infty}^{\infty} dz\left[\frac{1}{2}\left|\frac{d\psi}{dz}\right|^2 + 2\pi a_{1D}N\left(\left|\psi\right|^2 - \left|\psi_0\right|^2\right)^2\right] \tag{4.50}$$

From the soliton (4.43) the first integral is

$$\begin{aligned}\frac{1}{2}\int_{-\infty}^{\infty} dz \left|\frac{d\psi}{dz}\right|^2 &= \frac{1}{4}\frac{n_0\gamma^4}{N\xi^2}\int_{-\infty}^{\infty} dz \left[\operatorname{sech}^4\left(\gamma\frac{z-vt}{\sqrt{2}\xi}\right)\right] \\ &= \frac{1}{4}\frac{n_0\gamma^4}{N\xi^2}\left(\frac{4\sqrt{2}\xi}{3\gamma}\right) \\ &= \frac{\sqrt{2}n_0}{3N\xi}\gamma^3 \end{aligned} \tag{4.51}$$

here was used the integral $\int_{-\infty}^{\infty} dx \operatorname{sech}^4 x = 4/3$.

The second integral is written like

$$\begin{aligned}2\pi a_{1D}N\int_{-\infty}^{\infty} dz \left(|\Psi|^2 - |\Psi_0|^2\right)^2 &= 2\pi a_{1D}N\left(\frac{n_0}{N}\right)^2\int_{-\infty}^{\infty} dz \left[\gamma^2\tanh^2\left(\gamma\frac{z-vt}{\sqrt{2}\xi}\right) - \gamma^2\right]^2 \\ &= 2\pi a_{1D}N\left(\frac{n_0}{N}\right)^2\gamma^4\int_{-\infty}^{\infty} dz \operatorname{sech}^4\left(\gamma\frac{z-vt}{\sqrt{2}\xi}\right) \\ &= \frac{2\sqrt{2}\mathcal{N}\xi}{3}\left(\frac{n_0}{N}\right)^2\gamma^3 \end{aligned} \tag{4.52}$$

with $8\pi a_{1D}N = N/\left(\xi^2 n_0\right)$. Thus, the energy is

$$\epsilon = \frac{2}{3}\gamma^3\left(\frac{\sqrt{2}n_0}{\xi}\right) \tag{4.53}$$

and as $\xi = 1/\sqrt{2}s$, finally the soliton energy per unit surface can be written as [2, 4]

$$\epsilon = \frac{4}{3}n_0 s\left(1 - \frac{v^2}{s^2}\right)^{3/2} \tag{4.54}$$

Note that the dark soliton energy decreases when its velocity increases. This behavior implies that dissipative effects (e.g. collisions with thermal excitations) give rise due to the acceleration of the soliton which vanishes as $v \to s$. The soliton energy for $v \ll s$ is

$$\epsilon = \frac{4}{3}n_0 s\left(1 - \frac{v^2}{s^2}\right)^{3/2} \approx \frac{4}{3}n_0 s\left(1 - \frac{3v^2}{2s^2}\right) \tag{4.55}$$

Thus, the dissipative effect is given by the term $\approx -2n_0v^2/s$ [2, 79] agree with the fact that the density modulation corresponds to a hole rather than a particle.

4.5.3 Bright solitons

In the case of negative scattering length (focusing nonlinearity in optics) the GPE has other kind of solutions called bright solitons. These are harder to observe due to the

collapse of the system for suciently high number of atoms. Nevertheless, in 2002 two groups [75, 76], showed the generation and propagation of solitons in ^{7}Li condensates. The main difference in both experiments was the number of atoms allowing to create just one soliton [75], whereas in [76] were produced trains of several solitons and these trains oscillated in a weak attractive trapping potential. Later, were created bright solitons in ^{85}Rb [77].

The static bright soliton solution can be obtained from the quasi-one-dimensional GPE for attractive interactions $a < 0$ and for $\mu < 0$. Thus

$$|\mu|\,\psi(z) = \left[\frac{1}{2}\frac{d^2}{dz^2} + 4\pi N\,|a_{1D}|\,|\psi(z)|^2\right]\psi(z) \tag{4.56}$$

The validity of the adiabatic approximation to get the quasi-1D model of the GPE with bright solitons is discussed by [57]. In a same way using the procedure outlined earlier to the static dark soliton is possible to obtaining the equation

$$\left(\frac{d\psi}{dz}\right)^2 = 4\left[\frac{|\mu|}{2}\psi^2 - \pi N\,|a_{1D}|\,\psi^4\right] + c \tag{4.57}$$

the integration constant c, is given for the boundary conditions [51] such that both ψ and $d\psi/dz$ vanish as $z \to \pm\infty$, according to these $c = 0$. So

$$\frac{d\psi}{dz} = -\left(2\,|\mu|\,\psi^2 - 4\pi N\,|a_{1D}|\,\psi^4\right)^{1/2} \tag{4.58}$$

with the usual solution

$$z = \sqrt{\frac{1}{2\,|\mu|}}\,\mathrm{sech}^{-1}\left(\sqrt{\frac{2\pi N\,|a_{1D}|}{|\mu|}}\psi\right) \tag{4.59}$$

Or the static bright soliton (Figure 4.5)

$$\psi \;=\; \psi_0\,\mathrm{sech}\left(\frac{z}{\sqrt{2}\xi}\right) \tag{4.60}$$

where there were used the definitions $\psi_0^2 = |\mu|\,/\,(2\pi N\,|a_{1D}|)$ and $\xi^2 = 1/\,(8\pi N\,|a_{1D}|\,\psi_0^2)$ then $|\mu| = 1/\,(4\xi^2)$. The healing length ξ (Figure 4.6) characterizes the soliton width.

The Figure (4.7) compares the analytical bright soliton (4.60) with the numerical solution (obtained by the split-step Crank–Nicolson method [24]) of the quasi-one-dimensional GPE (4.10) for different values of the trapping potential frequency ω_z^2 in the z direction and the parameter $N\,|a_{1D}|$. The presence of the trap implies that the quasi-1D GPE doesn't have an analytical solution against the $V_z = 0$ case. Therefore is useful using a variational approximation which usually has a Gaussian form because of the relative ease for the different calculations. Although sometimes the soliton-like ansatz is applied too.

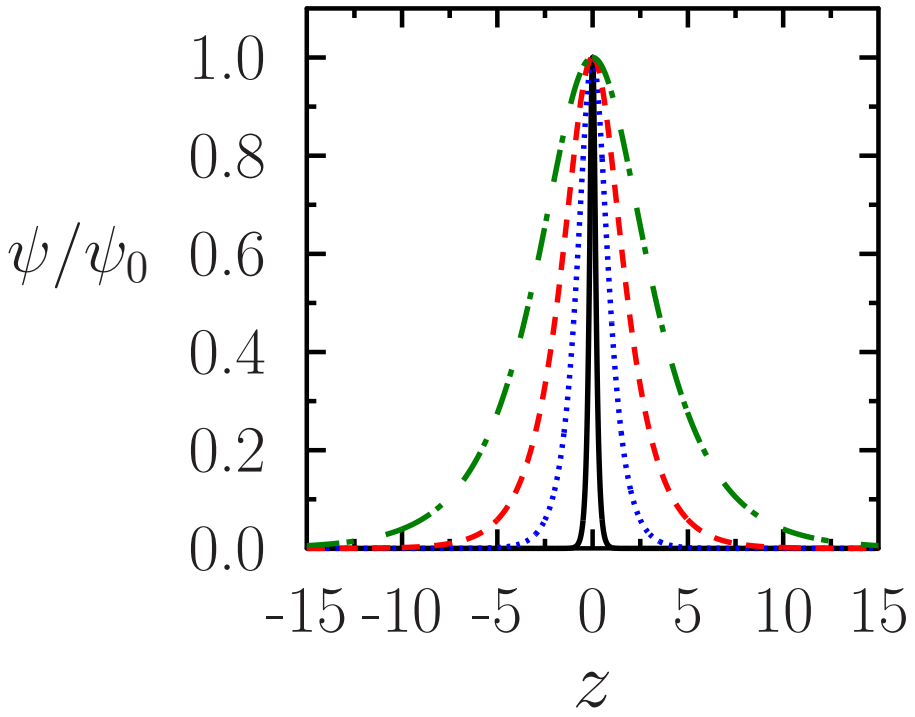

Figure 4.5: Profile of a bright soliton for different values of healing length. $\xi = 0.1$ (black solid line), $\xi = 0.5$ (blue dotted line), $\xi = 1$ (red dashed line) and $\xi = 1.8$ (green line and dot).

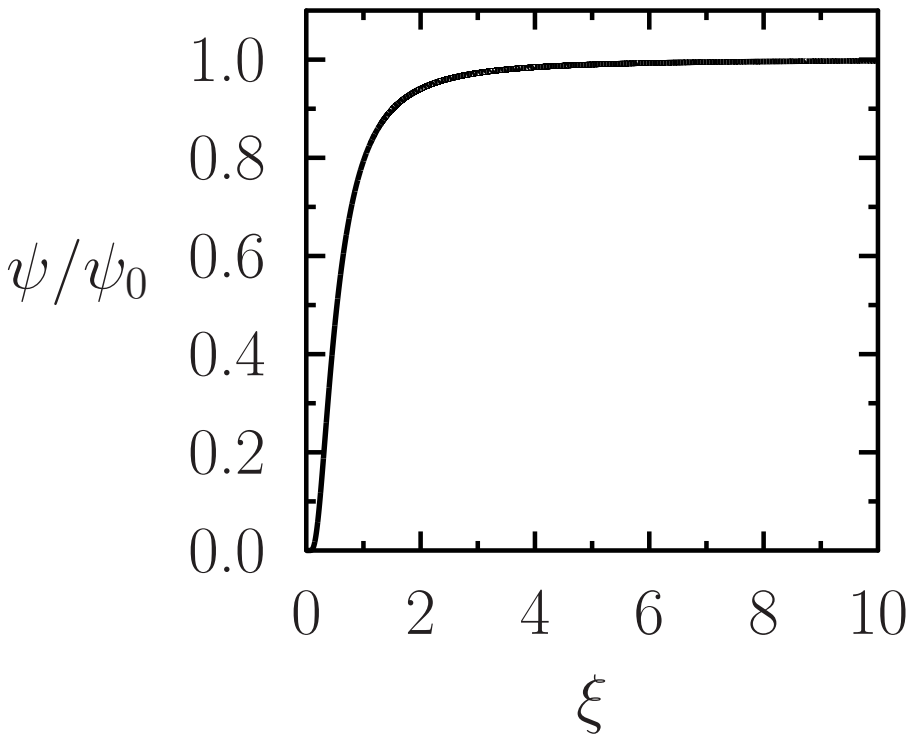

Figure 4.6: Effect of the healing length over the brigth soliton. While $\xi \to 0$ the soliton can be eliminated. When the coherence length $\xi \to \infty$ the wave function tends its bulk.

The absence of the trap allows prove that the theoretical solution matches with the numerical calculus and both profiles are very close to each. Nevertheless, when the trap is present and it is increasing its value, the condensate is getting thinner and longer, therefore the analytical solution (4.60) is not useful describing the system. As the goal of this dissertation is focused in the bright soliton theory of a condensate with dipolar interaction under transverse confinement, is useful to know the behavior in the non-dipolar case as part of such study. The Figure (4.8) presents some physical observables like the chemical

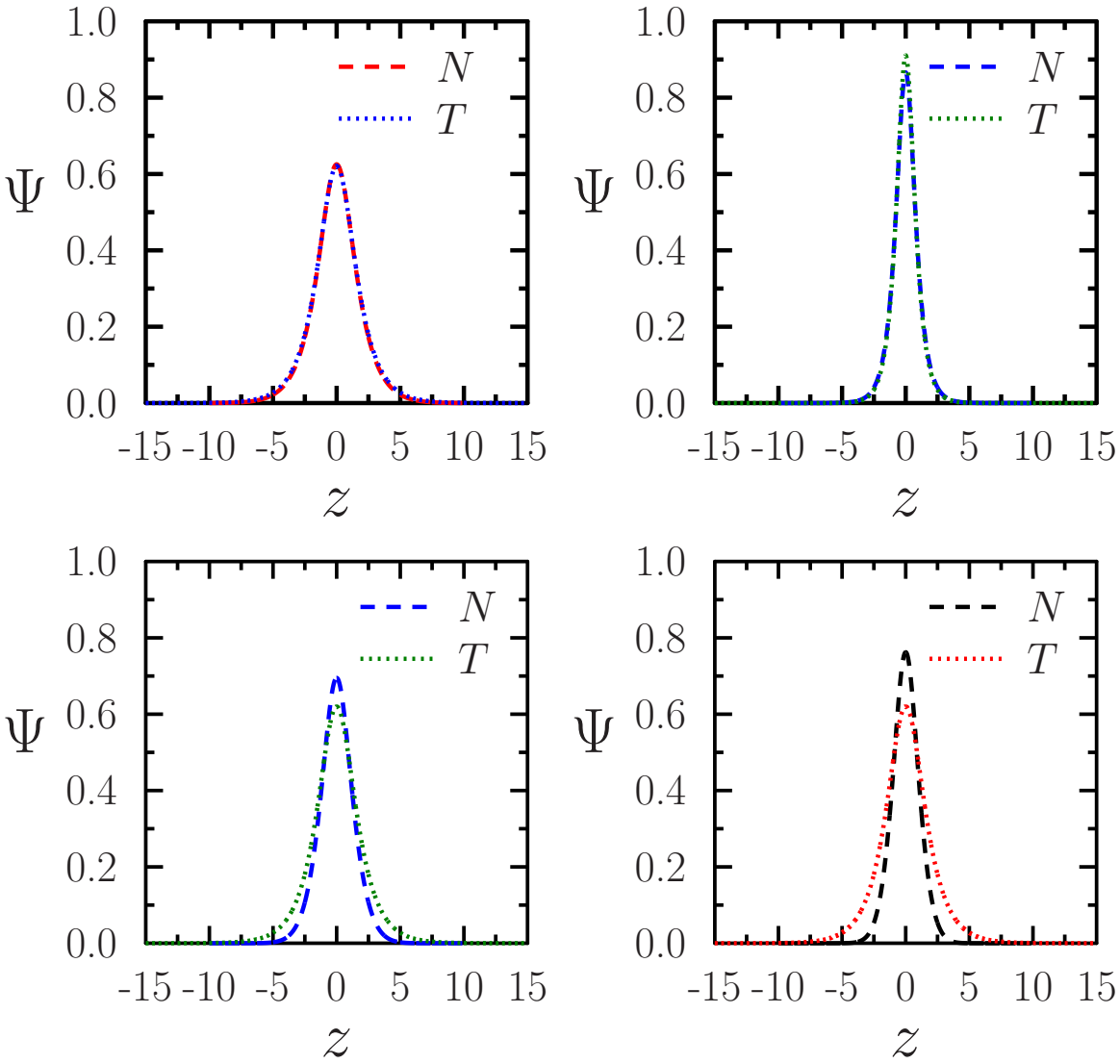

Figure 4.7: Numerical (N) and theoretical (T) ground state solution to the quasi-one-dimensional GPE (4.10) with different values of $N|a_{1D}|$ and the trapping potential frequency ω_z^2. In the upper both figures have $\omega_z = 0$. Top left $N|a_{1D}| = 1.5$ (red dashed line) and the analytical solution given by (4.60) (blue dotted line). Top right $N|a_{1D}| = 3.0$ (blue dashed line) and the theoretical solution (4.60) (green dotted line). The two lower figures have $N|a_{1D}| = 1.5$. Bottom left $\omega_z^2 = 0.1$ (blue dashed line) and theoretical soliton (green dotted line). Bottom right numerical solutions for $\omega_z^2 = 0.35$ (black dashed line) and the theoretical soliton (red dotted line). The numerical solutions were obtained by the programs provided in [24].

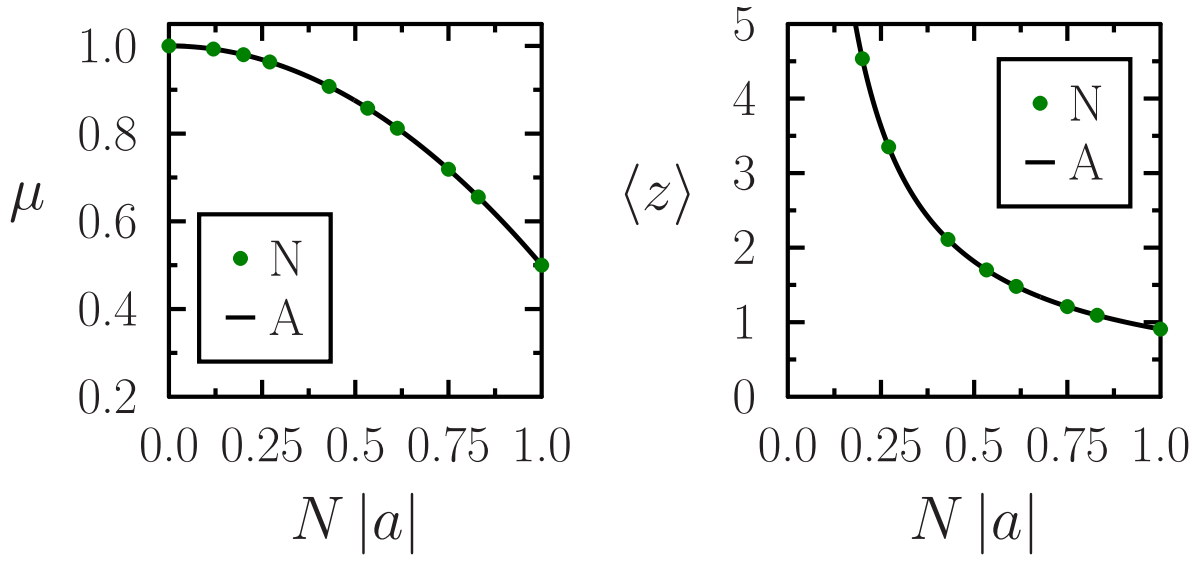

Figure 4.8: Chemical potential μ and root mean square size $\langle z \rangle$ versus $N\,|a|$ for a quasi-1D BEC. Are shown the numerical results (N) from the Crank–Nicolson method and the analytical solution (A) using the soliton of a BEC without trap (4.60).

potential μ and root mean square size $\langle z \rangle$ versus the parameter $N\,|a|$ of a quasi-1D BEC in the z direction, without the presence of the harmonic trap. Moreover the effect of the trap reduces the root mean square size $\langle z \rangle$ as expected and as it was above verified by means of the wave function of the Figure (4.7). Likewise those results agree with the numerical solution of the 3D GPE without trap in z direction as it will be seen later at the end of the Chapter in the Figure (4.12).

The analytical moving bright solitons can be obtained in more detail through the inverse scattering transform developed by Zakharov and Shabat (1971-1973), but these are also found by means of the Galilean invariance of the wave function to the GPE. The wave function that describes the BEC is not a Galilean invariant[¶], nevertheless the invariance can be satisfied using the transformation [4]

$$\psi\left(z,t\right) \rightarrow \psi\left(z-vt,t\right)\exp\left[i\left(vz-\frac{1}{2}v^{2}t\right)\right] \tag{4.61}$$

where the velocity v is constant. In the coordinate system where the condensate is in equilibrium the wave function is

$$\psi = \left(\frac{n_0}{N}\right)^{1/2}\exp(-i\mu t) \tag{4.62}$$

In the frame where the fluid moves with velocity v the wave function takes the form $\psi = \left(n_0/N\right)^{1/2}\exp(iS)$ where

$$S\left(z,t\right) = vz - \left(\mu + \frac{1}{2}v^{2}\right)t \tag{4.63}$$

[¶]The change in the wave function is related with the superfluid behavior displayed for the BEC [4]

The new phase shows that the superfluid velocity is proportional of its derived

$$v = \frac{\partial S(z,t)}{\partial z} \tag{4.64}$$

corresponding with (2.6) in the hydrodynamic study. Therefore, the moving bright soliton is [4]

$$\psi = \psi_0 \operatorname{sech}\left(\frac{z-vt}{\sqrt{2}\xi}\right) \exp\left\{-i\left[\left(\mu+\frac{1}{2}v^2\right)t - vz\right]\right\} \tag{4.65}$$

It is worth noting that the velocity of a dark soliton (4.43) cannot exceed the sound velocity, since there is not an inconvenient on the velocity of bright soliton (4.65).

4.6 Collapse of a BEC with attractive interactions

The presence of bright solitons in a BEC with attractive atomic interactions gives rise to rich nonlinear phenomena, e.g., in 3D and under transverse confinement, the bright soliton dynamics is present in the axial direction and their self-trapped nature allows these have significant advantages for atom interferometry applications [80]. Different numerical solutions and variational methods has been used to analyse the GPE solutions with attractive interactions [57, 74, 81, 82, 83], within a large range of axial trap geometries confining, expulsive and zero axial trapping. Another relevant property of attractive BECs in 3D is the instability by collapse (in 3D, a homogeneous condensate with attractive interactions is unstable and should collapse such as has seen in the Chapter one). However, the presence of a trap can stabilize the condensate and avoid the collapse up to a critical number of atoms. Here, it will be shown two kinds of variational ansatz to find the critical parameter $N_c|a|$ of the collapse in a 3D condensate under transverse confinement i.e., without trap in the z direction. The most common trial wave function is a Gaussian, however the procedure is also applicable to a soliton-like ansatz in the axial direction and Gaussian in the radial one. The most relevant scope shows that the variational algebraic equations to the widths (w_ρ and w_z), $\partial E/\partial w_\rho = \partial E/\partial w_z = 0$ have analytical solutions in terms of hyperbolic functions of the parameter $N|a|$. This kind of solutions are consistent with the numerical results.

4.6.1 Variational approximation and numerical results

For a 3D BEC with attractive interactions ($a < 0$) and under harmonic transverse confinement, the condensate energy from (1.33) is given by

$$E = \int d\mathbf{r}\left[\frac{N}{2}|\nabla\Psi(\mathbf{r})|^2 + \frac{\rho^2}{2}N|\Psi(\mathbf{r})|^2 - 2\pi|a|N^2|\Psi(\mathbf{r})|^4\right] \tag{4.66}$$

here $\Psi(\mathbf{r}) = \Psi(\rho, z)$. For ease the frequency of the trap is taken as $\omega_\perp^2 = 1$.

Taking as normalized trial ansatz a gaussian function [74, 82] in both transversal and axial direction. Thus,

$$\Psi(\rho, z) = \left(\frac{1}{w_\rho^2\, w_z \pi^{3/2}}\right)^{1/2} \exp\left[-\left(\frac{\rho^2}{2w_\rho^2} + \frac{z^2}{2w_z^2}\right)\right] \tag{4.67}$$

Where w_ρ and w_z are the variational parameters. Therefore the energy (4.66) is (for more details about the integrals see the Appendix E.1)

$$E = \frac{N}{4}\left[2\left(1 + \frac{1}{w_\rho^4}\right) w_\rho^2 + \frac{1}{w_z^2}\right] - \frac{N^2\,|a|}{\sqrt{2\pi} w_\rho^2\, w_z} \tag{4.68}$$

In a same way it was used as normalized trial ansatz a bright soliton-like function in the axial direction and a gaussian form in the radial one [74, 82, 83]. So,

$$\Psi(\rho, z) = \left(\frac{1}{2\pi w_z\, w_\rho^2}\right)^{1/2} \operatorname{sech}\left(\frac{z}{w_z}\right) \exp\left(-\frac{\rho^2}{2w_\rho^2}\right) \tag{4.69}$$

with the corresponding energy (4.66) (for more details about the integrals see the Appendix E.1)

$$E = \frac{N}{4}\left[2\left(1 + \frac{1}{w_\rho^4}\right) w_\rho^2 + \frac{2}{3w_z^2}\right] - \frac{N^2\,|a|}{3w_\rho^2\, w_z} \tag{4.70}$$

The procedure outlined below is for the Gaussian solution. Nevertheless, this also applies to the soliton-like solution giving rise to similar results. To obtain the collapse parameter $N_c\,|a|$, it is necessary find the minimal of the energy respect to the variational parameters w_ρ and w_z. So taking the partial derivatives of the Gaussian energy (4.68) with respect to w_ρ and w_z and equating to zero $\partial E/\partial w_\rho = \partial E/\partial w_z = 0$, the resulting equations to find the critical points are

$$w_\rho^4 - 1 + \frac{|\alpha|}{w_z} = 0 \tag{4.71}$$

$$w_z = \frac{w_\rho^2}{|\alpha|} \tag{4.72}$$

where $|\alpha| = 2N\,|a|/\sqrt{2\pi}$. The Jacobean $J = \left(\partial_{w_\rho}^2 E\right)\left(\partial_{w_z}^2 E\right) - \left(\partial_{w_\rho}\partial_{w_z} E\right)^2$, defines whether these critical points are saddle points, minima or maxima. If $J < 0$ there is a saddle point. If $J = 0$ the test is inconclusive. When $J > 0$ further it is necessary examining the sing of $\partial_{w_\rho}^2 E$ or $\partial_{w_z}^2 E$, if these second derivates are positive the point is a minimum, otherwise it is a maximum [83]. In the present case it will be considered the $J > 0$ stage. Substituting (4.72) in (4.71) the result is a sixth-degree polynomial equation, which can be treated as third degree polynomial equation (Appendix (E.2)).

$$w_\rho^6 - w_\rho^2 + |\alpha|^2 = 0 \tag{4.73}$$

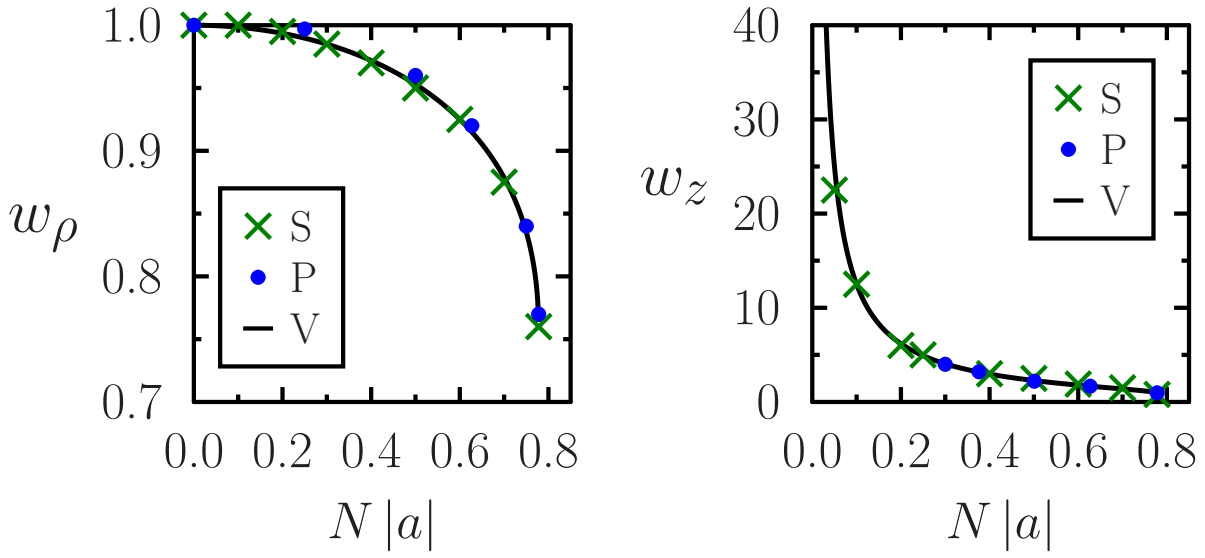

Figure 4.9: Gaussian variational approximation of a 3D bright soliton. Are compared the variational (V) functions to the widths w_ρ (4.74) and w_z (4.75) with the variational results of Salasnich (S) *et al* [81] and Pérez-García (P) *et al* [25].

The only solution to w_ρ which give rise a positive Jacobean and hence a minimum in the variational energy (4.68) it is shown in the Figure (4.9) and it is given by

$$w_\rho = \left\{ \frac{2}{\sqrt{3}} \cos\left[\frac{1}{3} \cos^{-1}\left(-\frac{3\sqrt{3}}{\pi} \left(N\,|a| \right)^2 \right) \right] \right\}^{1/2} \tag{4.74}$$

The respective solution to w_z is shown in the Figure (4.9), and this has the form

$$w_z = \sqrt{\frac{2\pi}{3}} \frac{1}{N\,|a|} \cos\left[\frac{1}{3} \cos^{-1}\left(-\frac{3\sqrt{3}}{\pi} \left(N\,|a| \right)^2 \right) \right] \tag{4.75}$$

These functions agrees with the variational results of Pérez-García *et al* [25] and Salasnich *et al* [81] as it is shown in the Figure (4.9).

From above solutions (4.74) and (4.75) the collapse point in a 3D BEC is present in the $\cos^{-1}$ argument, i.e. the $\cos^{-1}$ function is undefined when

$$-\frac{3\sqrt{3}}{\pi} \left(N\,|a| \right)^2 > -1 \tag{4.76}$$

hence, a BEC is unstable whereas

$$N\,|a| < \left(\frac{\pi^2}{27} \right)^{1/4} \approx 0.778 \tag{4.77}$$

In other words,

- for a gaussian ansatz in the variational approximation with attractive interactions a

BEC can be stable in the range

$$-0.778 < Na < 0 \tag{4.78}$$

- In a same way for a soliton-like ansatz in the variational approximation with attractive interactions, a BEC can be stable when

$$N|a| < \left(\frac{1}{3}\right)^{1/4} \approx 0.760 \tag{4.79}$$

or

$$-0.760 < Na < 0 \tag{4.80}$$

The physical meaning of the previous results shown that while the attractive interaction ($a < 0$) dominates the kinetic energy the condensate shrinks, but once $N|a| < N_c|a|$ this becomes so attractive that growth peak height is stopped by inelastic collisions. In consequence this presents a sudden explosion and the atoms are ejected outward[‖], However the collapse occurs intermittently (for more details a good reference is [84]). The Figures (4.10) and (4.11) plot the energy per particle in the Gaussian case for different values of the parameter $N|a|$ as function of the widths w_ρ and w_z respectively, including the collapse value $N_c|a|$. The other hand, when the radial trap frequency is different to 1, for a Gaussian ansatz, the critical parameter is given by $N_c|a| \approx 0.778/\omega_\perp^{1/2}$. For a soliton-like ansatz the critical parameter takes the form $N_c|a| \approx 0.760/\omega_\perp^{1/2}$. So it is possible manipulate the collapse range with the radial trap frequency.

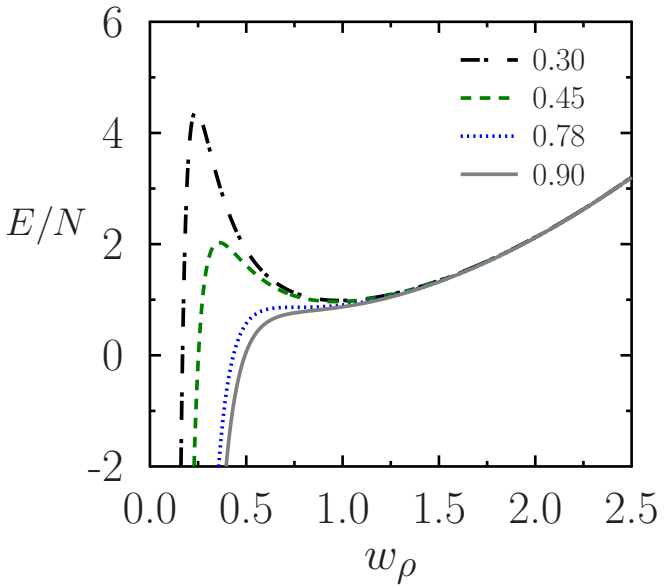

Figure 4.10: Energy per particle for a Gaussian ansatz as a function of the variational parameter w_ρ for different values of the interaction strength $N|a|$. The dotted curve corresponds to the critical value at which the condensate becomes unstable.

[‖]The phenomenon looks very familiar with a supernova, so the JILA group called it "Bosenova".

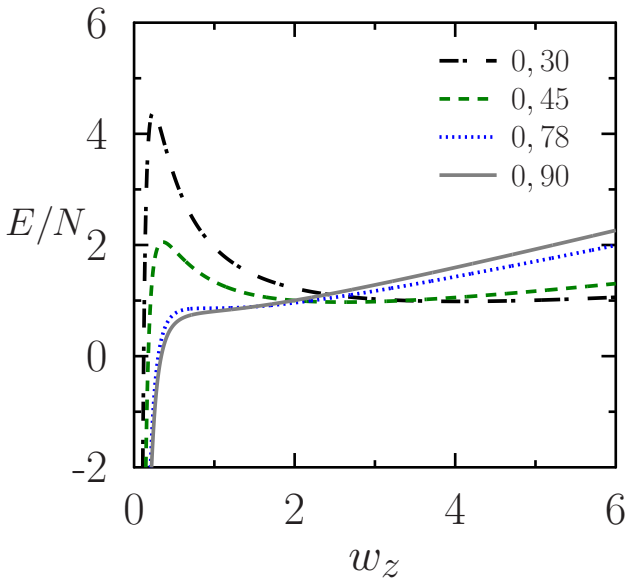

Figure 4.11: Energy per particle for a Gaussian ansatz as a function of the variational parameter w_z for different values of the interaction strength $N|a|$. The dotted curve corresponds to the critical value at which the condensate becomes unstable.

The above variational critical parameters in both cases Gaussian and soliton-like ansatz are consistent with the variational value -0.78 of [25, 81]. Solving numerically the GPE in three-dimensions without the trap potential in the z direction by means of the split-step Crank–Nicolson method, using the programs provided in [24], the collapse value is given by ≈ -0.679. This result is in good agreement with the numerical value -0.676 obtained in [57] where is minimized the mean-field Hamiltonian with the steepest-descent method; the numercial result -0.676 obtained in [85]; the value -0.67 from [86] in these two works is employed the Crank–Nicholson method and the result $-2/3$ from [81] where is used an analytic quasi-one-dimensional model. However, there is no match with the value -0.6268 ± 0.0035 from [83] obtained through the imaginary time relaxation method.

From the numerical solution (N) [24] and the variational approximation (V) (4.74) and (4.75) of the GPE in three dimensions under harmonic transverse confinement are plotted in the Figure (4.12) the results for the root mean square (rms) sizes $\langle\rho\rangle$ and $\langle z\rangle$ and the chemical potential μ. When the interaction vanishes the solution of the system corresponds with that of a harmonic oscillator in the ground state confined in the radial direction $\langle\rho\rangle$, free in the transverse axis $\langle z\rangle$ and with the chemical potential μ equal to the energy per particle as was expected. Likewise can be verified the instability value beyond which the condensate should collapse. The results of a condensate described by the three-dimensional mean-field GPE are consistent with those of the quasi-one-dimensional counterpart (Figure 4.8) nevertheless the instability linked to the collapse is a phenomenon that arises in a three-dimensional model as was expected.

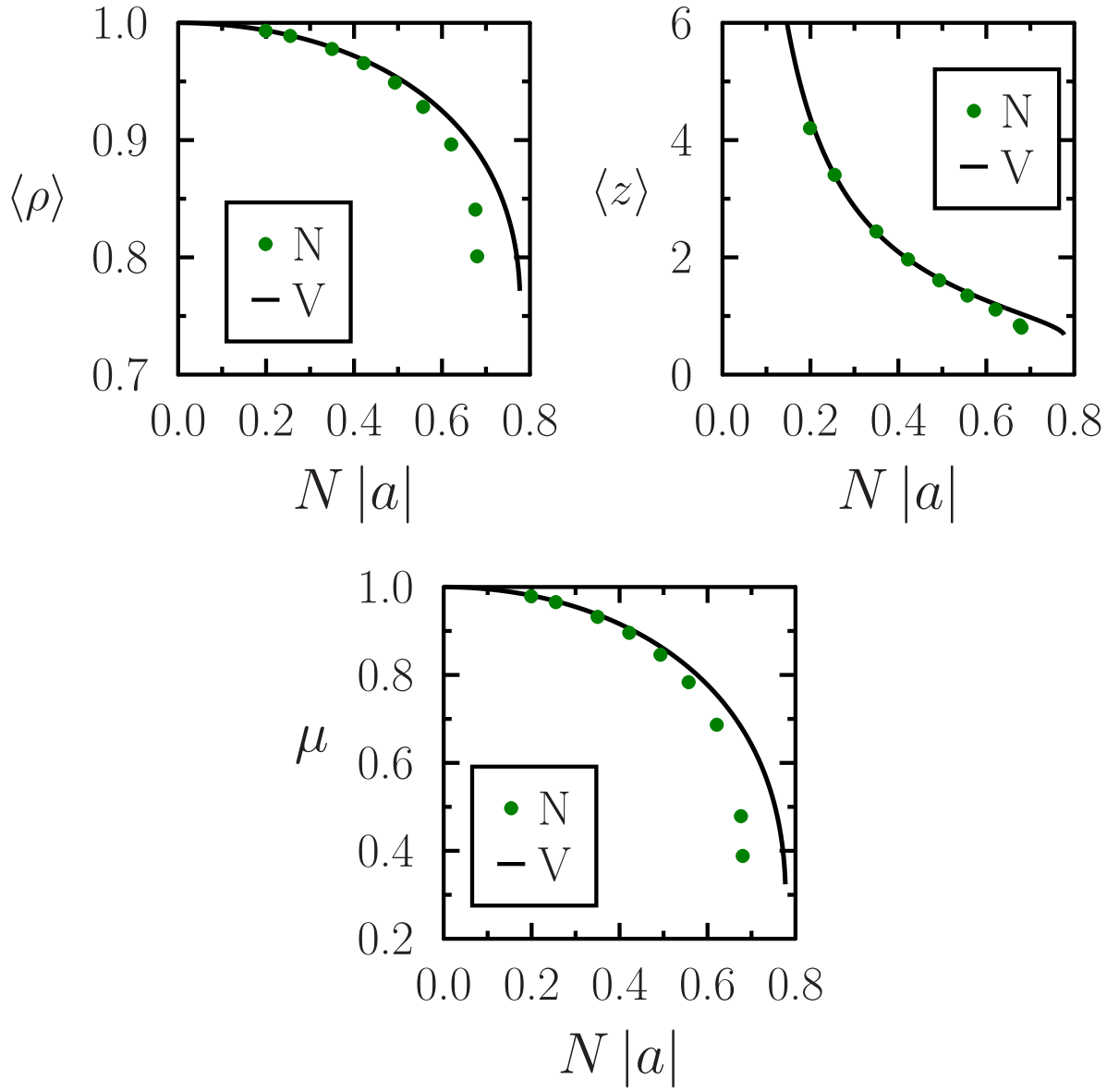

Figure 4.12: Root mean square (rms) sizes $\langle\rho\rangle$ and $\langle z\rangle$ and chemical potential μ from the numerical solution (N) and the variational approximation (V).

Chapter 5

Quasi-one-dimensional dipolar BEC

This Chapter is devoted to the study of the bright solitons existence in three different dipolar condensates ^{52}Cr, ^{168}Er and ^{164}Dy under harmonic transverse confinement. The study is performed to the three- and quasi-one-dimensional models. In analogy with the non-dipolar stage is introduced the dimensional reduction from 3D to 1D. The results obtained are plotted as stability diagrams, profiles of the wave function, plot of the chemical potential and the root mean square sizes. At the end of Chapter it is showing the effect of the phase diference δ with values $\delta = 0$ and $\delta = \pi$ for different velocities in the dynamics collision of a train of two bright solitons in the threee quasi-1D dipolar condensates above.

5.1 Reduction from 3D to 1D in the DGPE

In a same way as it was done the dimensional reduction from 3D to 1D in the Chapter 4 for a non-dipolar condensate, it is possible to find a counterpart in the dipolar condensate. The reduction from 3 to 1 dimension is achieved using the adiabatic approximation [54, 55, 56] such that the wave function to the mean-field equation (3.20) can be decomposed as $\Psi(\mathbf{r},t) = \kappa(\rho)\,\phi(z,t)$, or

$$\Psi(\mathbf{r},t) = \left(\frac{1}{\pi a_\rho^2}\right)^{1/2} \exp\left(-\frac{\rho^2}{2\,a_\rho^2}\right) \phi(z,t) \tag{5.1}$$

where a_ρ is the radial harmonic oscillator length and it fulfills $\omega_\perp a_\rho^2 = 1$. Substituting this ansatz $\Psi(\mathbf{r},t)$ in the DGPE (3.20), multipliying by $\kappa^*(\rho)$ and integrating in ρ (using the normalization* $\int d^2\rho\,|\kappa|^2 = 1$), this leads to the quasi-one-dimensional DGPE

$$\begin{aligned} i\frac{\partial\phi(z,t)}{\partial t} &= \left[-\frac{1}{2}\frac{\partial^2}{\partial z^2} + \frac{1}{2}\Omega_z^2 z^2 + \frac{2\,aN}{a_\rho^2}\,|\phi(z,t)|^2\right. \\ &+ \left. N\int_{-\infty}^{\infty} dz'\,U_{dd}^{1D}(z-z')\,|\phi(z',t)|^2\right]\phi(z,t) \end{aligned} \tag{5.2}$$

*Useful relations

$$\int_0^\infty d^2\rho\,|\kappa|^4 = \frac{1}{2\pi a_\rho^2} \qquad\qquad \phi(z,t) = \phi(z,t)\exp(i\omega_\rho t)$$

where [87] (for more details Appendix F)

$$U_{dd}^{1D}\left(z-z'\right)=\frac{1}{2\pi}\int_{-\infty}^{\infty}dq_z\exp\left(iq_zz\right)V_{1D}\left(q_z\right) \tag{5.3}$$

and

$$V_{1D}\left(q_z\right)=\frac{C_{dd}}{6\pi}\int_0^{\infty}dq_\rho\,q_\rho\left(3\frac{q_z^2}{q_\rho^2+q_z^2}-1\right)\exp\left(-\frac{q_\rho^2\,a_\rho^2}{2}\right) \tag{5.4}$$

5.2 Variational approximation

The time-independent Gaussian variational ansatz to the cigar-shaped DBEC is

$$\phi\left(z\right)=\left(\frac{1}{w_z^2\pi}\right)^{1/4}\exp\left(-\frac{z^2}{2w_z^2}\right) \tag{5.5}$$

with w_z the variational parameter. However, trying to find the energy using this wave function in the general form to the quasi-one-dimensional model (5.2) it implies integrals of the non-trivial dipolar contribution (5.3). Instead it is easier obtaining the three-dimensional Gaussian energy and considering the quasi-one-dimensional energy like a special case of this. Thus, the 3D Gaussian ansatz is (4.67)[11, 13, 87, 88]

$$\Psi\left(\rho,z\right)=\left(\frac{1}{w_\rho^2\,w_z\pi^{3/2}}\right)^{1/2}\exp\left[-\left(\frac{\rho^2}{2w_\rho^2}+\frac{z^2}{2w_z^2}\right)\right] \tag{5.6}$$

and substituting this wave function in the 3D dipolar energy (3.28), it leads to

$$E=\frac{N}{4}\left[2\left(\Omega_\rho^2+\frac{1}{w_\rho^4}\right)w_\rho^2+\frac{1}{w_z^2}+\Omega_z^2w_z^2\right]+\frac{N^2a}{\sqrt{2\pi}w_\rho^2\,w_z}+E_{dd} \tag{5.7}$$

here E_{dd} is the dipolar energy and the trap potential is defined as

$$V\left(\mathbf{r}\right)=\frac{1}{2}\left(\Omega_\rho^2\rho^2+\Omega_z^2z^2\right) \tag{5.8}$$

As mentioned in Appendix (F), the dipolar contribution is easily calculated in the Fourier space. So the energy takes the form (F.3)

$$E_{dd}=\frac{1}{2\left(2\pi\right)^3}\int d\mathbf{k}\,\tilde{n}^2\left(\mathbf{k}\right)\tilde{U}_{dd}\left(\mathbf{k}\right) \tag{5.9}$$

In a same way the Fourier transform of the density still a Gaussian, like (F.6)

$$\tilde{n}\left(\mathbf{k}\right)=\exp\left[-\frac{1}{4}\left(k_\rho^2w_\rho^2+k_z^2w_z^2\right)\right] \tag{5.10}$$

and the dipole dipole Fourier transform $\tilde{U}_{dd}\left(\mathbf{k}\right)$ (Appendix B)

$$\tilde{U}_{dd}\left(\mathbf{k}\right)=\frac{C_{dd}}{3}\left(3\frac{k_z^2}{\mathbf{k}^2}-1\right) \tag{5.11}$$

Using spherical coordinates (with magnetization in z direction), the substitution $q = kw_\rho$ and the definition $\kappa = w_\rho/w_z$ the dipolar energy takes the form

$$\begin{aligned} E_{dd} &= \frac{N^2 C_{dd}}{6\left(2\pi\right)^2 w_\rho^3} \int_0^\infty dq \int_0^\pi d\theta\, q^2 \sin\theta \left(3\cos^2\theta - 1\right) \exp\left[-\frac{q^2}{2}\left(\sin^2\theta + \kappa^{-2}\cos^2\theta\right)\right] \\ &= \frac{N^2 C_{dd}}{6\left(2\pi\right)^2 w_\rho^3} \sqrt{\frac{\pi}{2}} \int_0^\pi d\theta \frac{\sin\theta\left(3\cos^2\theta - 1\right)}{\left(\sin^2\theta + \kappa^{-2}\cos^2\theta\right)^{3/2}} \end{aligned} \tag{5.12}$$

with the substitution $u = \cos\theta$ the energy is

$$\begin{aligned} E_{dd} &= \frac{N^2 C_{dd}}{3\left(2\pi\right)^2 w_\rho^3} \sqrt{\frac{\pi}{2}} \int_0^1 du \frac{3u^2 - 1}{\left[1 + \left(\kappa^{-2} - 1\right) u^2\right]^{3/2}} \\ &= -\frac{N^2 a_{dd}}{\sqrt{2\pi} w_\rho^2 w_z} f\left(\kappa\right) \end{aligned} \tag{5.13}$$

where $a_{dd} = C_{dd}/12\pi$, $0 \leq \kappa < 1$[†] and the function $f\left(\kappa\right)$ is defined as [11, 13, 35, 89]

$$\begin{aligned} f\left(\kappa\right) &= \frac{1}{\kappa} \int_0^1 du \frac{1 - 3u^2}{\left[1 + \left(\kappa^{-2} - 1\right) u^2\right]^{3/2}} \\ &= \frac{1}{\kappa}\left[\kappa - \frac{3\kappa^3}{\left(1 - \kappa^2\right)^{3/2}}\left[\sinh^{-1}\sqrt{\kappa^{-2} - 1} - \tanh\left(\sinh^{-1}\sqrt{\kappa^{-2} - 1}\right)\right]\right] \end{aligned} \tag{5.14}$$

using the identity $\sinh^{-1}\sqrt{\kappa^{-2} - 1} = \tanh^{-1}\sqrt{1 - \kappa^2}$[‡] the function $f\left(\kappa\right)$ becomes

$$f\left(\kappa\right) = \frac{1 + 2\kappa^2 - 3\kappa^2 d\left(\kappa\right)}{1 - \kappa^2} \tag{5.15}$$

and the function $d\left(\kappa\right)$ is defined as

$$d\left(\kappa\right) = \frac{\tanh^{-1}\sqrt{1 - \kappa^2}}{\sqrt{1 - \kappa^2}} \qquad\qquad \kappa = \frac{w_\rho}{w_z} \tag{5.16}$$

The function $f\left(\kappa\right)$, is monotonically decreasing as it is plotted in the Figure (5.1). For $\kappa = 1$ the density distribution of the condensate is spherical and the dipole dipole interaction does not contribute. The function has asymptotic values $f\left(\kappa \to 0\right) = 1$ (cigar-shaped DBEC) and $f\left(\kappa \to \infty\right) = -2$ (disk-shaped DBEC) and it changes the sign in $\kappa = 1$.

[†]The other hand when $\kappa \geq 1$ it is necessary to performing the change

$$\frac{\tanh^{-1}\sqrt{1 - \kappa^2}}{\sqrt{1 - \kappa^2}} \to \frac{\tan^{-1}\sqrt{\kappa^2 - 1}}{\sqrt{\kappa^2 - 1}}$$

[‡]Defining $\sinh^{-1}\sqrt{\kappa^{-2} - 1} = x$ and from $\cosh^2 x - \sinh^2 x = 1$ then $\cosh^2 x = 1/\kappa^2$ and $x = \tanh^{-1}\sqrt{1 - \kappa^2}$

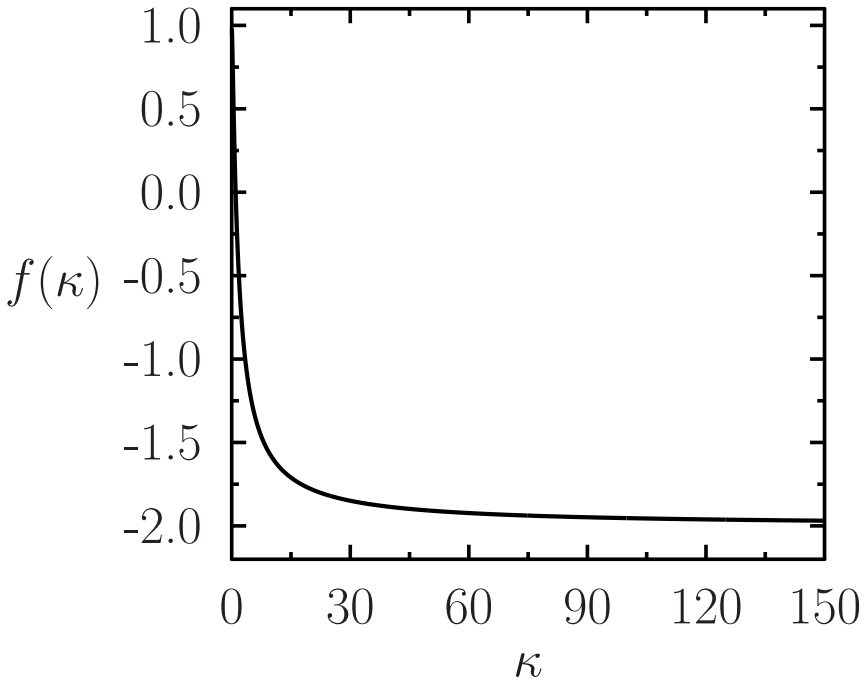

Figure 5.1: $f(\kappa)$ as function of κ in the dipolar mean-field energy.

Finally, the 3D dipolar BEC energy is given by [11, 87, 88]

$$E = \frac{N}{4}\left[2\left(\Omega_\rho^2 + \frac{1}{w_\rho^4}\right)w_\rho^2 + \frac{1}{w_z^2} + \Omega_z^2 w_z^2\right] + \frac{N^2}{\sqrt{2\pi}w_\rho^2\, w_z}\left[a - a_{dd} f(\kappa)\right] \tag{5.17}$$

The quasi-one-dimensional DBEC energy E_{1D}, can be obtained using $w_\rho = a_\rho$ in the dipolar contribution and neglecting the derivates respect to w_ρ in the kinetic energy term. So [87]

$$E_{1D} = \frac{N}{4}\left[\frac{1}{w_z^2} + \Omega_z^2 w_z^2\right] + \frac{N^2}{\sqrt{2\pi}a_\rho^2\, w_z}\left[a - a_{dd} f(\kappa_0)\right] \tag{5.18}$$

Where $\kappa_0 = a_\rho/w_z$. In a quasi-1D DBEC, the axial width is much larger than the transverse oscillator length, as well as $\kappa_0 \to 0$ then $f(\kappa_0) \to 1$ and the dipolar energy becomes in $-N^2 a_{dd}/\left(\sqrt{2\pi}a_\rho^2\, w_z\right)$. Therefore the variational approximation indicates that the dipolar interaction turns into a contact interaction. The total interaction (contact and dipolar), now is an effective contact interaction such that

$$a_{eff} \;=\; a - a_{dd} \tag{5.19}$$

From this effective scattering length the system becomes attractive whereas $a_{dd} > a$, i.e. is possible the bright soliton formation even for repulsive scattering length a (like it was shown for the 3D dipolar condensate [88]).

5.3 Existence of bright solitons and instability by collapse

Under appropriate conditions the existence of bright solitons may be regarded as a consequence of the anisotropy caused by the dipole dipole interaction. E.g. in [90] for a disk-shaped dipolar condensate are discussed the necessary conditions for the existence of stable 2D bright solitons trapped in the axial direction, with reversing the sign of the dipolar interaction (for magnetic dipoles is achieved by rotating the magnetic field) and the dipoles aligned in the same direction of the trap. Later, to a quasi-2D dipolar condensate with positive dipolar strength and atoms with the dipole moments polarized perpendicular to direction of the trap were predicted stable anisotropic bright solitons with the respective requirements to the collapse [91]. The collision of anisotropic quasi-2D bright solitons in a DBEC was performed in [92]. The analysis is carried out by means of both a numerical method with the split-operator for the grid calculations and a time-dependent variational approximation with coupled Gaussians. In a quasi-1D dipolar BEC with attractive interaction the bright solitons exist for an arbitrarily large number of atoms [93] because of there is no collapse in one-dimensional models with cubic nonlinearity. The numerical solution of the full three-dimensional mean-field GPE with positive dipolar strength, repulsive atomic interaction and under harmonic transverse confinement supports bright solitons below a critical number of particles whereas the scattering length is less than the dipolar strength [88].

5.3.1 Collapse of a 3D dipolar condensate

A BEC only with contact interaction in the attractive scenario $a < 0$ is unstable and it should collapse beyond a critical value. This event implies important scenarios such as the formation of soliton trains and energetic atoms, inter alia. Given the richness of the new interaction a similar idea to collapse in a dipolar condensate it was raised and experimentally it was carried out [17]. Nevertheless the collapse in a DBEC is more difficult to achieve than in the non-dipolar case, so it is interesting to make a short overview about this phenomenon. With a magnetic field $\mathbf{B}$ oriented along z direction for a stable dipolar condensate of ^{52}Cr, the scattering length a was decreased using Feshbach resonance [78], below the critical value a_{crit} of stability. After the ramp, the system evolved for an adjustable time t_{hold} and suddenly the trap was switched off. Later, the propagation of a laser beam along the x direction enables obtain images by absorption. The condensate evolves over time in a complicated way from an initial elongated shaped along z direction as it is shown in Figure (5.2). The experimental results are compared with a full 3D numerical simulation of GPE including both contact and dipolar interaction, also has been taken into account the three-body losses[§].

[§]In the GPE or in the DGPE corresponds to a term of the form $-\frac{i\hbar L_3}{2}\left|\Psi\right|^4\Psi$ [94], where L_3 is the recombination rate constant.

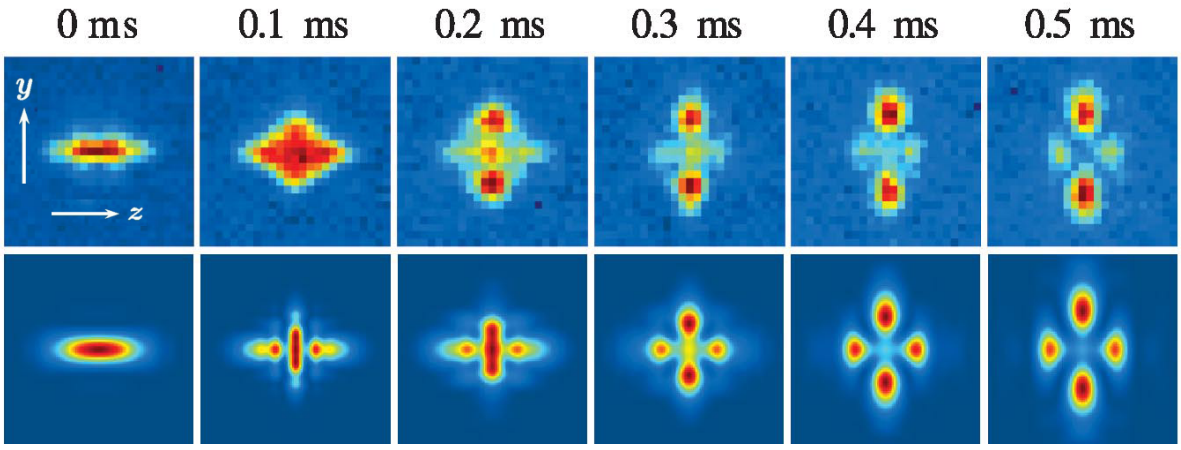

Figure 5.2: Collapse dynamics of a dipolar BEC. Experimental average of the absorption images (upper) and numerical simulation (lower), for different values of the adjustable time t_{hold} including both contact and dipolar interaction and the three-body losses [17].

5.3.2 Variational approximation and numerical results

The bright solitons can be regarded as stable stationary states and these are given by the minimum of the energy. Thus and similarly as it was done in the last Chapter, the widths of a dipolar BEC in the ground state can be obtained by a minimization of 3D energy (5.17) under harmonic transverse confinement ($\Omega_z = 0$) by $\partial E/\partial w_\rho = \partial E/\partial w_z = 0$. This procedure set the respective equations to the Gaussian widths as [88]

$$\frac{1}{w_\rho^3} - w_\rho + \frac{N\left[2a - a_{dd}\, g\left(\kappa\right)\right]}{\sqrt{2\pi}\, w_\rho^3\, w_z} = 0 \tag{5.20}$$

$$\frac{1}{2w_z^3} + \frac{N\left[a - a_{dd}\, h\left(\kappa\right)\right]}{\sqrt{2\pi}\, w_\rho^2\, w_z^2} = 0 \tag{5.21}$$

Henceforth the radial frequency is $\Omega_\rho = 1$. As it was outlined earlier the variation of the aspect ratio κ corresponds with three kinds of condensates: $\kappa < 1$ a cigar-shape, $\kappa = 1$ a spherical-shape and $\kappa > 1$ a disk-shape. The functions $g\left(\kappa\right)$ and $h\left(\kappa\right)$ can be read as

$$g\left(\kappa\right) = \frac{2 - 7\kappa^2 - 4\kappa^4 + 9\kappa^4 d\left(\kappa\right)}{\left(1 - \kappa^2\right)^2} \tag{5.22}$$

$$h\left(\kappa\right) = \frac{1 + 10\kappa^2 - 2\kappa^4 - 9\kappa^2 d\left(\kappa\right)}{\left(1 - \kappa^2\right)^2} \tag{5.23}$$

The variational approximation to the dipolar interaction is repulsive or attractive depending in the terms $-a_{dd}\, g\left(\kappa\right)$ and $-a_{dd}\, h\left(\kappa\right)$. The full effect of two interactions short and long-range is described in the bracket of (5.20) and (5.21), it giving rise to different interpretations to obtain stability or collapse in the condensate. In a disk-shaped trap whereas both the contact interaction a as the dipolar strength a_{dd} are repulsive (a, $a_{dd} > 0$), the functions $g\left(\kappa\right)$ and $h\left(\kappa\right)$ are negative and the collapse is not possible. The disk-shaped

configuration is always considered stable for any arbitrary number of atoms, but recently it was shown that it is not completely true [15] by means of a complete numerical solution of the dynamics of non-local GPE which leads to the collapse of a strongly disc-shaped dipolar BEC due to the long-range anisotropic dipolar interaction. This paper also shows that the variational approximation fails to predict collapse in several cases. The subject in this dissertation are the attractive interactions where the bright solitons exist and the

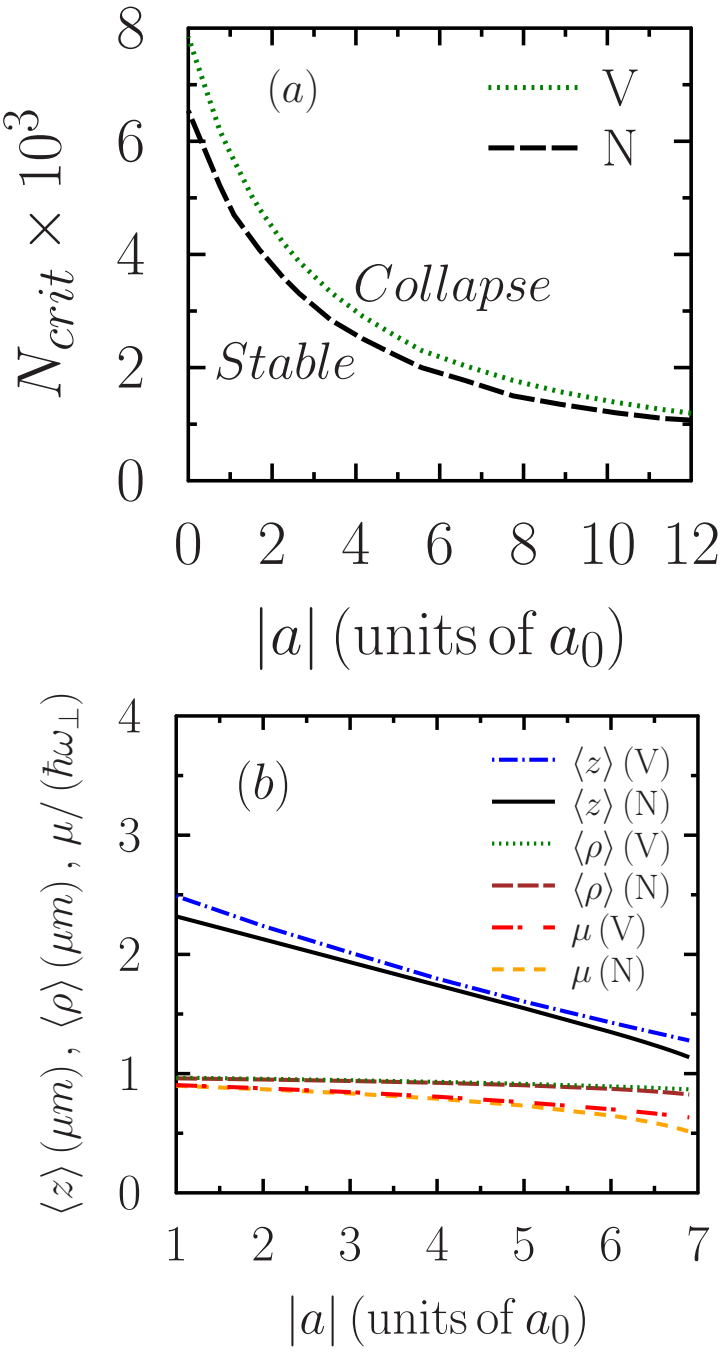

Figure 5.3: (a) The critical number of atoms N_{crit} of a dipolar condensate versus the scattering length $|a|$ for the dipolar strength $a_{dd} = 5a_0$. (b) Rms sizes $\langle\rho\rangle$ and $\langle z\rangle$ and chemical potential μ versus the scattering length $|a|$ of a dipolar condensate of 1500 atoms and $a_{dd} = 7a_0$. Numerical result (N) and varational approximation (V). The oscillator length applied is $1\,\mu m$.

condensate should collapse beyond a critical parameter. To an extreme cigar-shaped trap ($\kappa \to 0$, $h \to g/2 \to 1$), the variational collapse only exists for $a_{dd} > a$. Whereas that in a cigar-shaped condensate with $a > 0$ the functions $g(\kappa)$ and $h(\kappa)$ are positive with magnitude less than 1, the dipolar interaction should be attractive to giving rise to the collapse beyond a critical value of the dipolar strength [88]. Thus, in a cigar-shaped trap with $a_{dd} > 0$ the bright solitons exist while $-\infty < a < a_{dd}$ [88] because the dipolar interaction in (3.20) is attractive and it can be compensated by the atomic short-range repulsion ($a > 0$). The bright solitons always are predicted within the range $-\infty < a < 0$ to attractive atomic interaction ($a < 0$) and positive dipolar strength ($a_{dd} > 0$), and the condensate should collapse for $N > N_{crit}$. To this last stage the numerical and variational results of the stability diagram of bright solitons are plotted in the Figure (5.3 (a)) for $a_{dd} = 5a_0$ (here a_0 is the Bohr radius). Also for a dipolar BEC of 1500 atoms with $a_{dd} = 7a_0$ some physical observables are plotted in the Figure (5.3 (b)). The unit of length is taken as $1\mu m$ and it is given from the oscillator length $a_\perp = (\hbar/m\omega_\perp)^{1/2}$. In a same way once the dipolar strength is negative, the bright solitons are solutions only if $a < 0$.

In this dissertation, the three-dimensional GPE is solved numerically by the split-step Crank–Nicolson method in Cartesian coordinates [24]. The dipolar contribution is evaluated in the momentum space using the convolution theorem as

$$\int d\mathbf{r}'\, U_{dd}(\mathbf{r}-\mathbf{r}')\,|\Psi(\mathbf{r}')|^2 = \mathcal{F}^{-1}\left[\mathcal{F}\{U_{dd}\}(\mathbf{k})\,\mathcal{F}\left\{|\Psi|^2\right\}(\mathbf{k})\right](\mathbf{r}) \tag{5.24}$$

where the Fourier transform of the dipolar potential $\mathcal{F}\{U_{dd}\}(\mathbf{k})$ is given analytically (Appendix B). The term $\mathcal{F}\left\{|\Psi|^2\right\}(\mathbf{k})$ is evaluated numerically using the fast Fourier transform (FFT) [95] in Cartesian coordinates. The inverse Fourier transform is obtained by means of the FFT.

Likewise it was considered the stability diagram of a dipolar condensate with negative dipolar strength ($a_{dd} < 0$) and attractive atomic interaction ($a < 0$). The numerical results illustrate that the condensate should collapse for all values of $|a_{dd}|$ beyond of a critical number of particles (Figure 5.4). However, on the other hand the variational approximation fails to predict collapse as $|a_{dd}| \geq |a|$. This can be seen in the brackets of (5.20) and (5.21) because the system of equations has no solution for the dipolar condensate against to the numerical viewpoint. This issue lies in the variational treatment with a Gaussian ansatz because wrongly the long-range anisotropic dipolar interaction turns into a contact term. The variational approximation is correct describing the dipolar condensate in a small range of the parameter $|a_{dd}|$ such that $|a_{dd}| \gg 0$ and $|a_{dd}| \ll |a|$. When $|a_{dd}| \to 0$ the critical number of particles slowly changes and it is approximately constant with a boundary once the dipolar interaction vanishes. At this point the collapse value is completely given by the contact interaction and it agree the numerical and variational parameter $N_{crit}\,|a|$ found in the previous Chapter.

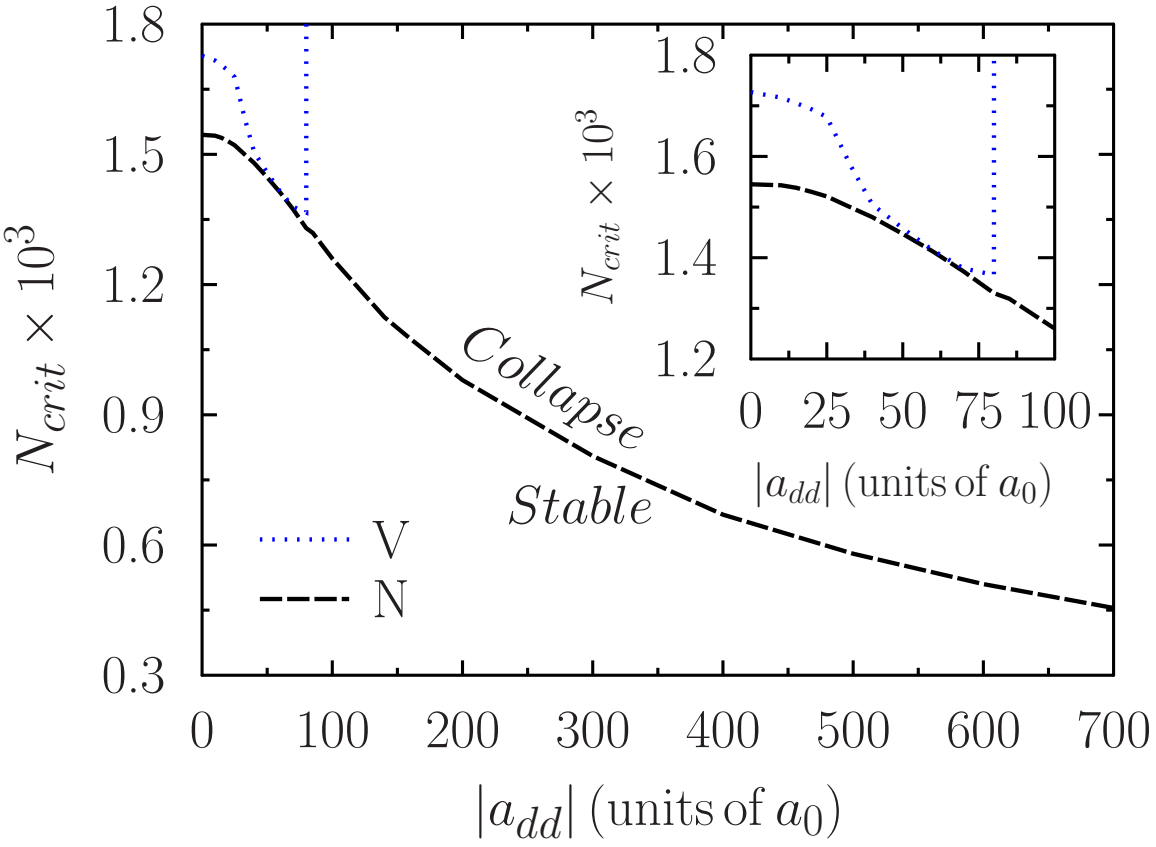

Figure 5.4: The critical number of atoms N_{crit} of a dipolar condensate versus the dipolar strength $|a_{dd}|$ for the attractive scattering length $a = -85.07a_0$. Numerical solution (N) and variational approximation (V). The oscillator unit applied is $10\mu m$.

Now, from reduced mean-field 1D GPE (5.2) with $V_z = 0$ and based on the work of bright solitons with repulsive atomic interaction in a 3D dipolar condensate [88], it is determined the rms size $\langle z \rangle$ and the chemical potential μ for three different quasi-one-dimensional dipolar BECs in the same regime of the atomic interaction ($a > 0$). The respective variational approximation is achieved recalling that quasi-1D equation is a special case of 3D one. Then, using $w_\rho \to a_\rho$ and $\kappa_0 = a_\rho / w_z$ in the dipolar contribution and neglecting the derivates respect to w_ρ (for this reason the equations (5.20) and (5.22) are not taken into account), the equation to the width w_z (5.21) becomes

$$\frac{1}{2w_z^3} + \frac{N\left[a - a_{dd}\, h\left(\kappa_0\right)\right]}{\sqrt{2\pi}\, a_\rho^2\, w_z^2} = 0 \tag{5.25}$$

The three dipolar condensates used are ^{52}Cr ($a_{dd} = 15a_0$), ^{168}Er ($a_{dd} = 66.6a_0$) and ^{164}Dy ($a_{dd} = 132.7a_0$), which are the experimental relevance. All of these with the same number of atoms $N = 1000$. Initially as illustrated in the Figure (5.5), it was solved numerically the quasi-1D GPE (5.2) with $a_{dd} = 15a_0$ ($a = 10a_0$) and $a_{dd} = 100a_0$ ($a = 75.6a_0$). The results for the profile of the square of the wave function $|\phi(z)|^2$ are compared with those of the full 3D equation and with the quasi-1D variational approximation (5.5). For convenience the trap parameter used to the 3D solution is $\Omega_\rho = 1$.

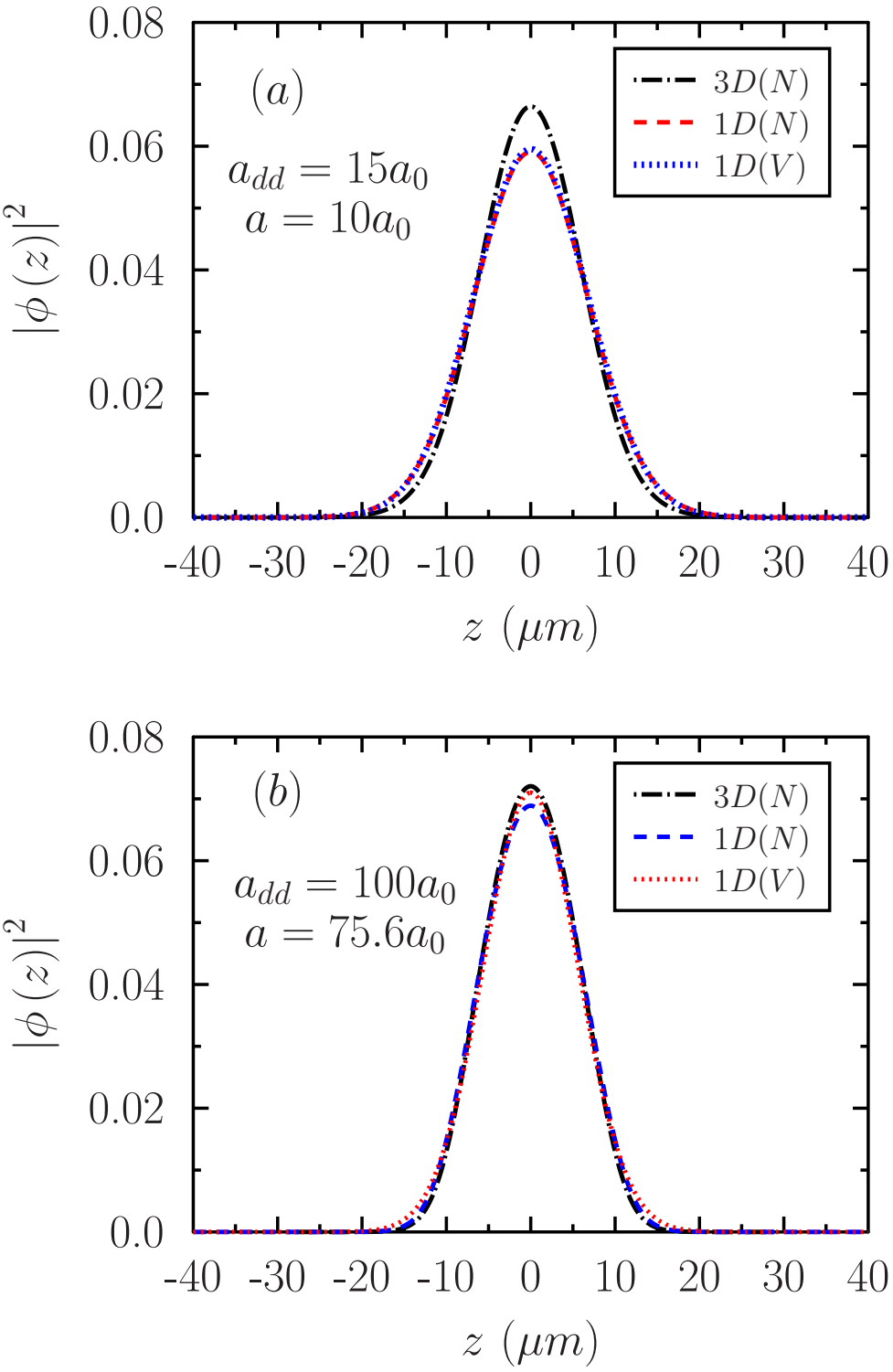

Figure 5.5: Profile of $|\phi(z)|^2$ to a dipolar condensate of 1000 atoms with trap parameter $\Omega_\rho = 1$. Numerical solution (N) of 3D (3.20 with $V_z = 0$) and quasi-1D model (5.2 with $V_z = 0$). The variational approximation (V) for the quasi-1D model is given by (5.5). (a) $a_{dd} = 15a_0$, $a = 10a_0$ and (b) $a_{dd} = 100a_0$, $a = 75.6a_0$. The oscillator length used is $1\,\mu m$.

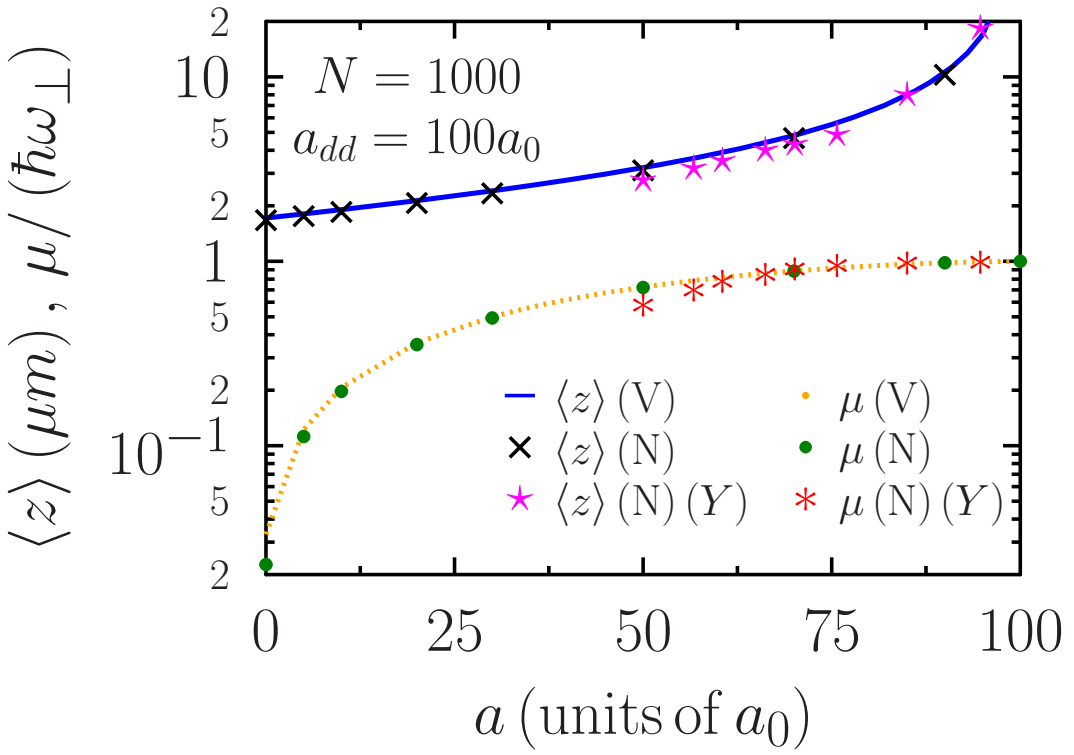

Figure 5.6: Chemical potential μ and rms size $\langle z\rangle$ versus the scattering length a of a quasi-1D and a 3D dipolar condensate of 1000 atoms with $a_{dd} = 100a_0$. Numerical solution (N), variational approximation (V) and Young *et al* (Y) [88]. The oscillator length used is $1\,\mu m$.

The effect of the trap parameters Ω_ρ and Ω_z in a dipolar condensate can be viewed in [87]. In both cases, variational and numerical results of the quasi-1D equation are in good agreement with those of the full 3D model. Likewise for $a_{dd} = 100a_0$ ($a = 75.6a_0$) it is compared the chemical potential μ and the root mean square $\langle z\rangle$ of the quasi-1D model with the full 3D (Figure 5.6). It is worth noting that the collapse is present only for the 3D condensate [88] and the range of existence of bright solitons is $50a_0 < a < 100a_0$, contrasting with the quasi-1D condensate where there is not collapse [93] and the bright solitons exist for an arbitrarily large number of atoms such that $0 \leq a \leq a_{dd}$.

After having established the appropriateness of the reduced 1D equation are plotted the chemical potential and the respective root mean square sizes for a three- and a quasi-1D dipolar condensate of ^{52}Cr, ^{168}Er and ^{164}Dy (Figure 5.7). The three dipolar BECs in 3D with the dipolar interaction attractive and the scattering length repulsive, should be stable only for a scattering length greater than a critical value such that the curves begin above this, as it is plotted in the Figure (5.7). This critical value is larger for ^{164}Dy atoms compared to that of ^{52}Cr and ^{168}Er atoms. Although the numerical solution of the reduced 1D model is simpler than the full 3D DGPE, this is still complicated because of the long-range anisotropic dipolar interaction. The variational approximation of this reduced model is relatively simple and could be used like an approximate solution.

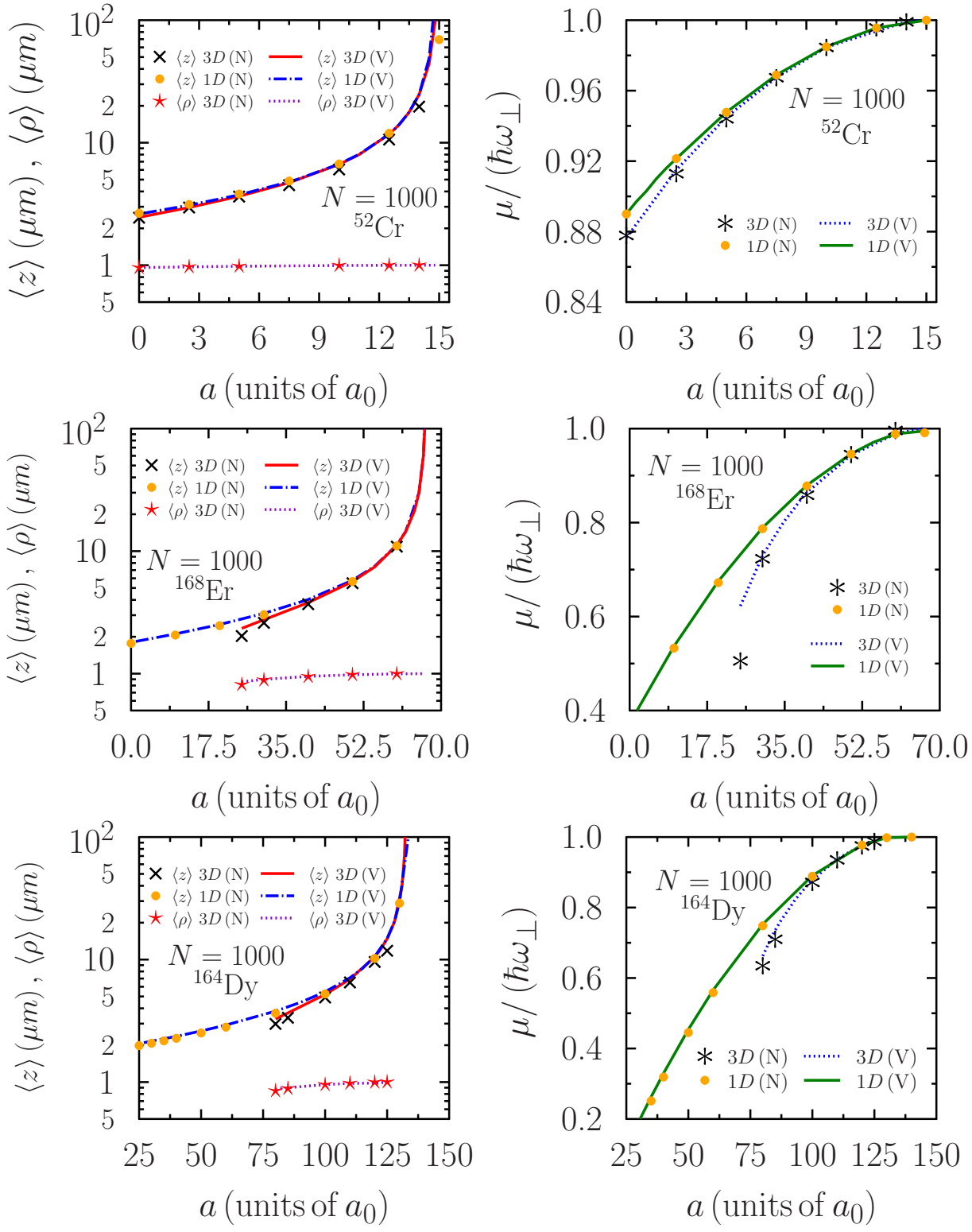

Figure 5.7: Chemical potential μ and rms size $\langle z\rangle$ versus the scattering length a of a three- and a quasi-1D dipolar condensate of 1000 atoms. In a same way it is presented the rms size $\langle\rho\rangle$ for the 3D dipolar condensate. (a) ^{52}Cr ($a_{dd} = 15a_0$). (b) ^{168}Er ($a_{dd} = 66.6a_0$). (c) ^{164}Dy ($a_{dd} = 132.7a_0$). Numerical (N) and variational (V) solution. The oscillator length used is $1\,\mu m$.

5.3.3 Collisions of bright solitons in a quasi-1D dipolar condensate

The numerical solution of the mean-field quasi-one-dimensional dipolar GPE enables the dynamics study of bright solitons. To investigate the collision between two bright solitons it is applied the following procedure. The first step is the creation of the soliton with a number of atoms $N = 1000$, employing imaginary-time propagation ($t \to -it$) in the Crank–Nicolson method. Afterwards two solitons are prepared at positions $\pm z_0$ with $2z_0$ the initial separation between these and these are then advanced by real-time propagation of (5.2) with $N = 2000$. To introduce the dynamics in the system, the two soliton are superposed with a phase difference δ and velocity zero. Here it is considered the following superposition [86]

$$\psi(z,t) = e^{i\delta} |\varphi(z - z_0, t)| + |\varphi(z + z_0, t)| \tag{5.26}$$

Similarly the dynamics can be obtained to a constant velocity v different from zero, where the soliton placed on the right hand is multiplied by a phase factor $\exp(ivz)$, while the soliton on the left hand is multiplied by a phase factor $\exp(-ivz)$, so [88, 92]

$$\psi(z,t) = e^{ivz} |\varphi(z - z_0, t)| + e^{-ivz} |\varphi(z + z_0, t)| \tag{5.27}$$

It should be noted that regardless of the form to generating the dynamics to keep constant the total number of atoms it is necessary normalize the new wave function $\psi(z,t)$ of the two solitons to 2 because it contains twice the particle number of a single soliton $\varphi(z,t)$. After the general explanation of the scheme used to obtain the collision dynamics of soliton are presented results about the effect of the phase difference between the solitons for $v = 0$ and for $v \neq 0$ in a train with two equal solitons in the three quasi-1D dipolar condensates ^{52}Cr, ^{168}Er and ^{164}Dy.

In a dipolar condensate of 2000 atoms of ^{52}Cr ($a_{dd} = 15a_0$) with scattering length $a = 10a_0$, velocity $v = 0$ and phase difference $\delta = 0$ is plotted the time evolution of the train of two such solitons by means of the profile of the square of the wave function versus z and t with initial positions $z = \pm 15.75\,\mu m$ in an interval of time $400\,ms$. Due to the dipolar attraction, the solitons come close, coalesce and oscillate forming a bound soliton molecule around $z = 0$ (Figure 5.8 top). For a phase difference $\delta = \pi$ in an interval of time $400\,ms$ the two solitons repel and away from each other, here these moved from positions $z = \pm 13.25\,\mu m$ to $z = \pm 23.75\,\mu m$ (Figure 5.8 bottom). The final solitons should be equal to the initial ones, however in this short time it is not seen due to the effect of the dipolar attraction which maintains the interaction between the solitons.

In the dynamics of two bright solitons in a dipolar condensate of 2000 atoms of ^{168}Er ($a_{dd} = 66.6a_0$) with scattering length $a = 50a_0$, the collision is insensitive to the initial phase difference $\delta = 0$ or $\delta = \pi$ when the velocity is $v = 3\,\mathrm{mm\,s^{-1}}$. The solitons come towards each other interact at $z = 0$, then these are separated and continue practically

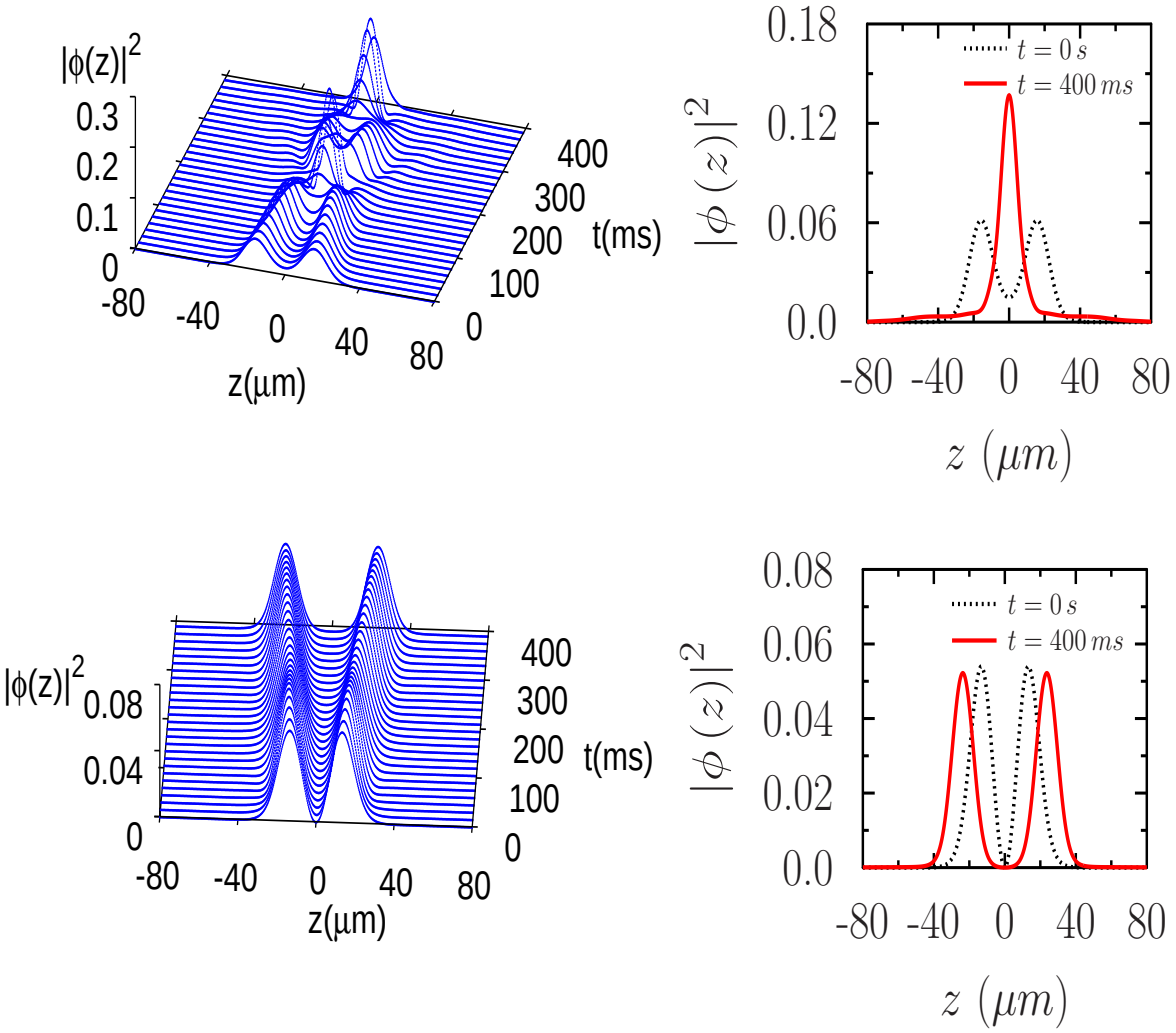

Figure 5.8: The profile of the square of the wave function $|\phi(z)|^2$ versus z and t for a train of two bright solitons in a quasi-1D dipolar condensate of ^{52}Cr ($a_{dd} = 15a_0$) with atomic scattering length $a = 10a_0$, 2000 atoms and velocity $v = 0$. The top corresponds with the phase difference $\delta = 0$ and the bottom with $\delta = \pi$. The oscillator length used is $1\,\mu m$.

unchanged. The solitons are placed at $z = \pm 38.4\,\mu m$ at $t = 0$ and each of these is advanced with a constant velocity $v = 3\,\mathrm{mm\,s^{-1}}$ towards centre $z = 0$. The real-time simulation of quasi-1D model (5.2) is terminated when the solitons reached approximately $z = \mp 38.4\,\mu m$ at time about $t = 24\,ms$. The collision dynamics is illustrated in Figure (5.9) where it is shown the evolution in t and z of the profile of the square of the wave function. As it is shown in the above Figure the final solitons are not equal to the initial ones, so the interaction is quasi-elastic and the final result is a quasi-soliton.

Finally, it is studied the effect of the phase difference with $\delta = 0$ and $\delta = \pi$ for the collision of two bright solitons in a dipolar condensate of 2000 atoms of ^{164}Dy ($a_{dd} = 132.7a_0$), scattering length $a = 120a_0$, and velocity $v = 0.2\,\mathrm{mm\,s^{-1}}$. As it is shown in the Figure (5.10) the collision is sensitive to the initial phase difference. In an interval of time $400\,ms$

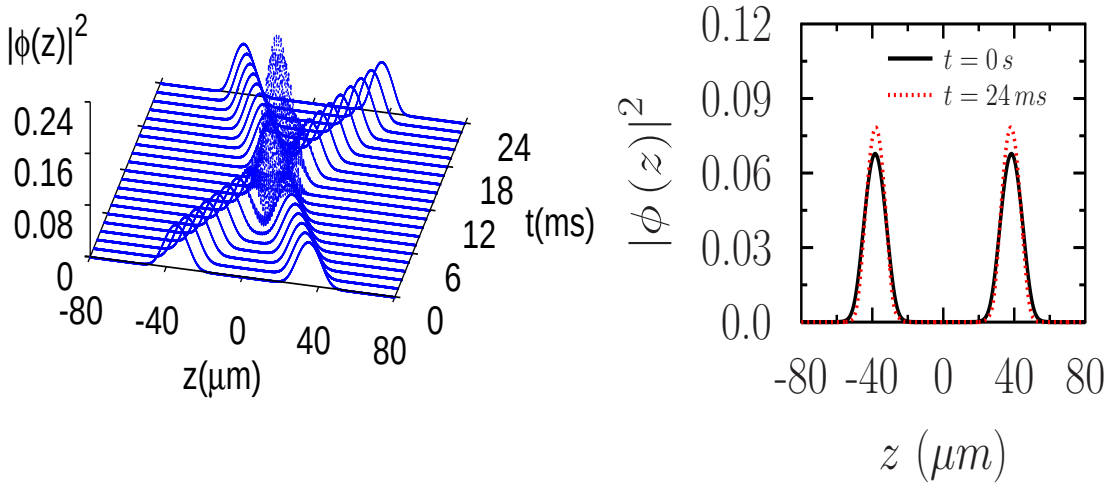

Figure 5.9: The profile of the square of the wave function $|\phi(z)|^2$ versus z and t for a train of two bright solitons in a quasi-1D dipolar condensate of ^{168}Er ($a_{dd} = 66.6a_0$) with atomic scattering length $a = 50a_0$, 2000 atoms and velocity $v = 3\,\mathrm{mm\,s^{-1}}$. The oscillator length used is $1\,\mu m$.

with initial positions $z = \pm 37.5\,\mu m$ and $\delta = 0$ the solitons come towards each other interact and the dipolar attraction along with the attractive phase difference allow the solitons are not separated thus forming a bound soliton molecule around $z = 0$ (Figure 5.10 top) similarly as when this was seen with zero velocity. For a phase difference $\delta = \pi$ in an interval of time $400\,ms$ the two solitons come towards each other and interact but unlike when the velocity is zero this time these don't coalesce because of the repulsive phase difference, so these repel and away from each other. The solitons are prepared with initial positions $z = \pm 40\,\mu m$ and these reach the final state in $z = \pm 44.5\,\mu m$ (Figure 5.10 bottom). At $400\,ms$ the final solitons still remain interacting and their shapes are not the same of initial solitons. To recovering the initial solitons it is necessary increasing the system time evolution.

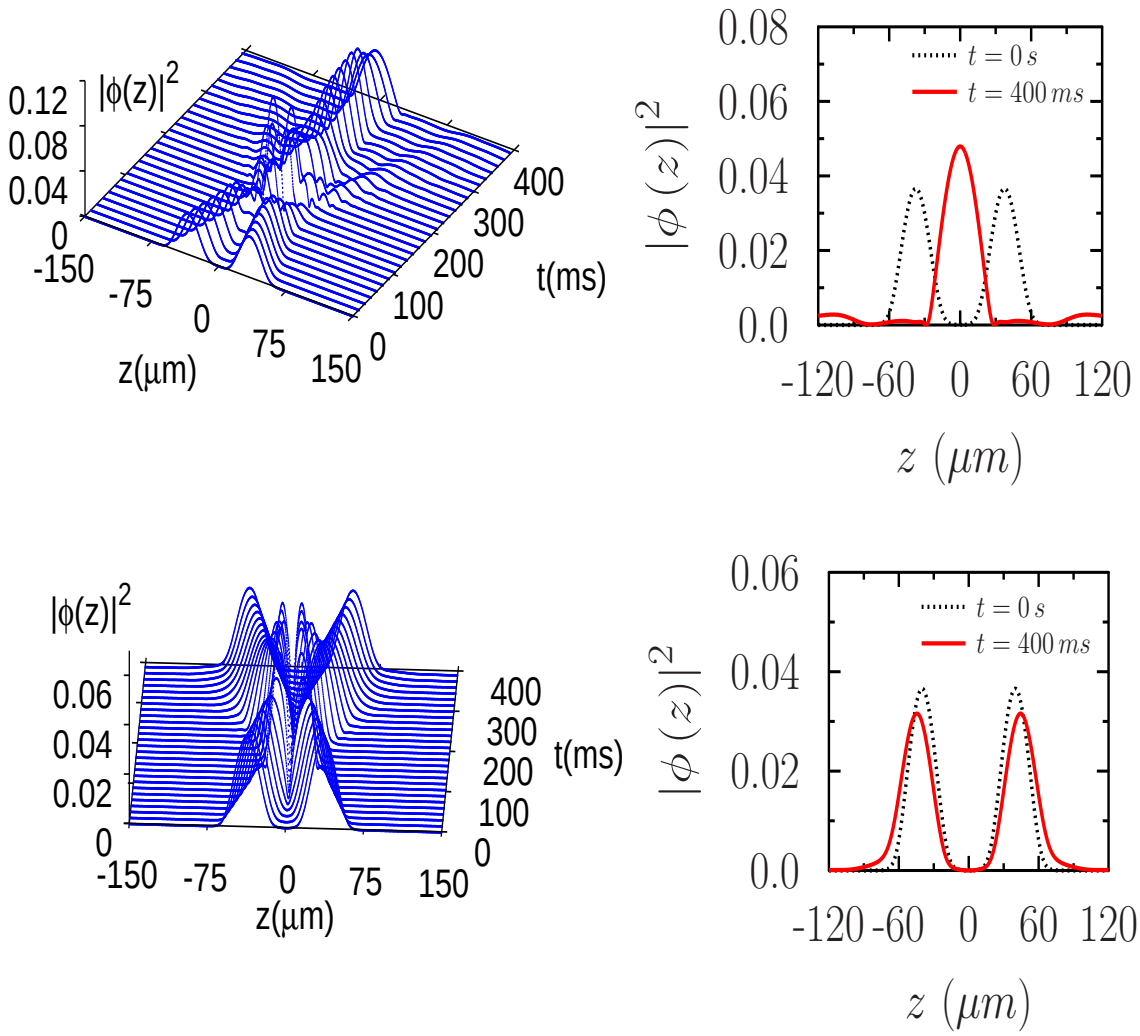

Figure 5.10: The profile of the square of the wave function $|\phi(z)|^2$ versus z and t for a train of two bright solitons in a quasi-1D dipolar condensate of ^{164}Dy ($a_{dd} = 132.7a_0$) with atomic scattering length $a = 120a_0$, 2000 atoms and velocity $v = 0.2\,\mathrm{mm\,s^{-1}}$. The top corresponds with the phase difference $\delta = 0$ and the bottom with $\delta = \pi$. The oscillator length used is $1\,\mu m$.

Summary and conclusions

This dissertation introduces the main ideas about the Bose-Einstein condensation with the dipole dipole interaction, this is focused on the bright solitons formation in the quasi-1D model obtained using dimensional reduction from three- to one-dimension. The richness of the new interaction is accompanied by a complicated theoretical treatment given by the long-range and the anisotropic character. So this work includes some basic features about the non-dipolar condensates as background of the dipolar study. Thus as part of the description of bright solitons in a dipolar condensate it is illustrated both numerical and variational the non-dipolar stage for one and three dimensions. The most relevant scope for a 3D condensate under harmonic transverse confinement shows that the system of variational algebraic equations to the widths (w_ρ and w_z), $\partial E/\partial w_\rho = \partial E/\partial w_z = 0$ have analytical solutions in terms of hyperbolic functions of the parameter $N|a|$. These solutions are consistent with the numerical results, maintaining the critical value of the instability by collapse whereas the atomic interaction is attractive.

From the hydrodynamic viewpoint, the long-range anisotropic dipolar interaction allows the existence of new intervals in the energy spectrum and sound of a homogeneous dipolar condensate, in some cases this is opposed with the contact interaction results. For a non-dipolar attractive condensate ($a < 0$) the speed of sound becomes purely imaginary involving instability. In the dipolar stage it is possible to get a real sound velocity as function of the dipolar anisotropy (reflected by the θ_q-angle dependence) since $|\epsilon_{dd}| \geq 1/2$. On the other hand, in a dipolar condensate with repulsive scattering length ($a > 0$) and within the range $0 \leq \epsilon_{dd} \leq 1$ the sound velocity exists as a function of the angle θ_q, but whether $\epsilon_{dd} > 1$, the angular dependence is constrained as it is seen at the end of Chapter 3.

Likewise and according to the two methods described in the Chapter 3 to define the character of a potential as long- or short-range, the numerical results obtained here for the dipolar potential in three dimensions agree with both. To one dimension only the solution of the two-body scattering problem for a potential r^{-3} agree, i.e. the dipolar potential in one dimension can be regarded as long-range by means of this method. In a dipolar condensate the numerical solution of the non-local Gross-Pitaevskii equation is a complicated issue because of the long-range anisotropic dipolar interaction. Nevertheless, the

reduced quasi-1D equation although also requires the Fourier transform and the inverse Fourier transform provides an alternative to the complete 3D equation. Regarding to the variational treatment of a 3D dipolar condensate, this gives good results in most cases, but in others this fails to predicting instability by collapse as it was outlined earlier in the Chapter 5. The variational approximation in the quasi-1D model is relatively simple and provides results for the stationary cigar DBEC in good agreement with the numerical solution of the respective GPE. The Chapter 5 suggests the existence possibility of bright solitons in a quasi-1D dipolar BEC for repulsive short-range interaction, thus it serving as a complementary work to that performed in 3D stage [88]. It was determined the statics by means of plots of rms size and chemical potential and the dynamics was analyzed using the collision of such solitons. It was studied the effect of the phase difference with values $\delta = 0$ and $\delta = \pi$ in the collision of two bright solitons with different velocities in three quasi-1D dipolar condensates of ^{52}Cr, ^{168}Er and ^{164}Dy.

As complement to the present dissertation it could be included the numerical and variational study of the bright solitons stability under a small breathing oscillation triggered by a sudden change in the scattering length. As perspectives for a future work it could be considered the study of dark solitons in this quasi-1D model and the study of two quasi-1D dipolar condensates coupled to compare these results with those produced by numerical integration of the full three-dimensional GPE. Likewise, at present the spin-orbit coupled is being considered in Bose-Einstein condensates with or without dipolar interaction, thus in these new systems the nonlinear waves will become an important research field and this dissertation may serve as a basis for this study.

Appendix A

Deduction of the GPE

A.1 The GPE from Schrödinger equation in the Hartree approximation

The Schrödinger equation to the condensate wave function using the Hartree approximation $\Psi(\mathbf{r}_1, \mathbf{r}_2, ..., \mathbf{r}_N, t) = \prod_{i=1}^{N} \phi(\mathbf{r}_i, t)$ can be written as

$$i\hbar \frac{\partial}{\partial t} \prod_{i=1}^{N} \phi(\mathbf{r}_i, t) = H \prod_{i=1}^{N} \phi(\mathbf{r}_i, t) \tag{A.1}$$

To obtain the motion equation for two particles (for ease performing a variable changes $\phi(\mathbf{r}_i, t) \to \phi_i,\ V(\mathbf{r}_i) \to V_i$) should be multiplied the Schrödinger equation by one single-particle wave function and integrating over this, thus

$$i\hbar \frac{\partial}{\partial t} [\phi_1 \phi_2] = H \phi_1 \phi_2 \tag{A.2}$$

$$i\hbar \int d\mathbf{r}_2\, \phi_2^* \frac{\partial}{\partial t} [\phi_1 \phi_2] = \int d\mathbf{r}_2\, \phi_2^* H \phi_1 \phi_2 \tag{A.3}$$

Taking the single-particle wave function normalization, the left hand is given by

$$\begin{aligned} i\hbar \int d\mathbf{r}_2\, \phi_2^* \frac{\partial}{\partial t} [\phi_1 \phi_2] &= i\hbar \int d\mathbf{r}_2\, \phi_2^* \left[\frac{\partial \phi_1}{\partial t} \phi_2 + \phi_1 \frac{\partial \phi_2}{\partial t} \right] \\ &= i\hbar \frac{\partial \phi_1}{\partial t} + i\hbar \phi_1 \int d\mathbf{r}_2\, \phi_2^* \frac{\partial \phi_2}{\partial t} \end{aligned} \tag{A.4}$$

again, with the single-particle wave function normalization the rigth hand term is

$$\begin{aligned} \int d\mathbf{r}_2\, \phi_2^* H \phi_1 \phi_2 &= \int d\mathbf{r}_2\, \phi_2^* \left[-\frac{\hbar^2}{2m} \left(\nabla_1^2 + \nabla_2^2 \right) + V_1 + V_2 + g\delta(\mathbf{r}_1 - \mathbf{r}_2) \right] \phi_1 \phi_2 \\ &= \left[-\frac{\hbar^2}{2m} \nabla_1^2 + V_1 + g |\phi_1|^2 \right] \phi_1 + \phi_1 \int d\mathbf{r}_2 \phi_2^* \left[-\frac{\hbar^2}{2m} \nabla_2^2 + V_2 \right] \phi_2 \end{aligned} \tag{A.5}$$

By comparing the expression (A.4) with (A.5), turns out the linear Schrödinger equation for one single-particle

$$i\hbar \int d\mathbf{r}_2\, \phi_2^* \frac{\partial \phi_2}{\partial t} = \int d\mathbf{r}_2\, \phi_2^* \left[-\frac{\hbar^2}{2m}\nabla_2^2 + V_2 \right] \phi_2 \tag{A.6}$$

or

$$i\hbar \frac{\partial \phi_2}{\partial t} = \left[-\frac{\hbar^2}{2m}\nabla_2^2 + V_2 \right] \phi_2 \tag{A.7}$$

and the other hand also turns out the motion equation to the particle in $\mathbf{r}_1$ interacting with the particle in $\mathbf{r}_2$

$$i\hbar \frac{\partial \phi_1}{\partial t} = -\frac{\hbar^2}{2m}\nabla_1^2 \phi_1 + V_1\phi_1 + g\left|\phi_1\right|^2 \phi_1 \tag{A.8}$$

In a same way for three particles, the Schrödinger equation becomes

$$i\hbar \int d\mathbf{r}_3\, \phi_3^* \int d\mathbf{r}_2\, \phi_2^* \frac{\partial}{\partial t}\left[\phi_1\phi_2\phi_3\right] = \int d\mathbf{r}_3\, \phi_3^* \int d\mathbf{r}_2\, \phi_2^* H \phi_1\phi_2\phi_3 \tag{A.9}$$

The left hand is

$$i\hbar \int d\mathbf{r}_3\, \phi_3^* \int d\mathbf{r}_2\, \phi_2^* \frac{\partial}{\partial t}\left[\phi_1\phi_2\phi_3\right] = i\hbar \frac{\partial \phi_1}{\partial t} + i\hbar\phi_1 \int d\mathbf{r}_2\, \phi_2^* \int d\mathbf{r}_3\, \phi_3^* \frac{\partial\left[\phi_2\phi_3\right]}{\partial t} \tag{A.10}$$

and the right hand is

$$\begin{aligned}
\int d\mathbf{r}_3\, \phi_3^* \int d\mathbf{r}_2\, \phi_2^* H \phi_1\phi_2\phi_3 &= \int d\mathbf{r}_3\, \phi_3^* \int d\mathbf{r}_2\, \phi_2^* \left[-\frac{\hbar^2}{2m}\left(\nabla_1^2 + \nabla_2^2 + \nabla_3^2\right) + V_1 + V_2 \right. \\
&+ \left. V_3 + g\Big[\delta\left(\mathbf{r}_1 - \mathbf{r}_2\right) + \delta\left(\mathbf{r}_1 - \mathbf{r}_3\right) + \delta\left(\mathbf{r}_2 - \mathbf{r}_3\right)\Big] \right] \phi_1\phi_2\phi_3 \\
&= -\frac{\hbar^2}{2m}\left[\nabla_1^2 + V_1 + 2g\left|\phi_1\right|^2\right]\phi_1 + \phi_1 \int d\mathbf{r}_2\, \phi_2^* \int d\mathbf{r}_3\, \phi_3^* \\
&\times \left[-\frac{\hbar^2}{2m}\left(\nabla_2^2 + \nabla_3^2\right) + V_2 + V_3 + g\delta\left(\mathbf{r}_2 - \mathbf{r}_3\right) \right] \phi_2\phi_3
\end{aligned} \tag{A.11}$$

By comparing the expression (A.10) with (A.11), then

$$i\hbar \frac{\partial\left[\phi_2\phi_3\right]}{\partial t} = \left[-\frac{\hbar^2}{2m}\left(\nabla_2^2 + \nabla_3^2\right) + V_2 + V_3 + g\delta\left(\mathbf{r}_2 - \mathbf{r}_3\right) \right] \phi_2\phi_3 \tag{A.12}$$

corresponding with the nonlinear Schrödinger equation for two particles such as (A.2). Therefore the motion equation to the particle in $\mathbf{r}_1$ interacting with the particle in $\mathbf{r}_2$ and the particle in $\mathbf{r}_3$ is

$$i\hbar \frac{\partial \phi_1}{\partial t} = -\frac{\hbar^2}{2m}\nabla_1^2 \phi_1 + V_1\phi_1 + 2g\left|\phi_1\right|^2 \phi_1 \tag{A.13}$$

A.2 Derivation of the GPE in the mean-field approximation

According the hamiltonian (1.44), the Heisenberg equation can be written as

$$\begin{aligned} i\hbar\frac{\partial}{\partial t}\hat{\Psi}\left(\mathbf{r}',t\right) &= \int d\mathbf{r}\left[\hat{\Psi}\left(\mathbf{r}',t\right),\hat{\Psi}^{\dagger}\left(\mathbf{r},t\right)\hat{H}_{0}\hat{\Psi}\left(\mathbf{r},t\right)\right] \\ &+ \frac{g}{2}\int d\mathbf{r}\left[\hat{\Psi}\left(\mathbf{r}',t\right),\hat{\Psi}^{\dagger}\left(\mathbf{r},t\right)\hat{\Psi}^{\dagger}\left(\mathbf{r},t\right)\hat{\Psi}\left(\mathbf{r},t\right)\hat{\Psi}\left(\mathbf{r},t\right)\right] \end{aligned} \tag{A.14}$$

Using the commutation relations for the boson fields operators (1.41 - 1.43) and their basic properties. To the first commutador

$$\begin{aligned} \left[\hat{\Psi}\left(\mathbf{r}',t\right),\hat{\Psi}^{\dagger}\left(\mathbf{r},t\right)\hat{H}_{0}\hat{\Psi}\left(\mathbf{r},t\right)\right] &= \left[\hat{\Psi}\left(\mathbf{r}',t\right),\hat{\Psi}^{\dagger}\left(\mathbf{r},t\right)\right]\hat{H}_{0}\hat{\Psi}\left(\mathbf{r},t\right) \\ &+ \hat{\Psi}^{\dagger}\left(\mathbf{r},t\right)\left[\hat{\Psi}\left(\mathbf{r}',t\right),\hat{H}_{0}\hat{\Psi}\left(\mathbf{r},t\right)\right] \\ &= \delta\left(\mathbf{r}'-\mathbf{r}\right)\hat{H}_{0}\hat{\Psi}\left(\mathbf{r},t\right) \end{aligned} \tag{A.15}$$

To the second commutador

$$\begin{aligned} \left[\hat{\Psi}\left(\mathbf{r}',t\right),\hat{\Psi}^{\dagger}\left(\mathbf{r},t\right)\hat{\Psi}^{\dagger}\left(\mathbf{r},t\right)\hat{\Psi}\left(\mathbf{r},t\right)\hat{\Psi}\left(\mathbf{r},t\right)\right] &= \left[\hat{\Psi}\left(\mathbf{r}',t\right),\hat{\Psi}^{\dagger}\left(\mathbf{r},t\right)\hat{\Psi}^{\dagger}\left(\mathbf{r},t\right)\right]\hat{\Psi}\left(\mathbf{r},t\right)\hat{\Psi}\left(\mathbf{r},t\right) \\ &+ \hat{\Psi}^{\dagger}\left(\mathbf{r},t\right)\hat{\Psi}^{\dagger}\left(\mathbf{r},t\right)\left[\hat{\Psi}\left(\mathbf{r}',t\right),\hat{\Psi}\left(\mathbf{r},t\right)\hat{\Psi}\left(\mathbf{r},t\right)\right] \\ &= \left[\left[\hat{\Psi}\left(\mathbf{r}',t\right),\hat{\Psi}^{\dagger}\left(\mathbf{r},t\right)\right]\hat{\Psi}^{\dagger}\left(\mathbf{r},t\right)\right. \\ &+ \left.\hat{\Psi}^{\dagger}\left(\mathbf{r},t\right)\left[\hat{\Psi}\left(\mathbf{r}',t\right),\hat{\Psi}^{\dagger}\left(\mathbf{r},t\right)\right]\right]\hat{\Psi}\left(\mathbf{r},t\right)\hat{\Psi}\left(\mathbf{r}\right) \\ &= 2\delta\left(\mathbf{r}'-\mathbf{r}\right)\hat{\Psi}^{\dagger}\left(\mathbf{r}\right)\hat{\Psi}\left(\mathbf{r}\right)\hat{\Psi}\left(\mathbf{r}\right) \end{aligned} \tag{A.16}$$

By replacing these commutators (A.15) and (A.16) on the Heisenberg equation (A.14) the result is a field operators equation

$$i\hbar\frac{\partial}{\partial t}\hat{\Psi}\left(\mathbf{r}',t\right)=\left(-\frac{\hbar^{2}}{2m}\nabla^{2}+V\left(\mathbf{r}'\right)+g\hat{\Psi}^{\dagger}\left(\mathbf{r}',t\right)\hat{\Psi}\left(\mathbf{r}',t\right)\right)\hat{\Psi}\left(\mathbf{r}',t\right) \tag{A.17}$$

Appendix B

Fourier transform of the dipolar interaction

There are differet ways of to calculate the Fourier transform of the dipolar term, e.g. in [46, 47], the appendix A in [11] (this is the most extensive method), or the appendix B in [48]. Here are presented two simple way to get the contribution from some works mentioned above.

B.1 First method

In general the dipolar interaction (3.23) can be written like [2, 46, 48]

$$U_{dd}\left(\mathbf{r}-\mathbf{r}'\right)=\frac{C_{dd}}{4\pi}\frac{1-3\cos^2\theta}{\left|\mathbf{r}-\mathbf{r}'\right|^3}=-\frac{C_{dd}}{4\pi}\left[\frac{\partial^2}{\partial z^2}\left(\frac{1}{\left|\mathbf{r}-\mathbf{r}'\right|}\right)+\frac{4\pi}{3}\delta\left(\mathbf{r}-\mathbf{r}'\right)\right] \tag{B.1}$$

In general taking

$$u_{dd}=-\frac{\partial^2}{\partial r_i\partial r_j}\left(\frac{1}{\left|\mathbf{r}-\mathbf{r}'\right|}\right)-\frac{4\pi}{3}\delta_{ij}\delta\left(\mathbf{r}-\mathbf{r}'\right) \tag{B.2}$$

The Fourier transform to $\tilde{u}_{dd}$ is easy calculated, the transform of the Dirac delta is equal to 1. For the first term is possible regularize the problem in the next way [21].

$$\begin{aligned}
\int d\mathbf{r}\frac{1}{|\mathbf{r}|}e^{-i\mathbf{q}\cdot\mathbf{r}} &= \lim_{\epsilon\to 0}\int d\mathbf{r}\frac{e^{-\epsilon|\mathbf{r}|}}{|\mathbf{r}|}e^{-i\mathbf{q}\cdot\mathbf{r}} \\
&= 2\pi\lim_{\epsilon\to 0}\int d\theta\, dr\, r^2\sin\theta\,\frac{e^{-\epsilon r}e^{-iqr\cos\theta}}{r} \\
&= -2\pi\lim_{\epsilon\to 0}\int_0^\infty dr\, re^{-\epsilon r}\int_0^\pi d\left(\cos\theta\right)e^{-iqr\cos\theta} \\
&= 2\pi\lim_{\epsilon\to 0}\int_0^\infty dr\, re^{-\epsilon r}\int_{-1}^1 d\left(\cos\theta\right)e^{-iqr\cos\theta}
\end{aligned}$$

$$
\begin{aligned}
&= 2\pi \lim_{\epsilon\to 0} \int_0^\infty dr\, r e^{-\epsilon r} \left[\frac{1}{iqr}\left(e^{iqr} - e^{-iqr}\right)\right] \\
&= \frac{4\pi}{q} \lim_{\epsilon\to 0} \int_0^\infty dr\, e^{-\epsilon r} \sin(qr) \\
&= \frac{4\pi}{q} \lim_{\epsilon\to 0} \mathrm{Im}\left(\int_0^\infty dr\, e^{-\epsilon r} e^{iqr}\right) \\
&= -\frac{4\pi}{q} \lim_{\epsilon\to 0} \mathrm{Im}\left(\frac{1}{iq-\epsilon}\right) \\
&= 4\pi \lim_{\epsilon\to 0} \frac{1}{q^2+\epsilon^2} = \frac{4\pi}{\mathbf{q}^2}
\end{aligned} \tag{B.3}
$$

Taking in the momentum space $\partial/\partial r_j \to -iq_j$. Therefore, the general Fourier transform of the interaction is

$$
\tilde{U}_{dd}(\mathbf{q}) = \frac{C_{dd}}{3} \sum_{ij}^{3} \left(4\pi \frac{q_i q_j}{\mathbf{q}^2} - \frac{4\pi}{3}\delta_{ij}\right) \tag{B.4}
$$

Particularly in the case where the dipolar interaction with polarization or magnetization along the z direction, the transform $\tilde{u}_{dd}$ becomes

$$
\tilde{u}_{dd} = \left(4\pi \frac{q_z^2}{\mathbf{q}^2} - \frac{4\pi}{3}\right) = 4\pi \left(\frac{q^2 \cos^2\theta_q}{q^2} - \frac{1}{3}\right) \tag{B.5}
$$

which leads to find the Fourier transform of the dipolar interaction in z direction as

$$
\tilde{U}_{dd}(\mathbf{q}) = \frac{C_{dd}}{3}\left(3\frac{q_z^2}{\mathbf{q}^2} - 1\right) = \frac{C_{dd}}{3}\left(3\cos^2\theta_q - 1\right) \tag{B.6}
$$

where θ_q is the angle between $\mathbf{q}$ and the polarization direction z.

B.2 Second method

From [47] the dipolar interaction can be written in terms of the spherical harmonics to $l = 2$ and $m = 0$, as

$$
U_{dd}(\mathbf{r}) = \frac{C_{dd}}{4\pi r^3}\left(-4\sqrt{\frac{\pi}{5}}\right) Y_{20}(\theta, \phi) \tag{B.7}
$$

the other hand is necessary using the expansion of a wave plane in spherical harmonics

$$
e^{-i\mathbf{q}\cdot\mathbf{r}} = 4\pi \sum_{l=0}^{\infty} i^l j_l(kr) \sum_{m=-l}^{l} Y_{lm}^*(\theta, \phi)\, Y_{lm}(\theta_q, \phi_q) \tag{B.8}
$$

and the orthonormality of the spherical harmonics

$$\int d\phi\, d\theta \sin\theta\, Y^*_{lm}(\theta,\phi)\, Y_{l'm'}(\theta,\phi) = \delta_{ll'}\delta_{mm'} \tag{B.9}$$

Thus the Fourier transform is

$$\tilde{U}_{dd}(\mathbf{q}) = \int d\mathbf{r}\, U_{dd}(\mathbf{r})\, e^{-i\mathbf{q}\cdot\mathbf{r}}$$

$$= \int r^2 dr\, \sin\theta\, d\theta\, d\phi\, \frac{C_{dd}}{4\pi r^3}\left(-4\sqrt{\frac{\pi}{5}}\right) Y_{20}(\theta,\phi)\left[4\pi\sum_{l=0}^{\infty} i^l j_l(kr)\sum_{m=-l}^{l} Y^*_{lm}(\theta,\phi)\, Y_{lm}(\theta_q,\phi_q)\right] \tag{B.10}$$

The integral of the spherical Bessel function is give by [42]

$$\int_0^\infty dr\, \frac{j_2(kr)}{r} = \int_0^\infty dr\, \left(\frac{3\sin r}{r^4} - \frac{\sin r}{r^2} + \frac{3\cos r}{r^3}\right) \tag{B.11}$$

integrating by parts the first term leads to

$$\int_0^\infty dr\, \frac{j_2(kr)}{r} = -\frac{\sin r}{r^3} - 2\int_0^\infty dr\, \left(\frac{\cos r}{r^3} + \frac{\sin r}{2r^2}\right) \tag{B.12}$$

again integrating by parts the first term

$$\int_0^\infty dr\, \frac{j_2(kr)}{r} = -\frac{\sin r}{r^3} + \frac{\cos r}{r^2}$$

$$= \lim_{r\to\infty}\left(-\frac{\sin r}{r^3} + \frac{\cos r}{r^2}\right) - \lim_{r\to 0}\left(-\frac{\sin r}{r^3} + \frac{\cos r}{r^2}\right) \tag{B.13}$$

the first one contribution is zero. To the second one with the $\sin r$ and $\cos r$ expansion the above equation becomes

$$\approx -\lim_{r\to 0}\left(-\frac{\sin r}{r^3} + \frac{\cos r}{r^2}\right) \approx -\lim_{r\to 0}\left[-\frac{1}{r^3}\left(r - \frac{r^3}{6}\right) + \frac{1}{r^2}\left(1 - \frac{r^2}{2}\right)\right] = \frac{1}{3} \tag{B.14}$$

Thus

$$\int_0^\infty dr\, \frac{j_2(kr)}{r} = \frac{1}{3} \tag{B.15}$$

As $l = 2$ and $m = 0$, the only contribution in the Fourier transform (B.10) turns out to be

$$\tilde{U}_{dd}(\mathbf{q}) = \frac{1}{3} C_{dd}\left(4\sqrt{\frac{\pi}{5}}\right)\int \sin\theta\, d\theta\, d\phi\, Y_{20}(\theta,\phi)\, Y^*_{20}(\theta,\phi)\, Y_{20}(\theta_q,\phi_q) \tag{B.16}$$

using the orthonormality of the spherical harmonics (B.9), leads to

$$\tilde{U}_{dd}(\mathbf{q}) = \frac{1}{3} C_{dd}\left(4\sqrt{\frac{\pi}{5}}\right) Y_{20}(\theta_q,\phi_q) \tag{B.17}$$

So, the Fourier transform with θ_q the angle between $\mathbf{q}$ and the polarization direction is

$$\tilde{U}_{dd}(\mathbf{q}) = \frac{C_{dd}}{3}\left(3\cos^2\theta_q - 1\right) \tag{B.18}$$

Appendix C

Virial theorem in Bose-Einstein condensation

C.1 Virial theorem of a BEC

In a system in equilibrium the virial theorem establishes relations which must fulfilled between the different energies. This theorem takes into account that the energy must be independent of a scaling transformation of the coordinates and besides that it imposes that the energy must be a minimum. So since the energy (1.33) is stationary for any variation of the wave function $\Psi(\mathbf{r})$ around the solution of the GPE, the same scaling in the three directions must be chosen $\mathbf{r} \rightarrow \widetilde{\mathbf{r}} = \nu\mathbf{r}$, where ν is an arbitrary real scaling parameter. The condensate wave function transforms as $\Psi(\mathbf{r}) \rightarrow \widetilde{\Psi}(\widetilde{\mathbf{r}}) = A\Psi(\nu\mathbf{r})$, where A is a normalization constant. From the principle of scale invariance the norm of the wave function must be preserved. Thus,

$$\int d\mathbf{r} \left|\Psi(\mathbf{r})\right|^2 = \int d\mathbf{r} \left|\widetilde{\Psi}(\widetilde{\mathbf{r}})\right|^2 = |A|^2 \int d\mathbf{r} \left|\Psi(\nu\mathbf{r})\right|^2 = 1 \tag{C.1}$$

In coordinates the normalization becomes

$$|A|^2 \int dxdydz \left|\Psi(\nu x, \nu y, \nu z)\right|^2 = 1 \tag{C.2}$$

$$|A|^2 \nu^{-3} \int d(\nu x)\, d(\nu y)\, d(\nu z) \left|\Psi(\nu x, \nu y, \nu z)\right|^2 = 1 \tag{C.3}$$

The integral is equal to 1, so the normalization constant is $A = \nu^{3/2}$. Using the scaling wave function $\widetilde{\Psi}(\widetilde{\mathbf{r}})$ the kinetic contribution (1.34) is given by

$$\widetilde{E}_{kin} = \frac{N}{2} \int d\mathbf{r} \left|\nabla_{\mathbf{r}} \Psi(\mathbf{r})\right|^2 = \frac{N}{2} \nu^3 \int d\mathbf{r} \left|\nabla_{\mathbf{r}} \Psi(\nu\mathbf{r})\right|^2 \tag{C.4}$$

In a same way like it was performed to get the normalization constant

$$\begin{aligned}\widetilde{E}_{kin} &= \frac{N}{2}\nu^3 \int \frac{d(\nu\mathbf{r})}{\nu^3} \left|\nabla_{\nu\mathbf{r}}\Psi(\nu\mathbf{r})\right|^2 \nu^2 \\ &= \nu^2 \frac{N}{2} \int d(\nu\mathbf{r}) \left|\nabla_{\nu\mathbf{r}}\Psi(\nu\mathbf{r})\right|^2 = \nu^2 E_{kin} \end{aligned} \tag{C.5}$$

The interaction energy (1.35) transforms as

$$\begin{aligned}\widetilde{E}_{int} &= 2\pi a N^2 \int d\mathbf{r} |\mathbf{\Psi}(\nu\mathbf{r})|^4 \nu^6 = 2\pi\nu^6 a N^2 \int \frac{d(\nu\mathbf{r})}{\nu^3} |\mathbf{\Psi}(\nu\mathbf{r})|^4 \\ &= 2\pi\nu^3 a N^2 \int d(\nu\mathbf{r}) |\mathbf{\Psi}(\nu\mathbf{r})|^4 = \nu^3 E_{int} \end{aligned} \tag{C.6}$$

Finally, transforming the harmonic oscillator energy (1.36) as

$$\begin{aligned}\widetilde{E}_{trap} &= N \int d\mathbf{r}\, V(\mathbf{r}) |\mathbf{\Psi}(\nu\mathbf{r})|^2 \nu^3 \\ &= \frac{N\nu^3}{2} \int \frac{d(\nu\mathbf{r})}{\nu^3} \left[\omega_x^2 (\nu x)^2 + \omega_y^2 (\nu y)^2 + \omega_z^2 (\nu z)^2\right] \frac{1}{\nu^2} |\mathbf{\Psi}(\nu\mathbf{r})|^2 \\ &= \frac{N}{2\nu^2} \int d(\nu\mathbf{r})\, V(\nu\mathbf{r}) |\mathbf{\Psi}(\nu\mathbf{r})|^2 = \nu^{-2} E_{trap} \end{aligned} \tag{C.7}$$

The total energy transformed is $\widetilde{E} = \nu^2 E_{kin} + \nu^3 E_{int} + \nu^{-2} E_{trap}$. So using the equilibrium condition $(dE/d\nu)|_{\nu=1} = 0$ the virial theorem of a non-dipolar condensate can be read as

$$2E_{kin} + 3E_{int} - 2E_{trap} = 0 \tag{C.8}$$

C.2 Virial theorem of a dipolar BEC

Considering the energy of a dipolar condensate (1.36) and using the procedure outlined earlier, in the virial theorem the dipolar contribution is given by

$$\begin{aligned}\widetilde{E}_{dd} &= \frac{N^2}{2} \int \frac{d(\nu\mathbf{r})}{\nu^3} \int \frac{d(\nu\mathbf{r}')}{\nu^3} U_{dd}(\nu\mathbf{r} - \nu\mathbf{r}') \nu^3\nu^3 |\Psi(\nu\mathbf{r}')|^2 \nu^3 |\nu\Psi(\mathbf{r})|^2 \\ &= \frac{N^2}{2}\nu^3 \int d(\nu\mathbf{r}) \int d(\nu\mathbf{r}')\, U_{dd}(\nu\mathbf{r} - \nu\mathbf{r}') |\Psi(\nu\mathbf{r}')|^2 |\nu\Psi(\mathbf{r})|^2 \\ &= \nu^3 E_{dd} \end{aligned} \tag{C.9}$$

Therefore, the virial theorem of a dipolar condensate is

$$2(E_{kin} - E_{trap}) + 3(E_{int} + E_{dd}) = 0 \tag{C.10}$$

Appendix D

Modulational instability

Using the perturbed solution (4.14) [51, 62, 65]

$$\psi(z,t) = [\psi_0 + \varphi(z,t)] \exp\{i[qz - \omega t + \alpha(z,t)]\} \tag{D.1}$$

in the GPE (4.11) such that

$$i\frac{\partial\psi}{\partial t} = \left[(s+\varphi)\left(\omega - \frac{\partial\alpha}{\partial t}\right) + i\frac{\partial\varphi}{\partial t}\right]\psi \tag{D.2}$$

$$\frac{\partial^2\psi}{\partial z^2} = \left[2i\frac{\partial\varphi}{\partial z}\left(q + \frac{\partial\alpha}{\partial z}\right) - (s+\varphi)\left(q + \frac{\partial\alpha}{\partial z}\right)^2 + i(s+\varphi)\frac{\partial^2\alpha}{\partial z^2} + \frac{\partial^2\varphi}{\partial z^2}\right]\psi \tag{D.3}$$

it is possible to get two equations, the first one from the imaginary part and the second one from the real part. Thus

$$\frac{\partial\varphi}{\partial t} + \frac{1}{2}\left[2\frac{\partial\varphi}{\partial z}\left(q + \frac{\partial\alpha}{\partial z}\right) + (s+\varphi)\frac{\partial^2\alpha}{\partial z^2}\right] = 0 \tag{D.4}$$

$$(s+\varphi)\left(\omega - \frac{\partial\alpha}{\partial t}\right) + \frac{1}{2}\left[\frac{\partial^2\varphi}{\partial z^2} - (s+\varphi)\left(q + \frac{\partial\alpha}{\partial z}\right)^2\right] \pm 4\pi N|a_{1D}||s+\varphi|^2(s+\varphi) = 0 \tag{D.5}$$

the linearization of these equations can be obtained considering the expansion to the perturbations $\varphi = \varphi(z,t)$ and $\alpha = \alpha(z,t)$ to first order in the parameter ϵ (which tends to zero). Thus,

$$\varphi \to \varphi_0(z,t) + \epsilon\varphi_1(z,t) \tag{D.6}$$

$$\alpha \to \alpha_0(z,t) + \epsilon\alpha_1(z,t) \tag{D.7}$$

Substituting these expressions in (D.4) and (D.5), again are obtained two expressions like (D.4) and (D.5) in terms of the variables φ_0 and α_0. Moreover, are gave rise to two new equations at first order in ϵ which represent the linearized equations of φ and α, given by

$$\frac{\partial\varphi_1}{\partial t} + \frac{1}{2}\left[2q\frac{\partial\varphi_1}{\partial z} + s\frac{\partial^2\alpha_1}{\partial z^2}\right] = 0 \tag{D.8}$$

$$-s\frac{\partial\alpha_1}{\partial t}+\omega\varphi_1+\frac{1}{2}\left[-2qs\frac{\partial\alpha_1}{\partial z}-q^2\varphi_1+\frac{\partial^2\varphi_1}{\partial z^2}\right]\pm 12\pi N\left|a_{1D}\right|s^2\varphi_1=0 \tag{D.9}$$

Here it was considered that both the functions φ_0 and α_0 as these derivates are small such that these can be neglected. The solution of this system of two coupled linear equations can be sought by mean of plane waves, as

$$\varphi_1 = A\exp\left[i\left(\Omega t-Qz\right)\right] \tag{D.10}$$

$$\alpha_1 = B\exp\left[i\left(\Omega t-Qz\right)\right] \tag{D.11}$$

Thereby the equations system resulting is

$$\begin{bmatrix} i\left(\Omega-qQ\right) & -\frac{1}{2}sQ^2 \\ \\ \omega+\frac{1}{2}\left[-q^2-Q^2\pm 24\pi N\left|a_{1D}\right|s^2\right] & -is\left(\Omega-qQ\right) \end{bmatrix}\begin{bmatrix} A \\ \\ B \end{bmatrix}=\begin{bmatrix} 0 \\ \\ 0 \end{bmatrix} \tag{D.12}$$

This system only has solution when the determinant is equal to zero. So

$$\left(\Omega-qQ\right)^2+\frac{1}{2}Q^2\left[\omega+\frac{1}{2}\left[-q^2-Q^2\pm 24\pi N\left|a_{1D}\right|s^2\right]\right] \;=\; 0 \tag{D.13}$$

from the dispersion relation (4.13)

$$\omega \;=\; \frac{1}{2}q^2\mp 4\pi N\left|a_{1D}\right|\psi_0^2 \tag{D.14}$$

is obtained the new dispersion relation for the perturbation

$$\left(\Omega-qQ\right)^2 \;=\; Q^2\left[\frac{1}{4}Q^2\pm 4\pi N\left|a_{1D}\right|\psi_0^2\right] \tag{D.15}$$

Appendix E

Useful math tools

E.1 Integrals

In the variational approximation implemented in the Chapter 4, are necessary some integrals, such as

- For the Gaussian ansatz

$$\int_{-\infty}^{\infty} d\mathbf{r}\,\rho^2 \exp\left[-\left(\frac{\rho^2}{w_\rho^2}+\frac{z^2}{w_z^2}\right)\right] = \left(w_\rho^6\pi\right)^{1/2}\left(w_\rho^2\pi\right)^{1/2}\left(w_z^2\pi\right)^{1/2} = \pi^{3/2}w_\rho^4 w_z \tag{E.1}$$

$$\int_{-\infty}^{\infty} d\mathbf{r}\,\frac{z^2}{w_z^4} \exp\left[-\left(\frac{\rho^2}{w_\rho^2}+\frac{z^2}{w_z^2}\right)\right] = \frac{w_\rho^2\pi}{2w_z^4}\left(w_z^6\pi\right)^{1/2} = \frac{1}{2}\pi^{3/2}\frac{w_\rho^2}{w_z} \tag{E.2}$$

- For the soliton-like ansatz

$$\int_{-\infty}^{\infty} dz\,\operatorname{sech} kz = \frac{1}{k}\tanh kz\Big|_{-\infty}^{\infty} = \frac{2}{k} \tag{E.3}$$

$$\int_{-\infty}^{\infty} dz\,\operatorname{sech}^4 kz = \frac{1}{3k}\left[\operatorname{sech}^2 kz + 2\right]\tanh kz\Big|_{-\infty}^{\infty} = \frac{4}{3k} \tag{E.4}$$

$$\int_{-\infty}^{\infty} dz\,\left(\tanh^2 kz\right)\left(\operatorname{sech}^2 kz\right) = \frac{1}{3k}\tanh^3 kz\Big|_{-\infty}^{\infty} = \frac{2}{3k} \tag{E.5}$$

E.2 Cubic equation

Performing the variable change $w_\rho^2 = x$, the sixth-degree polynomial equation (4.73) becomes in a third degree equation

$$x^3 - x + |\alpha|^2 = 0 \tag{E.6}$$

The nature of the roots is determined by its discriminant [96, 97, 98]

$$\triangle = -4 + 27\,|\alpha|^4 \tag{E.7}$$

The following cases need to be considered. While $\triangle < 0$ the equation has three distintic real roots. If $\triangle = 0$ there are three real roots of which at least two are equal. Whereas $\triangle > 0$ the equation has one real root and two complex conjugate roots. This last case is not useful because the real root is negative [96] and this is not a physical solution to the variational parameter w_ρ.

So it will be considered $\triangle < 0$ according to which while $N|a| < (\pi^2/27)^{1/4}$ or $N|a| < 0.778$ the cubic equation has three distintic real roots. However, it is necessary to know the sign of solutions because the negative ones are not physicals.

Performing the substitution $x = u\cos\theta$ such that u allows coincide (E.6) with the identity

$$4\cos^3\theta - 3\cos\theta = \cos 3\theta \tag{E.8}$$

i.e. choosing $u = 2/\sqrt{3}$ and dividing (E.6) by $u^3/4$ the new expression can be read as

$$4\cos^3\theta - 3\cos\theta = -\frac{3\sqrt{3}}{2}|\alpha|^2 \tag{E.9}$$

So, from (E.8) and (E.9)*

$$\theta = \frac{1}{3}\cos^{-1}\left(-\frac{3\sqrt{3}}{2}|\alpha|^2\right) + \frac{2\pi}{3}n \qquad\qquad n = 0, 1, 2 \tag{E.10}$$

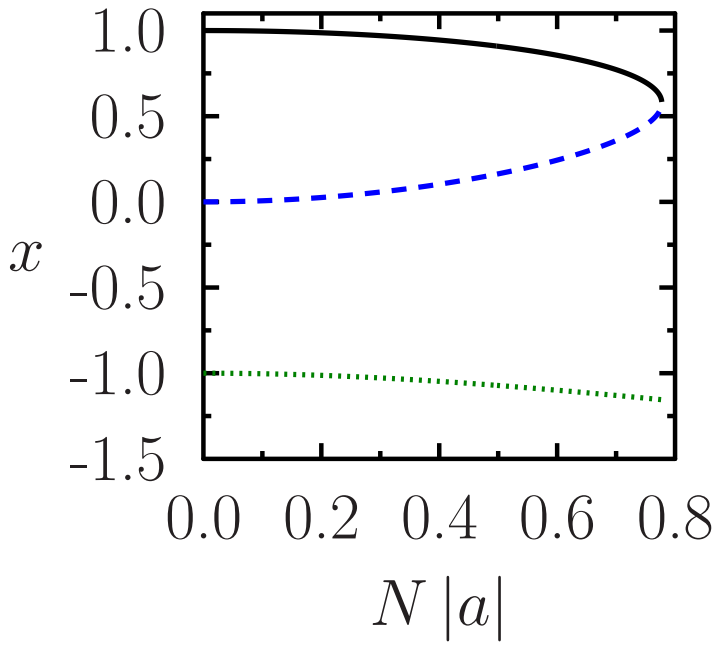

Figure E.1: The x solution to the cubic equation (E.6). For $n = 0$ (black solid line), $n = 1$ (green dotted line) and $n = 2$ (blue dashed line).

*This website has useful tools http://mathworld.wolfram.com/CubicFormula.html

Each value of the integer number n corresponds to each third degree polynomial equation solution (E.6) [98, 99]. Thus,

$$x = \frac{2}{\sqrt{3}} \cos\left[\frac{1}{3}\cos^{-1}\left[-\frac{3\sqrt{3}}{\pi}\left(N\left|a\right|\right)^2\right] + \frac{2\pi}{3}n\right] \tag{E.11}$$

The Figure (E.1) illustrates that two solutions to x are positive and therefore are physical solution to the sixth-degree polynomial equation in w_ρ (4.73). In a same way is confirmed the limit value $N\left|a\right| \approx 0.778$ of the existence of three real roots. Thus,

$$w_{1\rho} = \pm\left\{\frac{2}{\sqrt{3}} \cos\left[\frac{1}{3}\cos^{-1}\left[-\frac{3\sqrt{3}}{\pi}\left(N\left|a\right|\right)^2\right]\right]\right\}^{1/2} \tag{E.12}$$

$$w_{2\rho} = \pm\left\{\frac{2}{\sqrt{3}} \cos\left[\frac{1}{3}\cos^{-1}\left[-\frac{3\sqrt{3}}{\pi}\left(N\left|a\right|\right)^2\right] + \frac{4\pi}{3}\right]\right\}^{1/2} \tag{E.13}$$

Now, substituting these solutions in the Jacobean (by simplicity $\varepsilon = E/N$)

$$\begin{aligned} J &= \left[\frac{\partial^2\varepsilon}{\partial w_\rho^2}\right]\left[\frac{\partial^2\varepsilon}{\partial w_z^2}\right] - \left[\frac{\partial^2\varepsilon}{\partial w_\rho \partial w_z}\right]^2 \\ &= \left[1 + \frac{3}{w_\rho^4} - \frac{6N\left|a\right|}{\sqrt{2\pi}\, w_\rho^4\, w_z}\right]\left[\frac{3}{2\, w_z^4} - \frac{2N\left|a\right|}{\sqrt{2\pi}\, w_\rho^2\, w_z^3}\right] - \frac{2\left(N\left|a\right|\right)^2}{\pi w_\rho^6\, w_z^4} \end{aligned} \tag{E.14}$$

Only the solution $w_{1\rho}$ is physically useful because it gives rise a positive Jacobean and the respective derivates $\partial^2_{w_\rho}\varepsilon$ and $\partial^2_{w_z}\varepsilon$ are positive like is plotted in the Figure (E.2). Hence, this solution is a minimum in the variational energy (4.68).

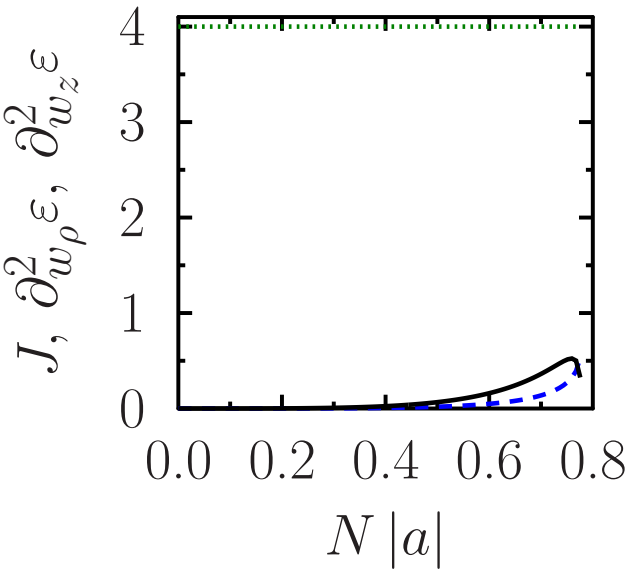

Figure E.2: The Jacobean J (black solid line) and the derivates $\partial^2_{w_\rho}\varepsilon$ (green dotted line) and $\partial^2_{w_z}\varepsilon$ (blue dashed line) using the positive solution $w_{1\rho}$ (By simplicity $\varepsilon = E/N$).

Appendix F

Quasi-one-dimensional dipolar interaction

The quasi-one-dimensional dipolar interaction can be obtained easily using the Fourier transform* of the 3D dipole dipole energy performing the dimensional reduction in the momentum space and returning to the configuration space [87].

The dipolar energy contribution can be read as

$$E_{dd} = \frac{N^2}{2} \int d\mathbf{r} \int d\mathbf{r}' \, U_{dd}\left(\mathbf{r} - \mathbf{r}'\right) \left|\Psi\left(\mathbf{r}'\right)\right|^2 \left|\Psi\left(\mathbf{r}\right)\right|^2 \tag{F.1}$$

where $U_{dd}\left(\mathbf{r} - \mathbf{r}'\right)$ is the dipole dipole interaction and it is given by (3.23). So, applying the Parseval theorem and the convolution theorem can be obtained the energy in the Fourier space [100]. By the Parseval theorem the dipolar energy is

$$E_{dd} = \frac{N^2}{2\left(2\pi\right)^3} \int d\mathbf{q} \, \mathcal{F}\left\{ \int d\mathbf{r}' \, U_{dd}\left(\mathbf{r} - \mathbf{r}'\right) \left|\Psi\left(\mathbf{r}'\right)\right|^2 \right\} \mathcal{F}\left\{ \left|\Psi\left(\mathbf{r}\right)\right|^2 \right\}^* \tag{F.2}$$

where $\mathcal{F}$ indicates the Fourier transform and the asterisk $(*)$ the complex conjugate. As the density is a real function and from the convolution theorem†, then the energy takes the form

$$E_{dd} = \frac{1}{2\left(2\pi\right)^3} \int d\mathbf{q} \, \tilde{n}^2\left(\mathbf{q}\right) \tilde{U}_{dd}\left(\mathbf{q}\right) \tag{F.3}$$

*Here the Fourier and the inverse Fourier transform in one dimension are defined respectively as

$$\mathcal{F}\left\{f\left(x\right)\right\} = \tilde{f}\left(k\right) = \int_{-\infty}^{\infty} f\left(x\right) \exp\left(-ik_x x\right) dx$$

$$\mathcal{F}^{-1}\left\{\tilde{f}\left(k\right)\right\} = f\left(x\right) = \frac{1}{2\pi} \int_{-\infty}^{\infty} \tilde{f}\left(k\right) \exp\left(ik_x x\right) dk_x$$

† A convolution of two function is defined as $\left(f \star g\right)\left(x\right) \equiv \int_{-\infty}^{\infty} dx' f\left(x - x'\right) g\left(x'\right)$ and the Fourier transform of this, is given by the product of each transformed $\mathcal{F}\left\{f \star g\right\}\left(x\right) \equiv \left[\mathcal{F}\left\{f\right\}\left(x\right)\right]\left[\mathcal{F}\left\{g\right\}\left(x\right)\right]$.

where the tilde represents the respective transform. With the density in the Fourier space as $\tilde{n}(\mathbf{q}) = \mathcal{F}\{n(\mathbf{r})\} = \mathcal{F}\left\{N|\Psi(\mathbf{r})|^2\right\}$ and the dipole dipole interaction in the momentum space (Appendix B)

$$\tilde{U}_{dd}(\mathbf{q}) = \frac{C_{dd}}{3}\left(3\frac{q_z^2}{\mathbf{q}^2} - 1\right) \tag{F.4}$$

The other hand, with the wave function of the condensate given by

$$\Psi(\mathbf{r}) = \left(\frac{1}{\pi a_\rho^2}\right)^{1/2} \exp\left(-\frac{\rho^2}{2\,a_\rho^2}\right)\phi(z) \tag{F.5}$$

such that $\omega_\perp a_\rho^2 = 1$. Then the density in the momentum space is

$$\begin{aligned}
\tilde{n}(\mathbf{q}) &= \int_{-\infty}^{\infty} d\mathbf{r}\exp(-i\mathbf{q}\cdot\mathbf{r})\, n(\mathbf{r}) \\
&= \frac{\tilde{n}_{1D}(q_z)}{\pi a_\rho^2}\int_{-\infty}^{\infty}\int_{-\infty}^{\infty} dx\,dy\,\exp\left(-iq_x x - iq_y y - \frac{x^2+y^2}{a_\rho^2}\right) \\
&= \tilde{n}_{1D}(q_z)\exp\left(-\frac{q_\rho^2\, a_\rho^2}{4}\right)
\end{aligned} \tag{F.6}$$

Now, substituting (F.4) and (F.6) in the energy (F.3), this latest taking the form

$$E_{dd} = \frac{1}{4\pi}\int_{-\infty}^{\infty} dq_z\,\tilde{n}_{1D}^2(q_z)\,V_{1D}(q_z) \tag{F.7}$$

Here

$$V_{1D}(q_z) = \frac{C_{dd}}{6\pi}\int_0^{\infty} dq_\rho\, q_\rho\left(3\frac{q_z^2}{q_\rho^2+q_z^2} - 1\right)\exp\left(-\frac{q_\rho^2\, a_\rho^2}{2}\right) \tag{F.8}$$

and the corresponding dipole dipole contribution in one dimension is given by the inverse Fourier transform of $V_{1D}(q_z)$. Thus,

$$U_{dd}^{1D}(z-z') = \frac{1}{2\pi}\int_{-\infty}^{\infty} dq_z\exp(iq_z z)\,V_{1D}(q_z) \tag{F.9}$$

References

[1] Fetter A. and Walecka J. Quantum Theory of many-particle systems. McGraw-Hill Book company. 1971.

[2] Pethick C. J. and Smith H. Bose-Einstein Condensation in dilute Gases. Cambridge university press. Second edition 2008.

[3] Dalfovo F., Giorgini S., Pitaevskii L., Stringari S. Rev. Mod. Phys. 71, 463 (1999).

[4] Pitaevskii and Stringari. Bose-Einstein Condensation. Oxford University. 2003.

[5] Anderson M., Ensher J., Matthews M., Wieman C., and Cornell E. Science, 269, 198-201 (1995).

[6] Bradley C., Sackett C., Tollett J., and Hulet R. Phys. Rev. Lett. 75, 1687–1690 (1995).

[7] Davis K., Mewes M., Andrews M., Druten N., Durfee D., Kurn D., and Ketterle W. Phys. Rev. Lett. 75, 3969–3973 (1995).

[8] Durfee D. and Ketterle W. 13 April 1998/ Vol. 2, No. 8/ OPTICS EXPRESS 300.

[9] Fetter A. L. and Foot C. J. arXiv:1203.3183v1 [cond-mat.quant-gas] 14 Mar 2012.

[10] Griesmaier A., Werner J., Hensler S., Stuhler J., and Pfau T. Phys. Rev. Lett. 94, 160401 (2005).

[11] Lahaye T., Menotti C., Santos L., Lewenstein M., and Pfau T. Rep. Prog. Phys. 72 126401 (2009).

[12] Baranov M. Physics Reports 464 (2008) 71–111.

[13] Pontes Lima. PhD. Dissertation. Berlin University 2010.

[14] Koch T., Lahaye T., Metz J., Fröhlich B., Griesmaier A., and Pfau T. 0710.3643v1 [cond-mat.other] 19 Oct 2007.

[15] Adhikari S. J. Phys. B: At. Mol. Opt. Phys. 46 (2013) 115301 (9pp).

[16] Metz J., Lahaye T., Fröhlich B., Griesmaier A., Pfau T., Saito H., Kawaguchi Y and Ueda M. New Journal of Physics 11 (2009) 055032.

[17] Lahaye T., Metz J., Fröhlich B., Koch T., Meister M., Griesmaier A., Pfau T., Saito H. Kawaguchi Y. and Ueda M. Phys. Rev. Lett. 101, 080401 (2008).

[18] Castin Y. arXiv:cond-mat/0105058v1 3 May 2001.

[19] Leggett A. J. Rev. Mod. Phys. 73, 307–356 (2001).

[20] Dalibard J. Collisional dynamics of ultra-cold atomic gases. Laboratoire Kastler-Brossel, France.

[21] Sakurai J. Modern quantum mechanics. Addison-Wesley Company. 1994.

[22] Huang K. Statistical mechanics. John Wiley & Sons. 1987.

[23] Young L., Adhikari S. and Muruganandam P. Phys. Rev. A 85, 033619 (2012).

[24] Muruganandam P. and Adhikari S.K. Computer Physics Communications 180 (2009) 1888–1912.

[25] Pérez-García, Michinel H., Cirac J. I., Lewenstein M. and Zoller P. Phys. Rev. A 56, 1424–1432 (1997).

[26] Salasnich L. arXiv:cond-mat/9908147v1 [cond-mat.stat-mech] 10 Aug 1999.

[27] Fetter A. arXiv:cond-mat/9510037v1 6 Oct 1995.

[28] Ruprecht P., Holland M., Burnett K., and Edwards M. Phys. Rev. A 51, 4704–4711 (1995).

[29] Gammal A., Frederico T., and Tomio L. Phys. Rev. A 64, 055602 (2001).

[30] Bogoliubov N., J. Phys. (USSR) 11, 23 (1947), reprinted in D. Pines, The Many-Body Problem, (New York, W. A. Benjamin, 1961), p. 292.

[31] Yi S. and You L. Phys. Rev. A 63, 053607 (2001).

[32] Santos L., Shlyapnikov G., Zoller P., and Lewenstein M. Phys. Rev. Lett. 85, 1791–1794 (2000).

[33] Giovanazzi S., Pedri P., Santos L., Griesmaier A., Fattori M. Koch T., Stuhler J., and Pfau T. arXiv:cond-mat/0605708v1 [cond-mat.other] 29 May 2006.

[34] Giovanazzi S., Görlitz A., and Pfau T. Phys. Rev. Lett. 89, 130401 (2002).

[35] Eberlein C., Giovanazzi S., and O'Dell D. Phys. Rev. A 71, 033618 (2005).

[36] O'Dell D., Giovanazzi S., and Eberlein C. Phys. Rev. Lett. 92 (25 Pt 1) 2004.

[37] Góral K., Rzazewski K., Pfau T. Phys. Rev. A 61, 051601 (2000).

[38] Lu M., Burdick N., Youn S., and Lev B. Phys. Rev. Lett. 107, 190401 (2011).

[39] Ospelkaus S., A. Peer, Ni K., Zirbel J., Neyenhuis B., Kotochigova S., Julienne P., Ye J., and Jin D. Nature Phys. 4, 622 (2008).

[40] Ni K., Ospelkaus S., H. de Miranda M., Peer A., Neyenhuis B., Zirbel J., Kotochigova S., Julienne P., Jin D., and Ye J. Science 322, 231 (2008).

[41] Griffiths D. Introduction to Electrodynamics. Prentice Hall. 1999.

[42] Jackson J. Classical Electrodynamics. Third Edition. Jhon Wiley & Songs. 1999.

[43] Dauxois T., Ruffo S., Arimondo E., and Wilkens M. arXiv:cond-mat/0208455v1 [cond-mat.stat-mech] 23 Aug 2002.

[44] Astrakharchik G., and Lozovik Y. Phys. Rev. A 77, 013404 (2008).

[45] Eberlein C., Giovanazzi S., and O'Dell D. arXiv:cond-mat/0311100v2 [cond-mat.soft] 23 Aug 2004.

[46] Cai Y., Rosenkranz M., Lei Z., and Bao W. arXiv:1006.4950v3 [cond-mat.quant-gas] 27 Oct 2010.

[47] Salomon C., Shlyapnikov G., and Cugliandolo L. Many-Body Physics with Ultracold Gases: Lecture Notes of the Les Houches 2010. Oxford University Press. 2013.

[48] Fregoso B., and Fradkin E. arXiv:1001.4167v4 [cond-mat.quant-gas] 1 Jul 2010.

[49] Scott A. Encyclopedia of nonlinear Science. Routledge 2005.

[50] Zabusky N., and Porter M. Solitons.

[51] Kivshar Y. and Agrawal G. Optical solitons from fibers to photonic crystals. Academic press (2003).

[52] The Nonlinear Schrödinger Equation. Bouchbinder E. December 2003.

[53] Parker N., Proukakis N., and Adams C. Dark soliton dynamics in confined Bose-Einstein condensates. University of Durham. 2004.

[54] Salasnich L., Parola A., and Reatto L. Phys. Rev. A 65, 043614-1 (2002).

[55] Muñoz A. and Delgado V. Phys. Rev. A 77, 013617 (2008).

[56] Buitrago C. and Adhikari S. J. Phys. B: At. Mol. Opt. Phys. 42 215306 (2009).

[57] Pérez-García, Michinel H., Herrero H. Phys. Rev. A 57, 3837–3842 (1998).

[58] Jackson A., Kavoulakis G., and Pethick C. Phys. Rev. A 58, 2417–2422 (1998).

[59] Abdullaev F., Gammal A., Kamchatnov A., and Tomio L. International Journal of Modern Physics B, 19, No. 22 (3415-3473) 2005.

[60] Görlitz A., Vogels J., Leanhardt A., Raman C., Gustavson T., Abo-Shaeer J., Chikkatur A., Gupta S. , Inouye S., Rosenband T., and Ketterle W. Phys. Rev. Lett. 87, 130402 (2001).

[61] Carretero-González R., Frantzeskakis D., and Kevrekidis P., Nonlinearity 21 (2008) R139–R202.

[62] Remoissenet M. Annales Des Télécommunications 51 (7-8), (297-303) 1996.

[63] Abdullaev F., Darmanyan S., and Garnier J. Modulational instability of electromagnetic waves in inhomogeneous and in discrete media. E. Wolf, Progress in Optics 44. Elsevier Science B.V 2002.

[64] Esbensen B., Wlotzka A., Bache M., Bang O., and Krolikowski W. Phys. Rev. A 84. 053854 (2011).

[65] Kivshar Y. and Luther-Davies B. Physics Reports 298 (81-197) 1998.

[66] Dauxois T., and Peyrard M. Physics of solitons. Cambridge university press. 2006.

[67] Frantzeskakis D. arXiv:1004.4071v1 [cond-mat.quant-gas] 23 Apr 2010.

[68] Proukakis N., Parker N., Frantzeskakis D., and Adams C. arXiv:cond-mat/0311141v2 [cond-mat.other] 3 Aug 2004.

[69] Middelkamp S.,Theocharis G., Kevrekidis P., Frantzeskakis D., and Schmelcher P. arXiv:1002.0552v3 [cond-mat.quant-gas] 20 May 2010.

[70] Burger S., Bongs K., Dettmer S., Ertmer W., Sengstock K., Sanpera A., Shlyapnikov G. and Lewenstein M. Phys. Rev. Lett. 83. 5198 (1999).

[71] Anderson B., Haljan P., Regal C., Feder D., Collins L., Clark C., and Cornell E. Phys. Rev. Lett. 86. 2926 (2001).

[72] Denschlag J., Simsarian J., Feder D., Clark C.,Collins L., Cubizolles J., Deng L., Hagley E., Helmerson K, Reinhardt W., Rolston S., Schneider B., and Phillips W. Science 287. 97 (2000).

[73] Kevrekidis P., Frantzeskakis D., and Carretero-González R. Emergent Nonlinear Phenomena in Bose-Einstein Condensates: Theory and Experiment. Springer 2008.

[74] Parker N. Cornish S., Adams C., and Martin A. J. Phys. B. At. Mol. Opt. Phys. 40 (2007).

[75] Strecker K., Partridge G., Truscott A., and Hulet R. 2002 Nature 417 150.

[76] Khaykovich L., Schreck F., Ferrari G., Bourdel T., Cubizolles J., Carr L., Castin Y., and Salomon C. 2002 Science 296 1290.

[77] Cornish S., Thompson S. and Wieman C. Phys. Rev. Lett. 96 170401 (2006).

[78] Timmermans E., Tommasini P., Hussein M., and Kerman A. Phys. Rep. (1999).

[79] Frantzeskakis D J. J. Phys. A: Math. Theor. 43 (2010) 213001 (68pp).

[80] Cronin A., Schmiedmayer J., and Pritchard D. Rev. Mod. Phys. 81, 1051 (2009).

[81] Salasnich L, Parola A and Reatto L Phys. Rev. A 66 043603. 2002.

[82] Billam T., Wrathmall S., and Gardiner S. Phys. Rev. A 85, 013627 (2012).

[83] Carr L. and Castin Y. arXiv:cond-mat/0205624v2 31 May 2002.

[84] Ueda M. and Saito H. J. Phys. Jpn. Vol 72 127-133 (2003).

[85] Gammal A., Tomio L., and Frederico T. Phys. Rev. A 66, 043619 (2002).

[86] Adhikari S. New Journal of Physics, v. 5, p. 137-137, 2003.

[87] Muruganandam P. and Adhikari S. K. Laser Physics 22 813-820 (2012).

[88] Young L., Muruganandam P., and Adhikari S. Phys. B: At. Mol. Opt. Phys. 44 101001 (6pp) 2011.

[89] Glaum K. and Pelster A. Phys. Rev. A 76, 023604 (2007).

[90] Pedri P. and Santos L. Phys. Rev. Lett. 95 200404 (2005).

[91] I. Tikhonenkov I., Malomed B. and Vardi A. Phys. Rev. Lett. 100 090406 (2008).

[92] Eichler R., Zajec D., Köberle P., Main J. and Wunner G. Phys. Rev. A 86, 053611 (2012)

[93] Cuevas J., Malomed B., Kevrekidis P. and Frantzeskakis D. Phys. Rev. A 79 053608 (2009).

[94] Kagan Y., Muryshev A., and Shlyapnikov G. Phys. Rev. Lett. 81, 933–937 (1998).

[95] Góral K. and Santos L. Phys. Rev. A 66 023613 (2002).

[96] Irving R. Integers, polynomials and rings. Springer. (2004).

[97] Birkhoff G. and Mac Lane S. A survey of modern algebra. Fourth edition. Macmillan Publishing Co. Inc. 1977.

[98] Zwillinger D. Standard mathematical tables and formulae. 2003.

[99] Holmes G. The use of hyperbolic cosines in solving cubic polynomials. Mathematical Gazette 86. 473–477. November 2002.

[100] Metz J. PhD. Dissertation. Stuttgart University. 2010.